49
43

Weak Narrow-Band Signal Detection In Multivariate Non-Gaussian Clutter

by

M.K.Sistanizadeh

Dissertation submitted to the Faculty of the

Virginia Polytechnic Institute and State University

in partial fulfillment of the requirements for the degree of

Doctor of Philosophy

in

Electrical Engineering

APPROVED:

Dr.Kai-Bor Yu, Chairman	Dr.R.E Nance
Dr.I.M Besieris	Dr.H.F Van Landingham
Dr.W.A Davis	Dr.L.W Johnson

November 1986

Blacksburg, Virginia

Weak Narrow-Band Signal Detection In Multivariate Non-Gaussian Clutter

by

M.K.Sistanizadeh

Dr.Kai-Bor Yu, Chairman

Electrical Engineering

(ABSTRACT)

This dissertation is concerned with the development and performance analysis of non-linear receivers for detection of weak narrow-band signals in multivariate non-Gaussian clutter. The novelty of the detection scheme lies in the utilization of both the complex measurement and the multivariate non-Gaussian character of the clutter. Two clutter models are developed based on the available partial information. Model (I) is based on the a priori knowledge of the first-order density, correlation structure of the amplitude, and the circular symmetric assumption of the in-phase and quadrature phase components. Model (II) is based on the first-order in-phase and quadrature phase densities and the complex correlation structure. These models completely specify a multivariate complex non-Gaussian density and can be used for clutter generation.

A class of optimum non-linear receiver structures based on weak signal level, canonically known as Locally Optimum Detectors (LOD) are derived under clutter Model (I). This can be considered to be a generalization of the LOD for the independent and identically distributed (i.i.d) clutter. The detectors utilize

complex measurements and their structures depend on whether the underlying hypothesis testing model is real or complex.

The performance of each of the proposed detector structures, based on the concept of Efficacy, is formulated. Then, the performance of the detectors are evaluated with respect to a reference detector using Asymptotic Relative Efficiency (ARE) criterion. Numerical evaluation of the performance expression is carried out for constant signal in Weibull distribution for various density parameters. Simulation results indicate that the performance of the developed detectors, based on ARE, is superior to (i.i.d) LOD detector and matched filter.

Finally, the sensitivity of the detector performance to parameter variation of the structural non-linearities is investigated.

Acknowledgements

I would like to express my sincere appreciation to Dr.Kai-Bor Yu, my supervising professor, for his valuable advice throughout the course of this research. I am indebted to my mentor, Dr.I.M Besieries, for his scholarly guidance during my Graduate studies at VPI&SU. I also wish to extend my gratitude to Dr.W.A Davis, my former advisor, for his constant encouragements and spiritual support. Also, I am sincerely grateful to Dr.H.F Van Landingham for his whole-hearted educational assistance throughout my studies at VPI&SU. My deep appreciation is extended to Dr.L.W Johnson, my Applied Mathematics Program Advisor, for his academic guidance and encouragements which made it possible to receive my M.Sc. degree in Applied Math. Finally, I would like to acknowledge my particular gratitude to Professor R.E. Nance, Head of the System Research Center at VPI&SU, without his financial support, this research would not have been achieved. This research is supported in part by the U.S. Navy under the contract N60921-83-G-A165(B008) through System Research Center at VPI&SU.

Table of Contents

List of Illustrations

I. Introduction

1.1. Statement of the Problem

This dissertation is concerned with the development and analysis of non-linear receiver structures for coherent and non-coherent detection of weak narrow-band signals in multivariate non-Gaussian noise. The fundamental concepts for the research reported in this dissertation are motivated by high-resolution radar detection problem in sea clutter. The terms "weak", "non-Gaussian", "multivariate", "coherent", "non-coherent", "narrow-band", and "complex" each have specific contributions to the overall problem under consideration.

In modern radar and communication systems, in order to realize low probability of intercept and high anti-jamming capability, one of the design objectives

is to minimize and disguise the transmitted signal by spreading it in time and frequency, thus making it more difficult to distinguish the signal from the background interfering noise. Furthermore, the transmitter's power, based on a'priori range information, may be constrained to a specific level to gain power economy and channel privacy. All these factors contribute to the notion of "weak" signal. Thus, as formulated analytically later, this concept is of significant interest.

Although, in the past, a Gaussian model of the additive noise has been a common approximation of the actual interfering environment, it is well established now that in many applications the noise should be modeled as non-Gaussian. This is well justified in the case of sea clutter, observed by high-resolution radar. In fact, the Gaussian assumption can lead to severe performance degradation, and in some cases to disastrous consequences. Thus, "non-Gaussianity" is another important factor in the formulation of the problem.

Various existing discrete-time formulation of the general detection problem consider the received noise samples to be independent and identically distributed. However, frequently, due to the physics of the noise generation, or the minimum sampling rate requirements of the receivers, the received samples are dependent. Thus, noise statistics are contained in an M-dimensional multivariate distribution, where M (duration of the signal) depends on specific application. Finding an appropriate multivariate distribution for dependent non-Gaussian noise is not a trivial problem and various characterization schemes exist that will be discussed later.

The coherent and non-coherent detection schemes are well known in communication systems, referring to the measurement and information extraction capability of the receivers. In coherent receivers, both the amplitude and phase of the received signals are available. That is, both the in-phase and quadrature phase components of the received signals are separately measurable. In particular, the complex envelope of the signal and noise processes are measured with respect to a known high frequency carrier and reference phase. However, in non-coherent receivers, only the amplitude information is available. The distinction between coherent and non-coherent has significant impact on the complexity of the receiver structure and the level of performance. Intuitively, more information implies better performance.

Finally, narrow-band signal implies that the bandwidth of the signal under consideration is much less than the carrier frequency (i.e., modulating signal).

In summary, the essential feature of the research presented in this dissertation will be the problem of coherent and non-coherent detection (hypothesis testing) of weak narrow-band signal embedded in complex or real multivariate non-Gaussian noise(clutter). In the sequel, the terms " noise " and " clutter " will be used interchangably.

1.2. Historical Background

In this section, a brief summary of available literature which is pertinent to the specific problem of weak signal detection in non-Gaussian noise is presented. The scope of the discussion is kept intentionally limited, since the full exposure to detection literature is beyond the scope of this dissertation. Three main issues are of concern: weak signal condition (vanishingly small compared with the additive complex or real noise), non-Gaussianity of the noise distribution, and dependency among the received samples.

In general, the class of detector which deal with small signal levels is called Locally Optimum Detector (LOD). The underlying statistical theory of this class is discussed by Middleton [1] and Ferguson [2]. A concise discussion of this theory will be presented later in Chapter III. Essentially, this type of detector maximizes the derivative of the Power Function (i.e., probability of detection) at the zero signal level, subject to a fixed false alarm probability.

In the case of low-pass signals, Rapport and Kurz [3] investigated a non-linear LOD for the detection problem of binary synchronous communication. The non-linear transformation of the received signal was proposed to render a Gaussian test statistic. Miller and Thomas [4,5] considered a locally optimum non-linearity and a Neyman-Pearson optimum non-linearity for the discrete-time detection of low-pass signals under a class of symmetric, unimodal, univariate probability density functions. They also discussed the robustness of a sub-class of locally optimum detectors against the possible errors incurred in the parame-

ters of density function [6]. Their significant contribution was that the LOD structure was a non-linearity followed by a matched filter that would be optimum for detection of lowpass signals in Gaussian noise. In 1978, Sheehy [7] applied the LOD technique to detect completely known signals, and zero-mean unknown low-pass signals.

In 1978, Poor and Thomas [8] considered purely zero-mean, small level stochastic signal in non-Gaussian noise. They introduced two models: additive noise and scale change models. Kassam [9] investigated the locally robust array detectors for the stochastic signals using the non-linear structure, identical to Sheehy [7]. These developments were all limited to the case of low-pass signals.

In the case of band-pass signals, Nirenberg [10] investigated non-coherent detection of digital communication signal over non-Gaussian channel. He approached the problem using the concept of characteristic function. The generality of this approach was sufficient to cover a large class of detection problems. Later, in 1979, Modestino and Ningo [11] extended the concept of LOD to coherent narrow-band signal detection. In their investigation, the LOD was developed for a class of narrow-band noise models possessing circularly symmetric probability distribution function (more will be covered about this concept in the next Chapter). Later, in 1981, Lu and Eisenstein [12] extended the method of characteristic function to develop detectors for weak band-pass signals of unknown level. Their approach was sufficiently general to be applied to low-pass unknown signals too.

Thus far, the discussion has been based on the assumption that the signal is embedded in independent and identically distributed (i.i.d) noise. The more real-

istic and difficult case is that of the dependent noise, where the received measurement vector possesses certain covariance structure. In this case, application of the detectors, designed optimally for independent noise, will lead to performance degradation and sub-optimal operation.

In 1979, Poor and Thomas [13] considered the memoryless discrete-time detection of constant signal in the so-called m-dependent noise. Their investigation lead to a non-linearity which was the solution of a Fredholm Integral Equation of the Second Kind. The kernel of the integral equation depended only on the bivariate probability distribution of the noise. This non-linearity was followed by a linear filter. Later, in 1980 and 1981, Halverson and Wise [14,15] investigated the memoryless detection of a constant and stochastic real signal in dependent noise. In the case of constant signal, they approximated the non-linearity by a polynomial, and in the case of stochastic signal, their design reduced to determining the solution of a Fredholm integral equation.

In 1982, Poor [16] considered the optimum detection of known constant signal in "weakly dependent" noise. He represented the dependency of the noise by a second-order moving-average model, and modified the optimum detector of the independent noise to accomodate for this weak dependence. Later, in 1984, Martinez, Swaszek, and Thomas [17] introduced the Transformation Noise Detector for optimal detection of known real signals in dependent noise. The various non-linear structures were based on the functional representation of the m-dimensional multivariate density function. They derived the detector based on maximizing the Efficacy(more will be discussed on this concept in Chapter V).

The overall structure of this detector was more complicated than previously investigated structure(non-linearity followed by a linear filter).

In summary, various LOD structures for the case of stochastic, constant, low-pass, and band-pass signals of known and unknown levels, embedded in independent and identically distributed noise have been studied. Also, in the case of band-pass signals, coherent detection, based on in-phase and quadrature phase information has been developed. In the case of dependent noise, for detection of weak real signals, all the proposed structures except for Martinez, et al. [17], have been based on a single non-linearity followed by a linear filter. It is only in [17] that several non-linearities have been proposed to comprise the detector.

Consequently, as a matter of higher level of detection methodology, what is needed is a general class of detectors for coherent(or non-coherent) weak band-pass signals embedded in complex (or real) multivariate non-Gaussian noise. This will necessitate a'priori knowledge of the complex (real) multivariate distribution function. It is the primary objective of this dissertation to provide the necessary analytical tools to satisfy the above-mentioned requirements.

In the next two sections, the methods of the approach, scope of the research, and limitations of the investigated techniques will be presented.

1.3. Outline of the Dissertation

Chapter II is devoted to the modeling of the complex multivariate clutter density. Two distinct models are presented. In Model (I), by imposing the circular-symmetry assumption on the in-phase and quadrature phase components of the clutter, the joint multivariate in-phase and quadrature phase density can be expressed as a function of the amplitude of the clutter samples. Then, this amplitude density function can be modeled (approximated) by the a'priori knowledge of the marginal density function and the covariance structure of the clutter. In particular, the problem reduces to Zero Memory Non-Linear (ZMNL) transformation of the multivariate Gaussian clutter with covariance structure based on the desired covariance of the non-Gaussian clutter. In Model (II), the complex multivariate non-Gaussian density is characterized by ZMNL transformation of the in-phase and quadrature phase components of a complex multivariate Gaussian density. The complex correlation of the Gaussian density is related to the desired non-Gaussian correlation structure, and the non-linear processing of the in-phase and quadrature phase components render the desired first-order densities. Then, sea clutter characteristics, observed through high-resolution radar, are discussed briefly, and the bivariate joint densities for Weibull distribution, based on Model (I) are illustrated. Finally, using the clutter Model (II), samples of complex non-Gaussian clutter for a specified non-Gaussian in-phase and quadrature densities are generated.

Chapter III is entirely devoted to the basic theoretical aspects of optimal detector design. The design methodologies for Neyman-Pearson and locally optimum detectors are discussed. Then different class of detectors based on complex and real signal, and measurement models are developed. These developments are all based on the dependent noise model. Specifically, the following hypothesis testing conditions are considered: a) multivariate complex noise and amplitude density model, b) multivariate complex noise and complex density Model (I), c) multivariate complex noise and complex density Model (II). Then, as a special case, the developed LOD are shown to collapse into the form of the previously reported detectors, based on the independent and identically distributed noise.

Chapter IV is concerned with the performance evaluation of the various detectors that have been developed in Chapter III. Since, the detectors are nonlinear functions of the complex or real measurements, one can not simply apply the usual criterion of signal to noise ratio, and a more general concept, known as "Efficacy" is needed. First, the Pittman-Noether Theorem and Efficacy are presented and their applications to performance evaluation are discussed. Second, the Efficacy of the various detectors are derived. Then, the concept of Asymptotic Relative Efficiency (ARE) is applied to compare various detectors with respect to a reference detector. Numerical results under specific density functions are presented, and their performances are evaluated.

In Chapter V, sub-optimum detectors, as an approximation to optimum detectors are presented. This approximation reduces the structural complexity of the locally optimum detectors without significant compromise in their performances.

Also, the concept of Asymptotic Optimum Detection (AOD) is considered briefly, and its relation to (LOD) is discussed.

Chapter VI concludes the dissertation with a discussion on the advantages and drawbacks of the proposed techniques. Finally, specific contributions of this dissertation are pointed out, and future directions of research in this area are identified.

1.4. Practical Motivations and Limitations of the Proposed Techniques

Throughout this dissertation, as with any other theoretical investigation, the development of the analytical results and the experimental verifications are motivated by a specific problem, and are based on certain assumptions. These assumptions are necessary for modeling and mathematical tractability of the problem under consideration. Consequently, the final results are only approximations of the true solution. As the discussion progresses, these assumptions will be pointed out, so that the scope of applicability of the proposed methods are clearly defined.

The underlying motivation for the imposition of certain assumptions is based on the utilization of the data from clutter measurements. In practical situation, the knowledge of the joint multivariate in-phase and quadrature phase probability density function is required. The approximation of such a density necessitates certain assumptions. Two multivariate non-Gaussian density models, Model (I) in section (2.2) and Model (II) in section (2.3), will be developed as an approximation of the true density function. Some of the fundamental assumptions discussed in characterization of Model (I) are: i) the circular-symmetry assumption on the joint multivariate in-phase and quadrature phase density function of the clutter, ii) assumption on the existence of the covariance structure for the sample amplitudes with uncorrelated phases, iii) multivariate amplitude density function approximation by marginal density and covariance structure of the clutter.

II. Complex Multivariate Non-Gaussian Noise Modeling

2.1. Statement of the Problem

In most modern communication and radar systems, operating at a carrier frequency, ω_c , the signal bandwidth, B , is small compared with ω_c (e.g., radar frequency in gigahertz). In such situations, it is convenient to represent the received signal n(t) in terms of its in-phase and quadrature phase components, as depicted in Figure(1). The received signal (which might be just due to noise) is:

$$n(t) = A(t)\cos(\omega_c t + \theta) \qquad (2.1 - 1)$$

where n(t) and A(t) are narrow-band and low-pass processes respectively. This means that the spectral density of n(t) is concentrated around $(\omega = \omega_c)$, and that of A(t) is located around $(\omega = 0)$.

The narrow-band process n(t) can be converted into a low-pass process as shown in Figure(1). The signals $n_I(t)$ and $n_Q(t)$ in the two channels are the low-pass in-phase and quadrature phase components of the n(t) respectively. They are obtained as:

$$n_I(t) = LPF_B[n(t)\cos(\omega_c t)] \qquad (2.1-2a)$$

$$n_Q(t) = LPF_B[n(t)\sin(\omega_c t)] \qquad (2.1-2b)$$

where LPF_B denotes the low-pass filtering operation with bandwith of B. Also, the low-pass amplitude and the phase of n(t) are obtained as:

$$A(t) = \sqrt{n_I^2(t) + n_Q^2(t)} \qquad (2.1-3)$$

$$\theta(t) = \tan^{-1}\left(\frac{n_Q(t)}{n_I(t)}\right) \qquad (2.1-4)$$

Now, the term coherent system (i.e., radar system) means that both A(t) and $\theta(t)$ are available information ($n_I(t)$ and $n_Q(t)$ are measurable), whereas non-coherent system implies that only A(t) is available for measurement.

In the discrete-time detection problem, if the detection system is coherent, both samples of $n_I(t)$ and $n_Q(t)$ are available, and are samples of a low-pass random process. In order to formulate the detection problem, the statistical information such as the density function is required. Hence, modeling of the density function is of great interest. It is noted that the in-phase and quadrature phase components of a sample, obtained at the same instant, can be shown to be un-

correlated, and if the underlying narrow-band process n(t) is Gaussian, they are also statistically independent [18]. However, in general, if n(t) is non-Gaussian, then $n_I(t)$ and $n_Q(t)$ are not statistically independent.

As will be described in Chapter III, for coherent detection of signals embedded in non-Gaussian noise, joint non-linear processing of both in-phase and quadrature phase components of the received signal is required. This means that marginal density $p_{n_I}(I)$ and $p_{n_Q}(Q)$ are not sufficient information, and joint density function $p_{n_I, n_Q}(I,Q)$ is required. Moreover, based on the covariance structure of the noise samples (dependent noise) or the receiver capability, an M-vector complex or real measurement is performed before a decision is made by the detector. Statistically, this means that one requires the knowledge of the joint multivariate non-Gaussian in-phase and quadrature phase density function of the noise denoted as:

$$p_{n_{I_1}, n_{Q_1}, ..., n_{I_M}, n_{Q_M}}(I_1, Q_1, ..., I_M, Q_M) \qquad (2.1 - 5)$$

In this Chapter, the discussion is concerned with the modeling (approximating) of the density function given by (2.1-5). Two distinct models are developed. Model (I) is based on Zero Memory Non-Linear (ZMNL) transformation of a correlated real Gaussian clutter with uniform phase distribution. Model (II) is based on ZMNL transformation of a correlated complex Gaussian clutter with separate in-phase and quadrature phase components processing. As a special case, if the noise samples are statistically independent, then (2.1-5) can be reduced to:

$$p_{n_{I_1}, n_{Q_1}, \ldots, n_{I_M}, n_{Q_M}}(I_1, Q_1, \ldots, I_M, Q_M) = \prod_{i=1}^{M} p_{n_{I_i}, n_{Q_i}}(I_i, Q_i) \qquad (2.1 - 6)$$

In the past, since most of the research in this area has been based on the independent assumption, equation (2.1-6) has been used extensively.

It should be pointed out that the noise sample dependence and in-phase and quadrature phase dependence of a single sample are different issues under consideration. The sample to sample dependence of the received signal is due to the physics of the problem and/or the sampling rate of the receiver structure; whereas the in-phase and quadrature phase dependence is due to non-Gaussianity of the underlying narrow-band process. In general, equation (2.1-5) is the most general density function that incorporates both aspects of dependence. In the next section, multivariate non-Gaussian clutter density is characterized based on Model (I).

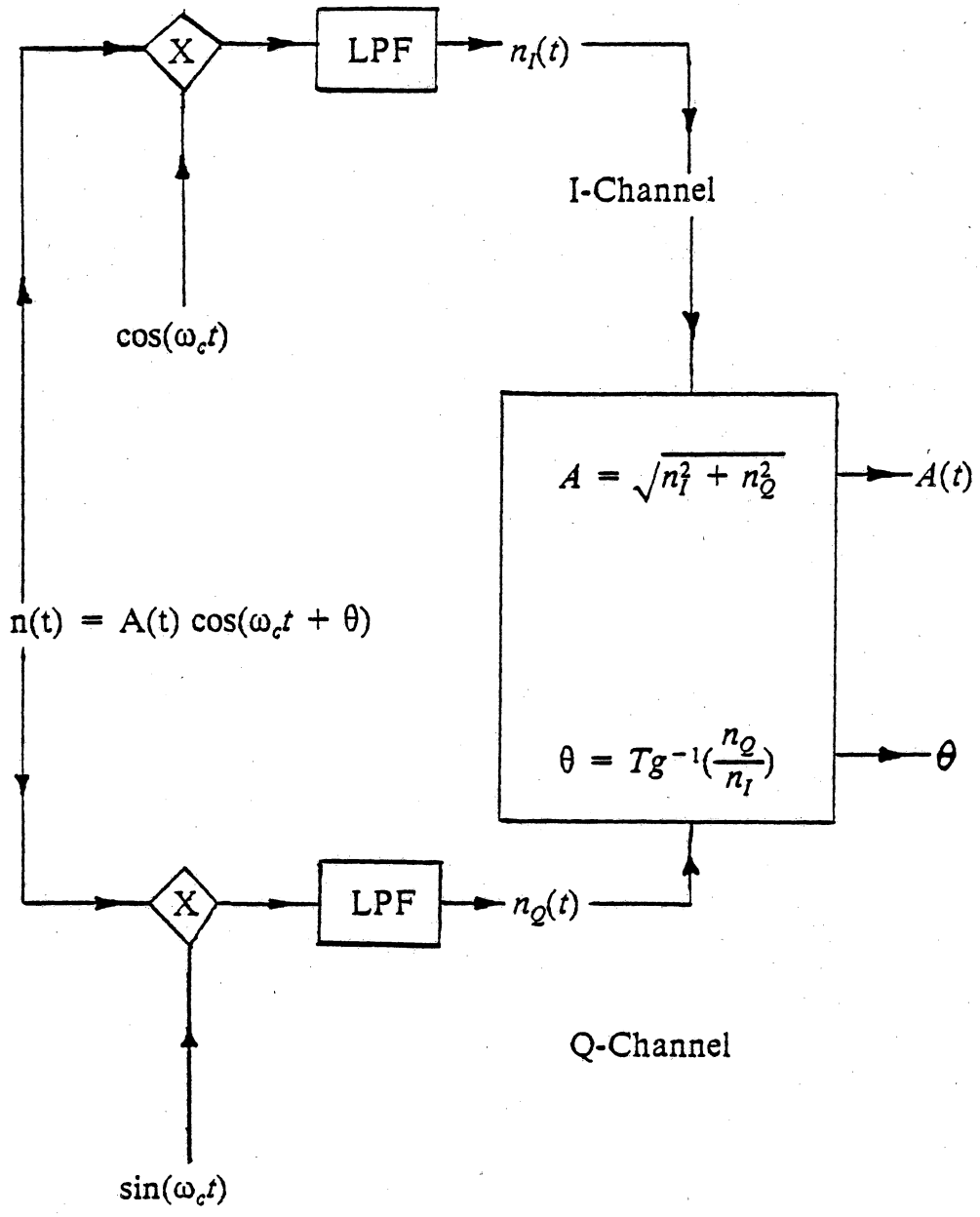

Figure 1. In-phase and Quadrature Phase Representation of the Received Signal.

2.2. Multivariate Non-Gaussian Density Model (I)

This section is concerned with modeling (approximation) of the joint multivariate non-Gaussian in-phase and quadrature phase density function of the narrow-band noise process: $p_{n_{I_1}, n_{Q_1}, ..., n_{I_M}, n_{Q_M}}(I_1, Q_1, ..., I_M, Q_M)$. The required information for the implementation of this model are the first-order amplitude density and the amplitude correlation structure of the clutter.

As a first major proposition, it is assumed that the multivariate density function possesses "circular symmetry". That is, the density function is assumed to depend only on the amplitude(envelope) of the received noise samples:

$$p_{n_{I_1}, n_{Q_1}, ..., n_{I_M}, n_{Q_M}}(I_1, Q_1, ..., I_M, Q_M) = f(\sqrt{I_1^2 + Q_1^2}, ..., \sqrt{I_M^2 + Q_M^2}) \qquad (2.2 - 1)$$

This implies that the amplitude and phase are statistically independent, and in particular, the phase is uniformly distributed. This assumption has both theoretical merit and practical validity. Theoretically, as will be seen in the sequel, it will lead to a formulation which is easily amenable for modeling and computational purpose. Practically, it implies that a'priori knowledge on the phase distribution is minimal: uniformly distributed (worst case).

To find the explicit form of the function $f(\sqrt{I_1^2 + Q_1^2}, ..., \sqrt{I_M^2 + Q_M^2})$, consider the relations between amplitude, phase, quadrature, and in-phase components of the M-sample as:

$$I_1 = A_1 \cos \varphi_1 \ , \ \ Q_1 = A_1 \sin \varphi_1 \qquad (2.2 - 2a)$$

. .

. .

. .

$$I_M = A_M \cos \varphi_M \ , \ \ Q_M = A_M \sin \varphi_M \qquad (2.2 - 2b)$$

Now, using the Jacobian of the transformation, one can represent $p_{n_{I_1}, n_{Q_1}, ..., n_{I_M}, n_{Q_M}}(I_1, Q_1, ..., I_M, Q_M)$ as a function of amplitude and phase as:

$$p_{n_{I_1}, n_{Q_1}, ..., n_{I_M}, n_{Q_M}}(I_1, Q_1, ..., I_M, Q_M) = \frac{p(A_1, ..., A_M, \varphi_1, ..., \varphi_M)}{|J|} \qquad (2.2 - 3)$$

where J, Jacobian of the transformation, is obtained from:

$$J = \det(D_1) ... \det(D_M) \qquad (2.2 - 4)$$

where D_i is a (2 × 2) i-th sample transformation matrix , associated with the Jacobian, defined as:

$$D_i = \begin{bmatrix} \dfrac{\partial I_i}{\partial A_i} & \dfrac{\partial Q_i}{\partial A_i} \\ \dfrac{\partial I_i}{\partial \varphi_i} & \dfrac{\partial Q_i}{\partial \varphi_i} \end{bmatrix} = \begin{bmatrix} \cos\varphi_i & \sin\varphi_i \\ -A_i \sin\varphi_i & A_i \cos\varphi_i \end{bmatrix} \qquad (2.2-5)$$

Substituting (2.2-5) and (2.2-4) in (2.2-3), one obtains:

$$p_{n_{I_1}, n_{Q_1}, \ldots, n_{I_M}, n_{Q_M}}(I_1, Q_1, \ldots, I_M, Q_M) = \frac{p(A_1, \ldots, A_M, \varphi_1, \ldots, \varphi_M)}{(A_1 A_2 \ldots A_M)} \qquad (2.2-6)$$

Now, by assuming that the phase and amplitude are statistically independent, and also each of the sample phases are uniformly distributed, equation (2.2-6) reduces to:

$$p_{n_{I_1}, n_{Q_1}, \ldots, n_{I_M}, n_{Q_M}}(I_1, Q_1, \ldots, I_M, Q_M) =$$

$$\frac{1}{(2\pi)^M} \frac{p(\sqrt{I_1^2 + Q_1^2}, \ldots, \sqrt{I_M^2 + Q_M^2})}{\prod_{i=1}^{M} \sqrt{I_i^2 + Q_i^2}} \qquad (2.2-7)$$

This form of the joint density is a function of the amplitudes of the measured samples only. Naturally, the next step is to find a model for the numerator of equation (2.2-7): the joint multivariate amplitude density function.

In general, there is no single best method to characterize a multivariate non-Gaussian distribution. There exist several techniques that each have their own advantages and drawbacks. A first approach is to employ the multivariate

Gaussian density function as a basic model of multivariate density. This is mathematically tractable. However, it can be a very poor model if the conditions of the Central Limit Theorem are not satisfied.

A second approach is to replace the argument of a univariate density function with the square root of a quadratic form. This produces the so-called " elliptically symmetric " density [19], denoted as:

$$p(\underline{x}) = kg(Q(x)) \qquad (2.2-8)$$

where k is a constant, g(.) is a univariate density, and Q(x) is a quadratic function of $\underline{x}$. As an example, consider a bivariate, elliptically symmetric density, $f(\underline{z})$, whose marginal density f(x) is Laplacian:

$$f(x) = \frac{1}{\sqrt{2\sigma^2}} e^{-\sqrt{2}\frac{|x|}{\sigma}} \qquad (2.2-9a)$$

with bivariate density:

$$f(\underline{z}) = \frac{1}{\pi |R|^{\frac{1}{2}}} K_0(\sqrt{2\underline{z}^T \underline{R}^{-1} \underline{z}}) \qquad (2.2-9b)$$

where $\underline{z} = [x \ y]^T$, $|\underline{R}| = \sigma^2(1-\rho^2)$ is the determinant of the covariance matrix, with ρ as the correlation coefficient, and K_0 is the Modified Bessel Function of

Second Kind and order zero. This method is also mathematicaly tractable, but the dependence (correlation) structure may not be well preserved.

The third approach is to use Gram-Charlier multivariate series expansion [20,21]. However, in this approach, the choice of the proper basis function is not well-resolved. Moreover, the number of coefficients in the series increases as $O(m^2)$ [17], and the expansion requires cross-moments estimates. Also, due to truncation of the series, the tail regions of the density function may not be well represented (this issue is the same as the Gaussian-Sum approach to univariate density approximation).

The approach that will be pursued here is the so-called " Transformation Noise " model. This model, in the multivariate setting, is the extension of the method for generation of desired univariate density function by non-linear transformation of known densities [22]. In the multivariate case, the non-linearity requires memory. However, if one restricts the non-linearity to be " invertible and memoryless, " then a computationally tractable procedure results. This type of modeling was proposed by Liu [23] for modeling and used by Martinez, et al.[17] for detection.

The modeling problem can be stated formally as: given a known multivariate density function at the input, a Zero Memory Non-Linearity (ZMNL) can be chosen such that, at the output, the multivariate density function has the desired marginal density. This is depicted in Figure(2), where $p(x_1, x_2, ..., x_M)$ is a known multivariate density whose marginal distribution $p_x(x_i)$ are known, $g^{-1}(.)$ is a specific invertible ZMNL (i.e. $g(.)$ exist), and $p(n_1, n_2, ..., n_M)$ is the output

multivariate density with the desired marginal $p_n(n_i)$. The matrices, $\underline{R}_x$ and $\underline{R}_n$ denote the correlation structures of the input and output samples respectively.

In practice, the available information is the correlation structure of the output $\underline{R}_n$ and the marginal density $p_n(n_i)$. In order to characterize the clutter model, first the ZMNL associated with Figure (2) should be specified. Since, the nonlinearity is memoryless this can be found by equating the marginal cumulative distribution functions of input and output as follows:

$$Prob\left[x_i \leq x\right] = Prob\left[n_i \leq g^{-1}(x)\right] \qquad (2.2-10)$$

or equivalently:

$$Prob\left[x_i \leq g(x)\right] = Prob\left[n_i \leq x\right] \qquad (2.2-11)$$

and by definition of the distribution function, (2.2-11) reduces to :

$$F_{x_i}(g(x)) = F_{n_i}(x) \qquad (2.2-12)$$

Since, x_i is Gaussian, $F_{x_i}(g(x))$ is obtained by Error Function as:

$$\Phi[g(x)] = F_{x_i}(g(x)) = \int_{-\infty}^{g(x)} \frac{1}{\sqrt{2\pi}} e^{-\frac{u^2}{2}} du \qquad (2.2-13)$$

Thus:

$$g(x) = \Phi^{-1}\left[F_{n_i}(x) \right] \qquad (2.2-14a)$$

This is the inverse of the required ZMNL which will be used in the computation of the joint density function. To find ZMNL, one can observe from (2.2-12) that:

$$g^{-1}(x) = F_{n_i}^{-1}\left[F_{x_i}(x) \right] \qquad (2.2-14b)$$

Now, referring to Figure(2), due to the imposed invertibility condition on $g^{-1}(.)$, one can observe:

$$\begin{aligned} x_1 &= g(n_1) \\ x_2 &= g(n_2) \qquad (2.2-15) \\ &\cdots \quad \cdots \\ x_M &= g(n_M) \end{aligned}$$

Using the Jacobian of the transformation, one can formally write:

$$p_{NG}(n_1, n_2, ..., n_M) = \frac{P_G[g(n_1), g(n_2), ..., g(n_M)]}{|J(x_1, x_2, ..., x_M)|} \qquad (2.2-16)$$

where J, the Jacobian, can easily be shown to be:

$$J(x_1, x_2, ..., x_M) = \frac{1}{\prod_{i=0}^{M} g'(n_i)} \qquad (2.2 - 17)$$

Thus, the multivariate non-Gaussian output density can be written as:

$$p_{NG}(n_1, n_2, ..., n_M) = p_G[\, g(n_1), g(n_2), ..., g(n_M)\,] \left| \prod_{i=0}^{M} g'(n_i) \right| \qquad (2.2 - 18)$$

where $p_G[\, g(n_1), g(n_2), ..., g(n_M)\,]$ is the multivariate Gaussian input density with zero mean vector, covariance structure of $\underline{R}_x$, and $g'(n_i)$ is the derivative of $g(n_i)$ that is obtainable from (2.2-14) as follows:

$$g'(n_i) = \frac{p_{NG}(n_i)}{p_G(g(n_i))} \qquad (2.2 - 19)$$

where $p_{NG}(n_i)$ is the marginal non-Gaussian density function at the output of the non-linearity $g^{-1}(.)$, and $p_G(.)$ is the marginal (Gaussian) density at the input.

Next, the characterization of $\underline{R}_x$, the correlation structure of the multivariate Gaussian density is required. In order to find $\underline{R}_x$ from $\underline{R}_n$, the correlation mapping described in [22], or the Hermite polynomial expansion method of [23] can be applied. In the latter approach, the problem reduces to the solution of the

non-linear equations involving the normalized correlation sequence of the input and output correlation sequence, given by:

$$R_n(m) = \sum_{k=0}^{\infty} d_k^2 \left[\rho_x(m)\right]^k \qquad (2.2-20)$$

where

$$d_k^2 = \frac{1}{k!}\left[\int_{-\infty}^{+\infty} g^{-1}(x)\, H_k\left(\frac{x}{\sigma_x}\right) \frac{e^{-\frac{x^2}{2\sigma_x^2}}}{\sqrt{2\pi}\,\sigma_x} dx\right]^2 \qquad (2.2-21)$$

and

$$g^{-1}(x) = \sum_{k=0}^{\infty} \left(\frac{d_k}{\sqrt{k!}}\right) H_k\left(\frac{x}{\sigma_x}\right) \qquad (2.2-22)$$

Solution of equation (2.2-20) for $\rho_x(m)$, given $R_n(m)$, completely determines $\underline{R}_x$.

Now, if $\underline{x}$ has a multivariate Gaussian distribution $N(0,\underline{R}_x)$, the transformation noise can be modeled as shown in Figure(3). It is well known that any correlation matrix can be factorized into a unique lower triangular matrix $\underline{L}$ by the Cholesky decomposition algorithm as:

$$\underline{R} = \underline{L}\ \underline{L}^T \qquad (2.2-23)$$

Thus, if $\underline{R}_x$ is known, then the multivariate Gaussian density $N(0,\underline{R}_x)$ can be generated by linear transformation of a Gaussian vector $\underline{z}$, whose components are N(0,1) independent and identically distributed random variables.

In summary, equations (2.2-18), (2.2-19), and (2.2-20) completely specify the multivariate non-Gaussian Model (I). These three equations approximate a multivariate non-Gaussian density by a priori knowledge of only the marginal density and correlation structure. Approximation of a multivariate non-Gaussian density by its first-order density and correlation structure is the second major assumption of this dissertation.

Using this model, the numerator of equation (2.2-7) can now be expressed as:

$$p(\sqrt{I_1^2 + Q_1^2}, ..., \sqrt{I_M^2 + Q_M^2}) =$$

$$p_G[\, g(\sqrt{I_1^2 + Q_1^2}), ..., g(\sqrt{I_M^2 + Q_M^2})\,] \; \Big| \prod_{i=0}^{M} g'(\sqrt{I_i^2 + Q_i^2}) \Big| \qquad (2.2-24)$$

Equation (2.2-24) will be used extensively in Chapter III, in the design of optimum detectors. In the next section, another model for characterization of complex multivariate non-Gaussian clutter is developed.

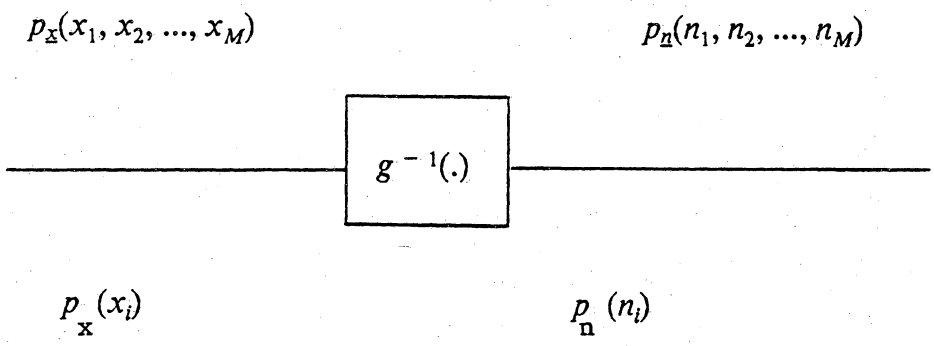

Figure 2. Transformation Noise Model

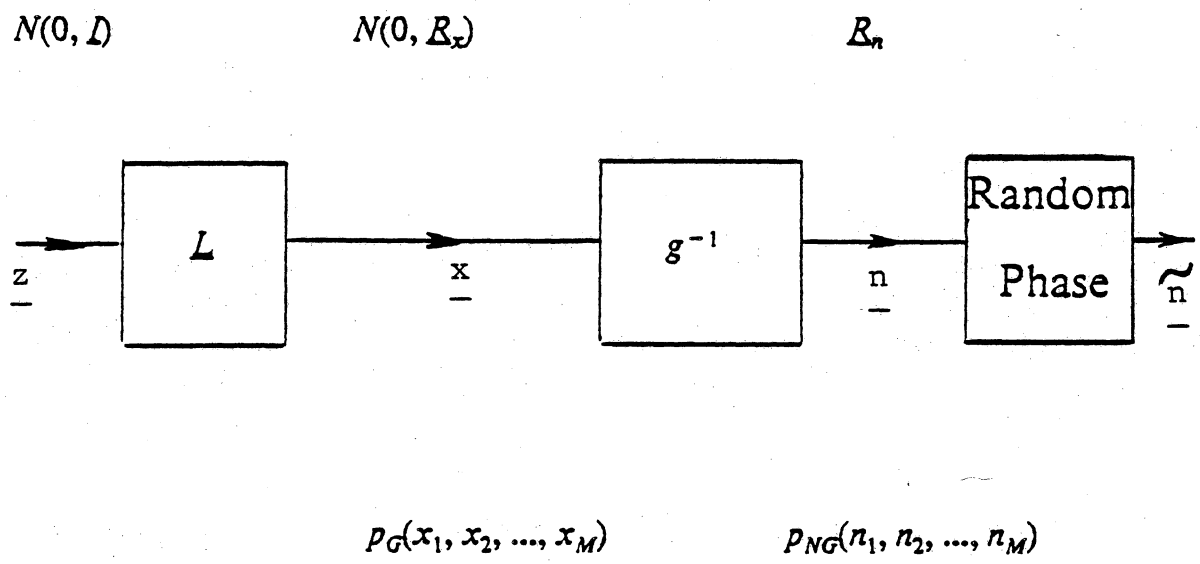

Figure 3. Gaussian Transformation Noise Model (I)

2.3. Multivariate Non-Gaussian Density Model (II)

In this section, the second model (approximation) to the complex multivariate non-Gaussian clutter density is presented. The problem is modeling of the density of the narrow-band noise process: $p_{n_{I_1}, n_{Q_1}, ..., n_{I_M}, n_{Q_M}}(I_1, Q_1, ..., I_M, Q_M)$.

The given information for characterizing Model (II) are the first-order in-phase and quadrature phase density and the complex correlation structure of the non-Gaussian clutter (noise). The block diagram of this model is illustrated in Figure (4). In this model, the in-phase and quadrature phase components are modelled separately. First, the in-phase and quadrature phase components of the complex non-Gaussian variables are modelled as Zero Memory Non-Linear (ZMNL) transformation of two distinct Gaussian variables. Formally, the input and output of ZMNL are related by their marginal cumulative distribution function. Thus the required non-linearities are characterized by:

$$g_I^{-1}(.) = F_{n_I}^{-1}[F_{x_I}(.)] \qquad (2.3-1)$$

and

$$g_Q^{-1}(.) = F_{n_Q}^{-1}[F_{x_Q}(.)] \qquad (2.3-2)$$

By the Jacobian of transformation, it can be shown that the multivariate input and output densities of the ZMNL are related by:

$$P_{\underline{N}_I}(n_{I_1}, n_{I_2}, \ldots, n_{I_M}) = P_{\underline{X}_I}[g_I(n_{I_1}), \ldots, g_I(n_{I_M})] \mid \prod_{i=1}^{M} g'_I(n_{I_i}) \mid$$

(2.3 − 3)

$$P_{\underline{N}_Q}(n_{Q_1}, n_{Q_2}, \ldots, n_{Q_M}) = P_{\underline{X}_Q}[g_Q(n_{Q_1}), \ldots, g_Q(n_{Q_M})] \mid \prod_{i=1}^{M} g'_Q(n_{Q_i}) \mid$$

(2.3 − 4)

where $P_{\underline{X}_I}$ and $P_{\underline{X}_Q}$ are the multivariate Gaussian densities, characterized by:

$$P_{\underline{X}_I} = P_G(\underline{0}, R_{\underline{X}_I}) \qquad (2.3 - 5)$$

$$P_{\underline{X}_Q} = P_G(\underline{0}, R_{\underline{X}_Q}) \qquad (2.3 - 6)$$

where $(\underline{0})$ is the mean of the multivariate density function with $R_{\underline{X}_I}$ and $R_{\underline{X}_Q}$ as the I-phase and Q-phase correlation structures. Consequently, the joint in-phase and quadrature phase density of the non-Gaussian clutter can be expressed as:

$$P_{\underline{N}}(n_{I_1}, n_{Q_1}, \ldots, n_{I_M}, n_{Q_M}) =$$

$$P_{\underline{X}}[g_I(n_{I_1}), g_Q(n_{Q_1}) \ldots, g_I(n_{I_M}), g_Q(n_{Q_M})] \mid \prod_{i=1}^{M} g'_I(n_{I_i})\, g'_Q(n_{Q_i}) \mid$$

(2.3 − 7)

with

$$P_{\underline{X}} = P_G(\underline{0}, \tilde{\underline{R}}) \qquad (2.3-8)$$

Next, in order to complete the information requirements of equation (2.3-7), the complex Gaussian correlation structure associated with (2.3-8) should be specified. This correlation structure is related to the desired non-Gaussian correlation structure by correlation mapping, described in [23], as:

$$(R_{\underline{X}_I})_{ij} = \sum_{k=0}^{\infty} [(\rho_{ij})_{\underline{n}_I}]^k \, b_{k_I}^2 \qquad (2.3-9)$$

$$(R_{\underline{X}_Q})_{ij} = \sum_{k=0}^{\infty} [(\rho_{ij})_{\underline{n}_Q}]^k \, b_{k_Q}^2 \qquad (2.3-10)$$

$$(R_{\underline{X}_I \underline{X}_Q})_{ij} = \sum_{k=0}^{\infty} [(\rho_{ij})_{\underline{n}_I \underline{n}_Q}]^n \, b_{k_I} \, b_{k_Q} \qquad (2.3-11)$$

where the correlation coefficient, ρ, is defined as:

$$\rho_{ij}(.) = \frac{R_{ij}(.)}{\sigma^2} \qquad (2.3-12)$$

and the constants b_k are the coefficients of the Hermite Polynomial expansion of the ZMNL as:

$$g^{-1}(x) = \sum_{k=0}^{\infty} \frac{1}{\sqrt{k!}} b_k \, H_k(\frac{x}{\sigma_x}) \qquad (2.3-13)$$

and

$$b_k = \frac{1}{\sqrt{2\pi k!}\,\sigma_x} \int_{-\infty}^{+\infty} g^{-1}(x)\, \exp\left(-\frac{x^2}{2\sigma_x^2}\right)\, H_k\left(\frac{x}{\sigma_x}\right)\, dx \qquad (2.3-14)$$

Solution of the non-linear equations, given by (2.3-9) through (2.3-11), specify the correlation structure of the Gaussian density. Thus, the characterization of complex multivariate non-Gaussian density, given by (2.3-7) is complete.

Since, the marginal density function $p_{NG}(n_i) = f(\sqrt{I_i^2 + Q_i^2})$ is essential in the determination of the non-linearity $g(x)$, the next section will briefly discuss such non-Gaussian marginal densities, associated with sea clutter. Also, clutter generation techniques will be reviewed.

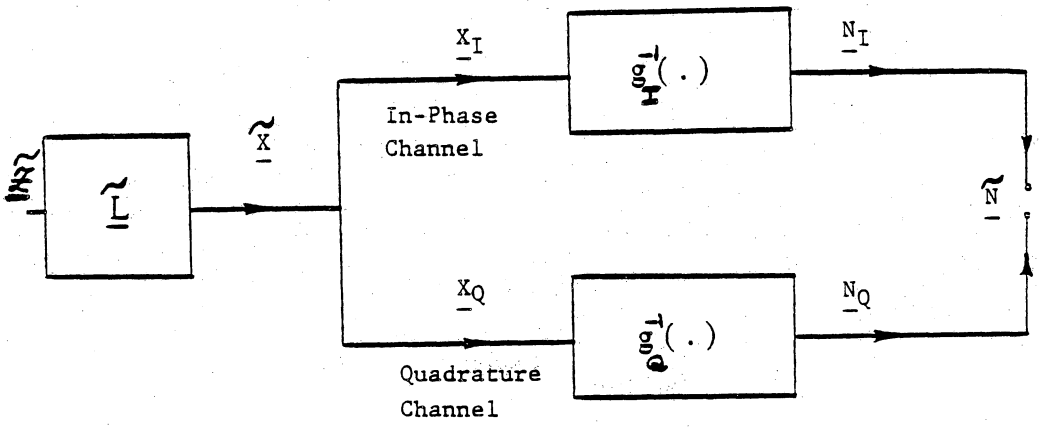

Figure 4. Complex Gaussian Transformation Noise Model (II)

2.4. Sea Clutter Characteristics

This section is devoted to a brief discussion on sea-clutter characteristics. Since the earliest days of radar, detection of desired targets has been complicated due to masking of the target echo by "clutter" (undesirable echo). Example of unwanted echoes are numerous: chaff, land, sea, rain, snow, clouds, birds, atmospheric turbulences, ionized media, etc. Generally, clutters have spatial and temporal distributions, and can be homogeneous or non-homogeneous. Echoes from land or sea are known as "surface" clutter, and those from the atmospheric phenomena are called "volume" clutter [24].

The mechanism of sea clutter generation and its characteristics have been under investigation since the earliest stages of radar development. Sea clutter is a very complex phenomenon. It is dependent on various parameters such as: depression angle(angle below horizontal at which sea is viewed), polarization of the incident wave, frequency and pulse-width of the radar, state of the sea(according to World Meteorological Organization, there are nine sea states), speed and direction of the wind, existence of white-caps on the waves, and surface area under illumination.

To develop a unified theory to take into consideration all the dependent parameters is very complicated, if not impossible. This fact has been the major reason for the radar system engineers to rely on experimentation and data collection for some of their design parameters.

In 1957, Katzin [25] presented a theory on the mechanism of radar sea clutter. In his development, the scatterers were assumed to be the small patches or "facets" of the sea surface, and their reflection characteristics with respect to depression angle and the frequency of radar were described. He also explained the appearance of "spikes" at small depression angles. Assuming that the scattered fields from various facets were completely random, he concluded that the most efficient reflective facets are in the order of wavelength.

In 1970, Guinard, et al.[26] presented a theory based on the concept of "composite surface", where a rough scattering surface was assumed to be superimposed on a larger surface structure. Also, in 1970, Trunk, et al.[27] used the measurements of high-resolution X-band radar, with low grazing angle, to conclude that the clutter cross-section was Non-Rayleigh. They proposed Log-Normal and Contaminated-Normal(heavier tail than Gaussian) distributions. Their experimental results showed that with horizontal polarization, the tail had larger value, that is more spikes were present.

Later, in 1976, Jakeman, et al.[28] developed a model for Non-Rayleigh microwave sea echo. They considered the spatial and temporal probability distribution of the envelope of the returned signal, and introduced the "K-distribution", a class of Modified Bessel functions.

In 1977, Fay, et al.[29] applied Weibull distribution to amplitude density function of sea-echo. Later, in 1981, Ward [30] proposed a model with compound distribution: one with a large correlation time and Chi-distributed, and the other Rayleigh, which led the overall amplitude to be K-distributed.

In 1981, Glaser, et al.[31] reported the results of an extensive measurement that took place between 1979 and 1980 by Boeing Company. Approximately, **two billion** range-gate amplitude were recorded under different sea state conditions and wind-speeds. They concluded that the Weibull distribution for amplitude distribution best fits their data. The radar was S-band with horizontal polarization.

In 1982, Maaloe [32] reported the results of X-band radar measurements at low grazing angle with horizontal polarization. The data indicated that at close ranges for radar, the Weibull distribution fits the best, and at large range the log-Normal is more representative for amplitude distributions.

There are numerous other reports on sea-clutter measurements and modeling. Although, the purpose of all the experiments were to determine the statistics of the sea-clutter, one should note that they were performed under various radar systems and sea-state conditions. From the above discussion, three important conclusions can be drawn:

1) clutter statistics are not Gaussian; thus, the detection schemes under Gaussian assumptions are not only sub-optimum, but also increase the false alarm rate,

2) no single Non-Gaussian model accurately describes the possible variety of clutter types under different sea-state conditions,

3) for optimum system performance, a sea clutter model should be obtained for a given radar system under its intended application.

As discussed previously, the non-Rayleigh measurement of amplitude distribution implies that the in-phase and quadrature phase of the noise are not samples of Gaussian processes. The measurement results indicate strongly that Log-Normal, Weibull, and K-distributed are the most agreed-upon distributions, specially for high-resolution radar. That is, they are the best fit to the spiky and infrequently high amplitude nature of the sea clutter measurements. These are the desired marginal distributions that are required for modeling of the multivariate non-Gaussian density function of section (2.1). Mathematically, they are formulated as follows:

Log-Normal:

$$p(x) = (ax\sqrt{2\pi})^{-1} \exp\left(-\frac{1}{2}\frac{(\ln(x) - m)^2}{a^2}\right) \quad x > 0 \qquad (2.4-1)$$

Weibull:

$$p(x) = \frac{c}{b}\left(\frac{x}{b}\right)^{c-1} \exp\left(-\left(\frac{x}{b}\right)^{c}\right) \quad x > 0, b > 0, c > 0 \qquad (2.4-2)$$

K-distributed:

$$p(x) = ax^{\nu}\frac{K_{\nu-1}(x)}{\Gamma(\nu)} \qquad (2.4-3)$$

where a and b are scaling parameters, m and c are shaping parameters (c=2 Weibull is identical to Rayleigh), x is $\sqrt{I^2 + Q^2}$ where I^2 and Q^2 are square of the amplitude of the in-phase and quadrature phase channels, and K is the Modified Bessel Function.

In the next section, a numerical example of modeling the multivariate non-Gaussian amplitude density function, based on the Weibull marginal density, will be presented, and an explicit expression for the non-linearity involved with Weibull density function will be derived.

2.5. Multivariate Weibull Clutter

In this section, computer simulation and numerical examples concerning the multivariate non-Gaussian density modeling, developed in Section (2.2) as Model (I), are presented. The required modeling equations are as follows:

$$R_n(m) = \sum_{k=0}^{\infty} d_k^2 \left[\rho_x(m)\right]^k \qquad (2.5-1)$$

$$p_{NG}(n_1, n_2, ..., n_M) = p_G\left[\, g(n_1), g(n_2), ..., g(n_M) \,\right] \left| \prod_{i=0}^{M} g'(n_i) \right| \qquad (2.5-2)$$

$$g'(n_i) = \frac{p_{NG}(n_i)}{p_G(g(n_i))} \qquad (2.5-3)$$

As a specific example, the marginal density, $p_{NG}(\sqrt{I_i^2 + Q_i^2}) = p_{NG}(x_i)$, at the output of the ZMNL, is chosen to be Weibull:

$$p_{NG}(x) = (\frac{\alpha}{b})(\frac{x}{b})^{\alpha-1} \exp(-(\frac{x}{b})^{\alpha}) \quad x \geq 0\,,\ b > 0\,,\ \alpha > 0 \qquad (2.5-4)$$

and for illustration, the scale parameter (b) is set to be 1. The shape parameter (α) is chosen to be in the range: ($1.4 < \alpha < 2.0$) , which is the representative of

the sea-clutter measurements [31,32]. Figure(5) illustrates the effect of (α) on the shape of density function for the range: $1.1 \leq \alpha \leq 2.0$. As a special case, when $\alpha = 2.0$, the Weibull collapses into Rayleigh density function. Also, as noticed from the Figure, with decreasing value of (α), the density has heavier tail, emphasizing the heavy-tail non-Rayleigh, and consequently, the spiky nature of the sea clutter.

The cumulative distribution function associated with (2.5-4) is:

$$F_{x_i}(x) = 1 - e^{-(\frac{x}{b})^{\alpha}} \quad x \geq 0 \qquad (2.5-5)$$

Thus, from (2.2-14b), the corresponding ZMNL can be obtained as:

$$g^{-1}(x) = F_{n_i}^{-1}(F_{x_i}(x)) = \left[\ln \left[\frac{1}{1 - F_G(x)} \right] \right]^{\frac{1}{\alpha}} \qquad (2.5-6)$$

where

$$F_G(x) = \Phi(x) = \int_{-\infty}^{x} \frac{1}{\sqrt{2\pi}} e^{-\frac{u^2}{2}} du \qquad (2.5-7)$$

Figure(6) illustrates this non-linearity for various values of (α) . As noticed, the ZMNL is nearly linear. As will be discussed in Chapter V, this property will have a practical impact in the computation of $\underline{R}_x$. Figure(7) depicts the inverse of ZMNL , g(x), which is obtained from (2.5-3).

The computation of g(x) requires special care, since the argument of the Inverse Error Function, Φ^{-1}, should be strictly greater than zero and less than one (theoretically, $g(0) = -\infty, g(\infty) = +\infty$). For practical purpose, the limits of the plot in Figure (7) gives sufficient information.

Next, for the sake of numerical simplification, it is assumed that the input normalized correlation sequence is known and has either Markov or triangular structure. That is, the sequence is of the form:

$$\rho_x(m) = (\rho)^m \quad |\rho| < 1 \qquad (2.5-8)$$

for Markov structure, and

$$\rho_x(m) = 1 - |\frac{m}{20}| \qquad |m| \leq 20 \qquad (2.5-9)$$

for triangular structure ($\rho_x(m) = 0, \quad |m| > 20$). With the ZMNL given by (2.5-6), and employing (2.2-21) and (2.2-22), one can find $R_n(m)$ from:

$$R_n(m) = \sum_{k=0}^{\infty} d_k^2 \left[\rho_x(m)\right]^k \qquad (2.5-10)$$

Figures (8) through (13) illustrate the input and output correlation sequence $R_x(m)$(Var(x) = 1) and $R_n(m)$ for specific value of $\rho = 0.9$, and α = (1.1, 1.4, 1.9) for both Markov and triangular input correlation structures. As observed from these Figures, the values of the input and output correlation sequences become approximately equal as the degree of non-Gaussianity diminishes (i.e., as α increases). This proximity is due to " piecewise or nearly " linear behaviour of the ZMNL. This result has also been verified experimentally, for various density functions, by Liu [23].

Finally, applying equations (2.2-18) and (2.2-19), one can write the bivariate non-Gaussian density function as:

$$p_{NG}(x,y) = p_G[g(x), g(y)] \; |g'(x)| \; |g'(y)| \qquad (2.5-11)$$

with

$$g'(x) = \sqrt{2\pi}\,(x)^{\alpha-1}\, e^{-x^{\alpha}}\, e^{g^2(x)} \qquad (2.5-12)$$

Figures (14) and (15) illustrate the bi-variate Weibull density function for parameters of ($\rho = 0.9, \alpha = 1.5$) and ($\rho = 0.5, \alpha = 1.5$) respectively.

In the next section, clutter generation techniques will be discussed briefly, and clutter samples will be generated for specific first-order in-phase and quadrature phase non-Gaussian density.

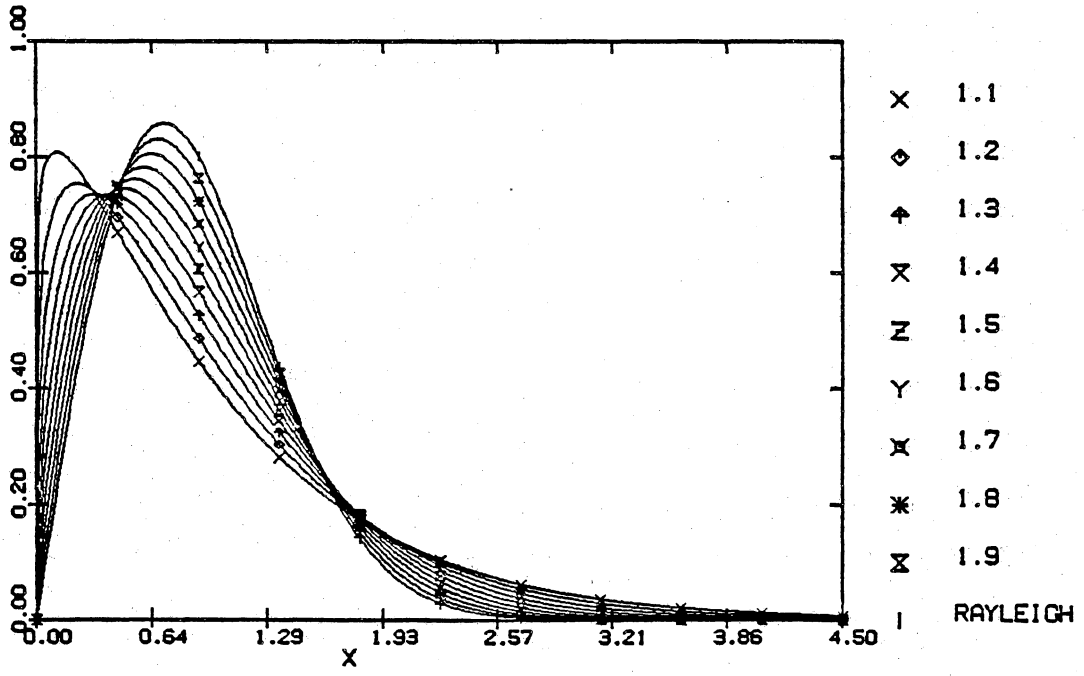

Figure 5. Weibull Density for Various Values of Density Parameter.

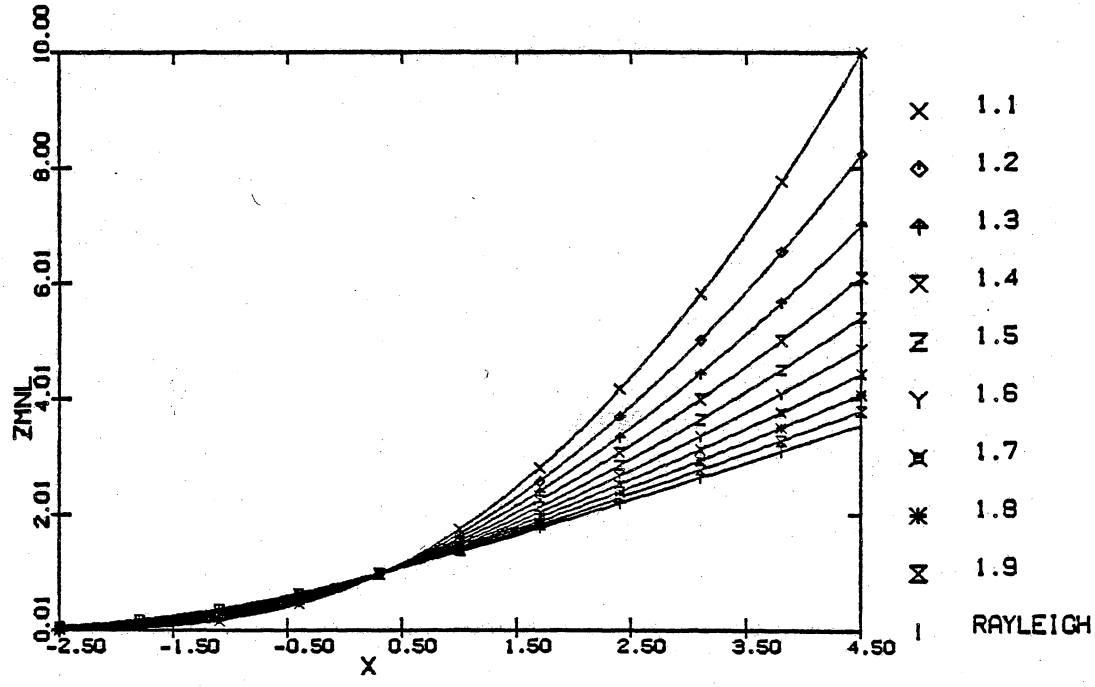

Figure 6. The Zero Memory Non-Linearity for (1.1 < α < 2.0).

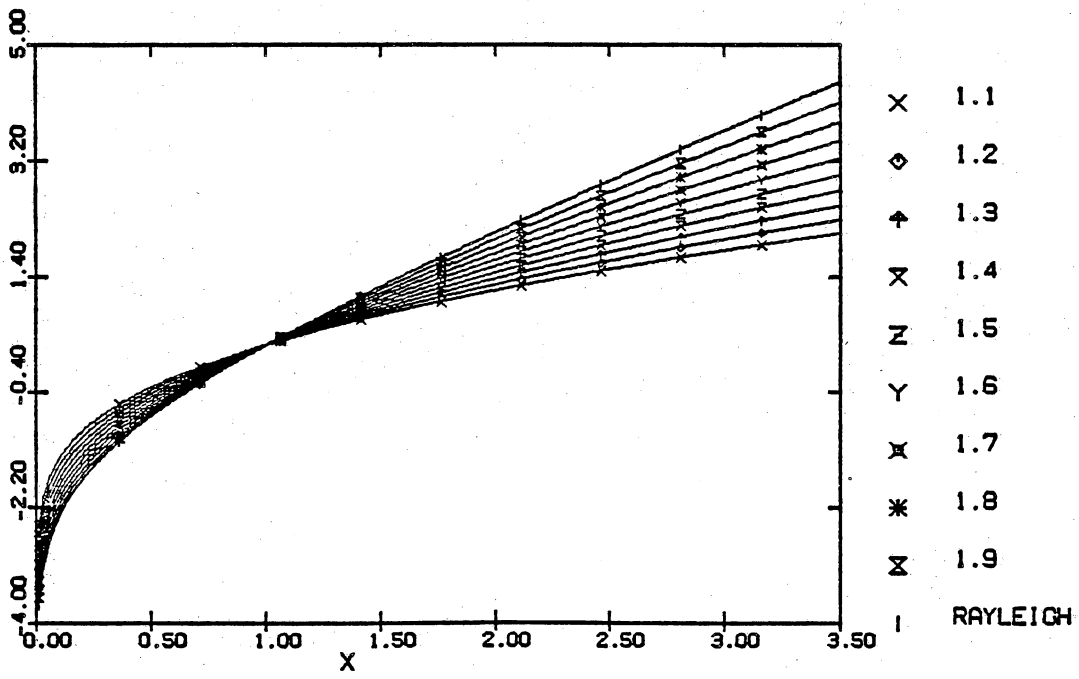

Figure 7. The Inverse of ZMNL(g(x)) for (1.1 < α < 2.0).

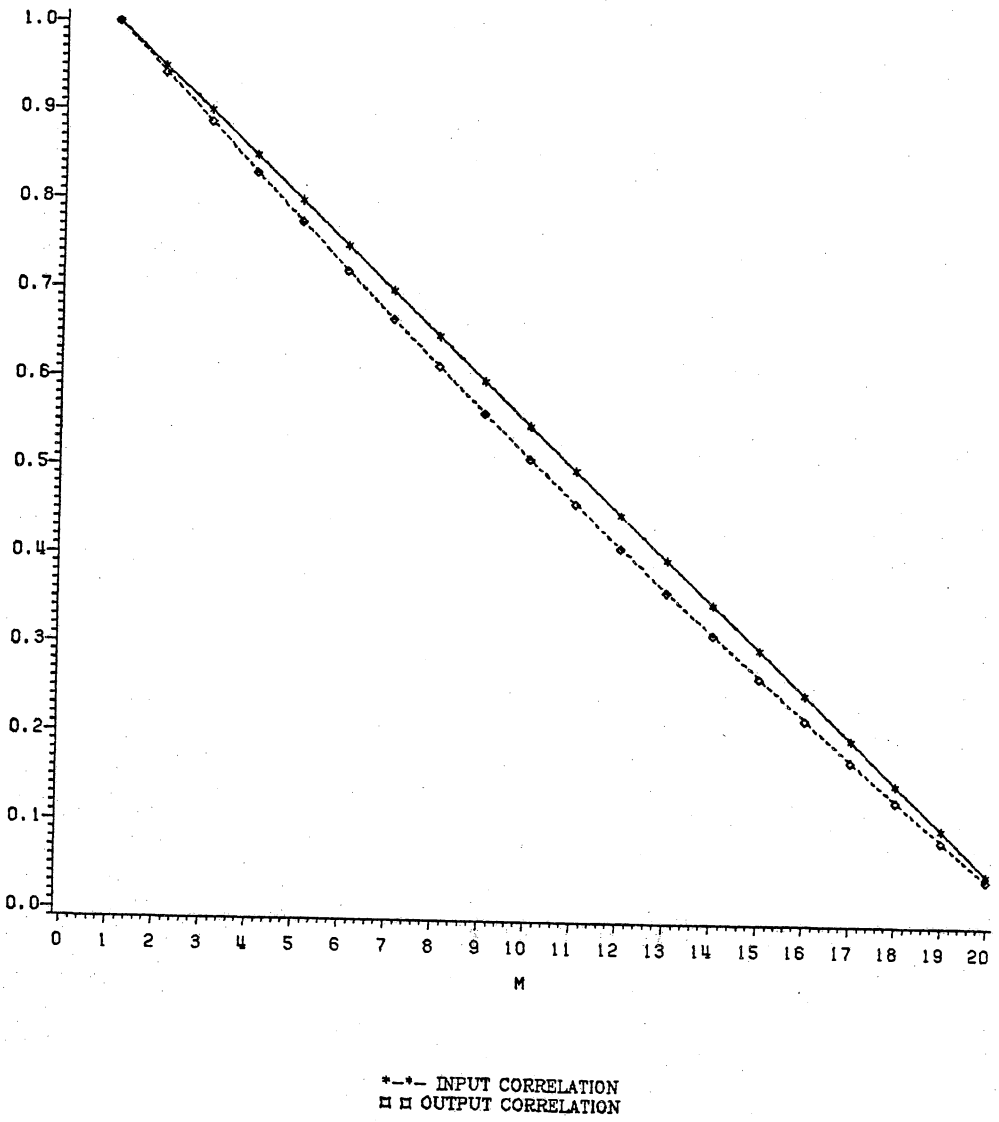

Figure 8. Input and Output Triangular Correlation Sequence ($\rho = 0.9$, $\alpha = 1.1$).

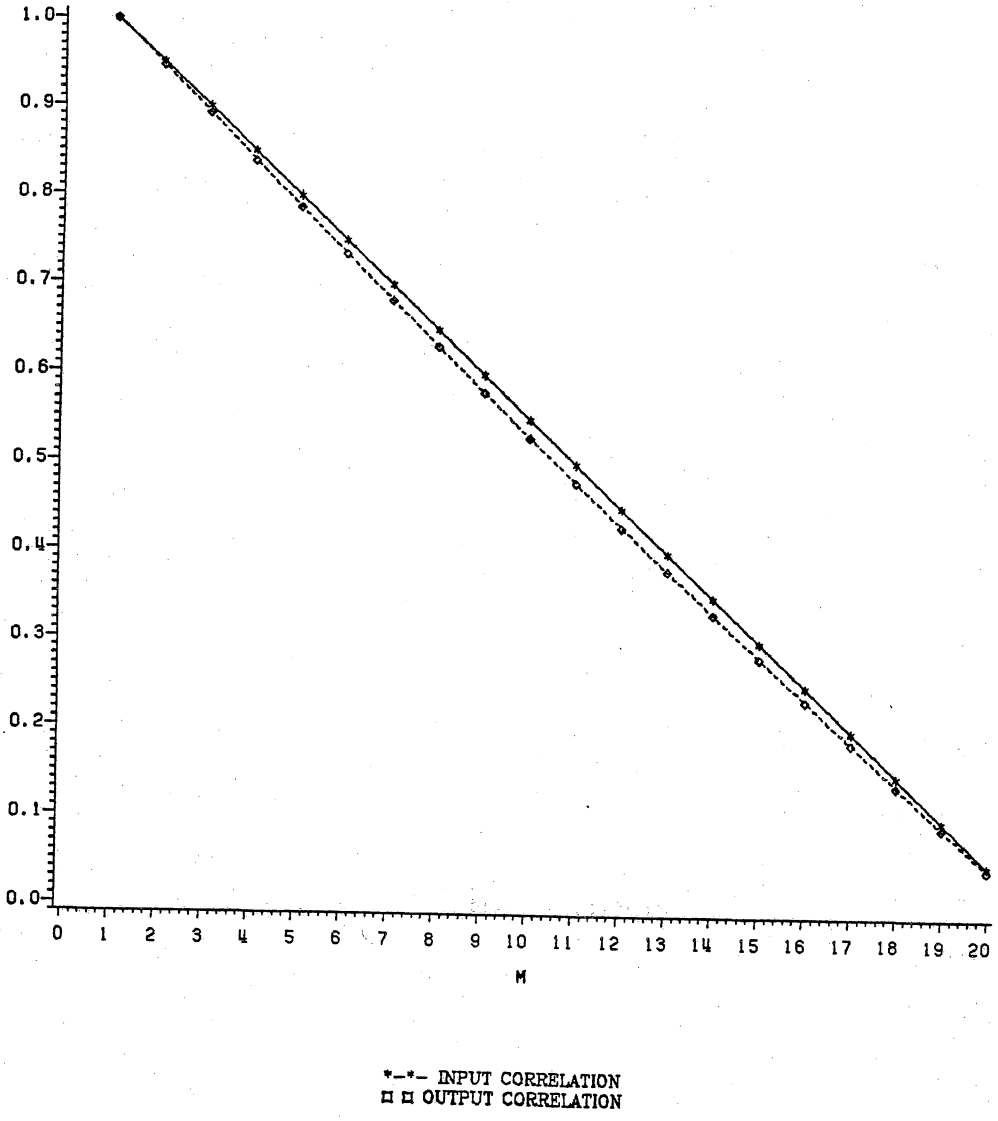

Figure 9. Input and Output Triangular Correlation Sequence ($\rho = 0.9$, $\alpha = 1.4$).

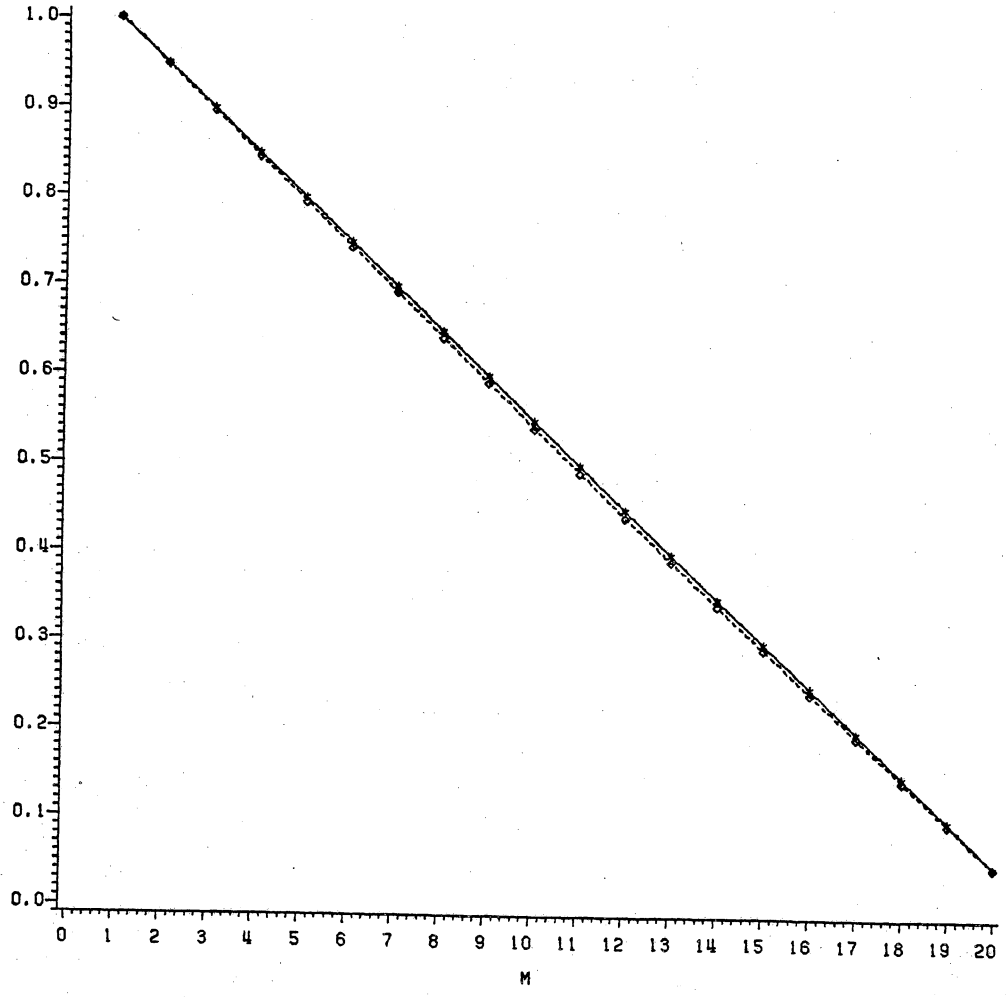

Figure 10. Input and Output Triangular Correlation Sequence ($\rho = 0.9$, $\alpha = 1.9$).

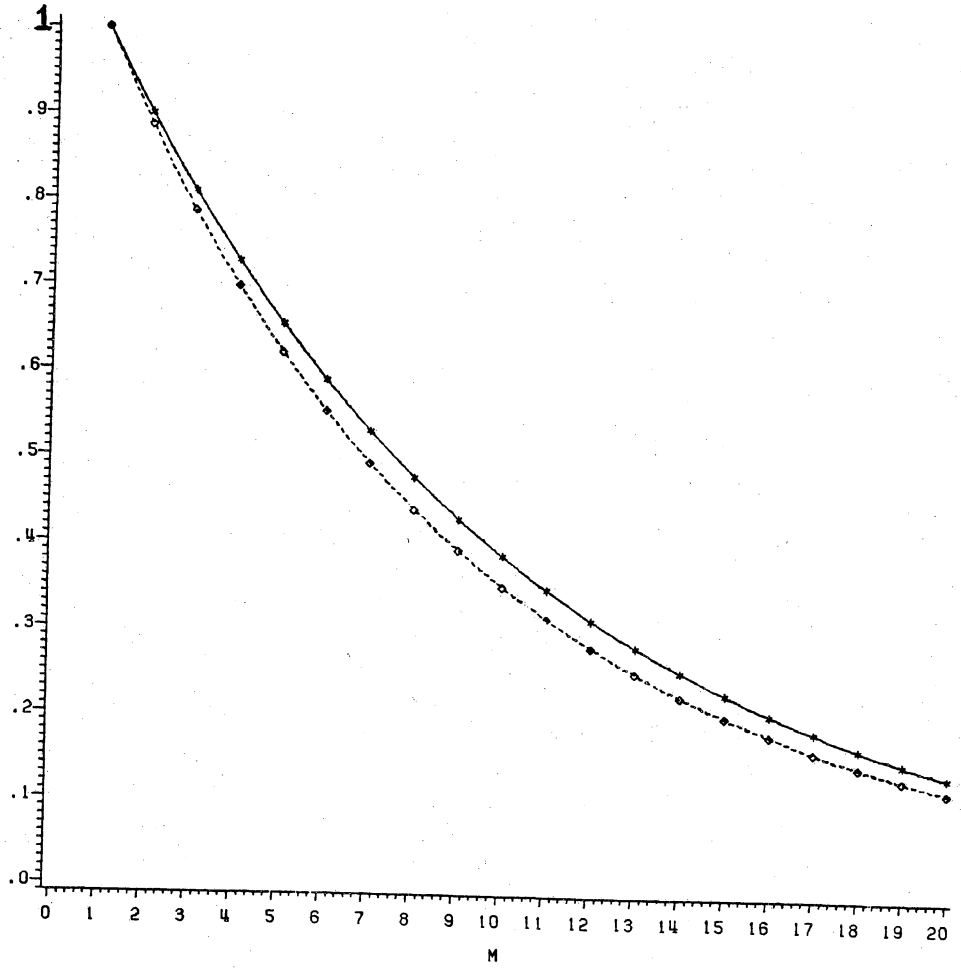

Figure 11. Input and Output Markov Correlation Sequence ($\rho = 0.9$, $\alpha = 1.1$).

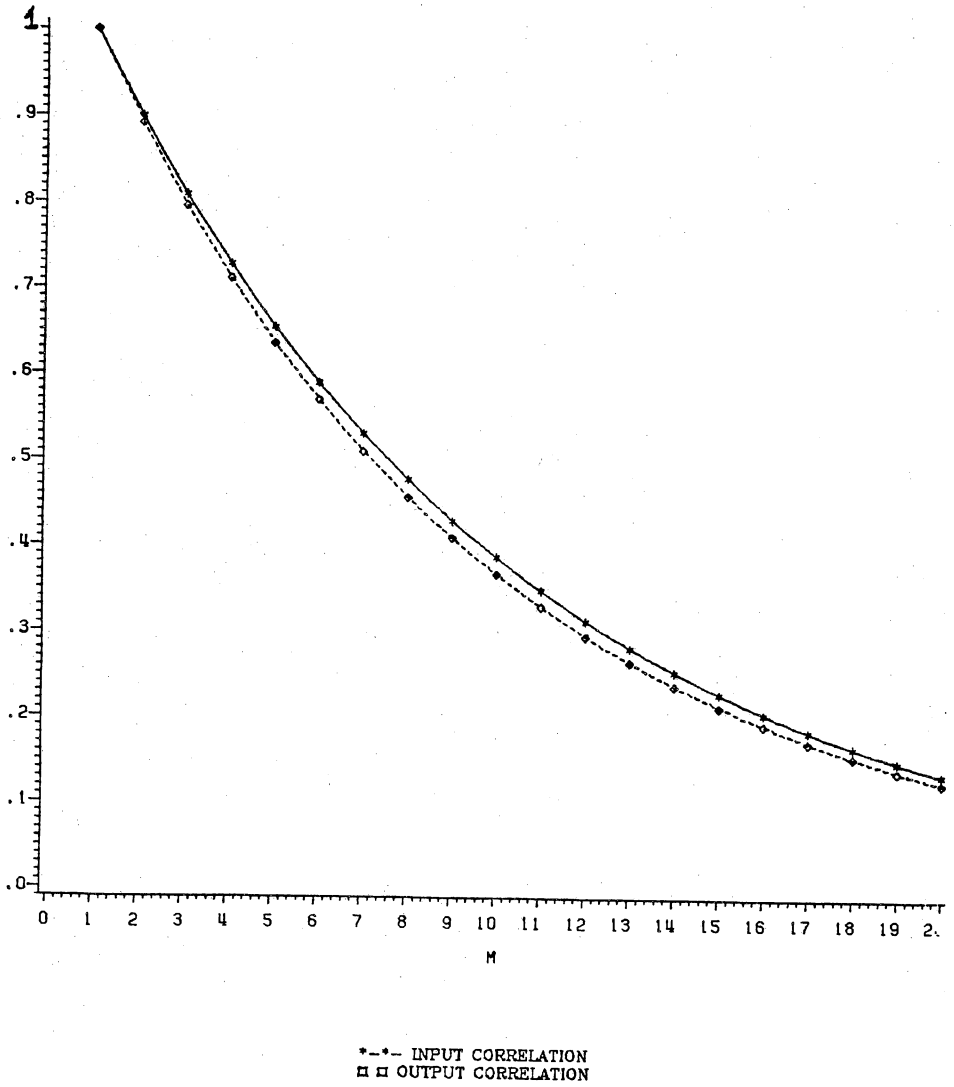

Figure 12. Input and Output Markov Correlation Sequence ($\rho = 0.9$, $\alpha = 1.4$).

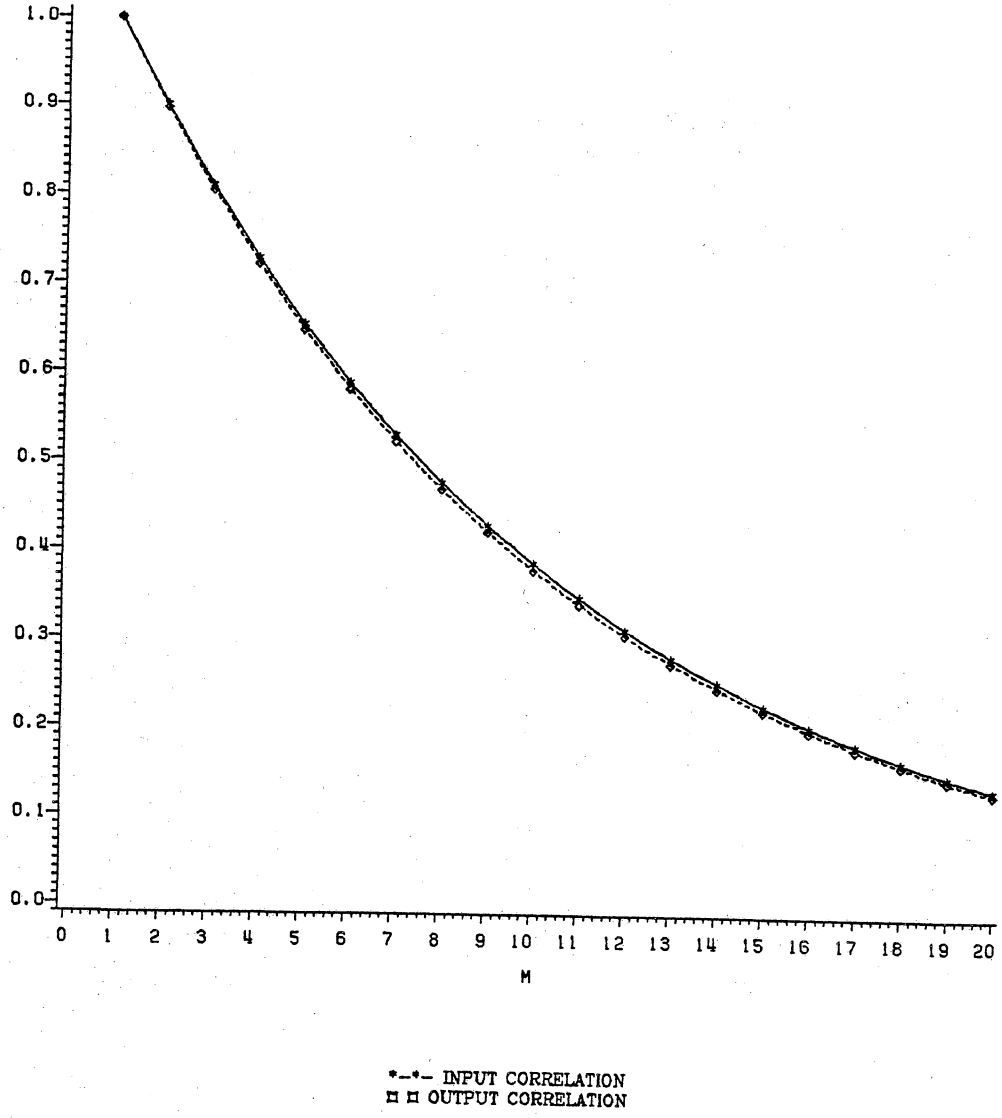

Figure 13. Input and Output Markov Correlation Sequence ($\rho = 0.9$, $\alpha = 1.9$).

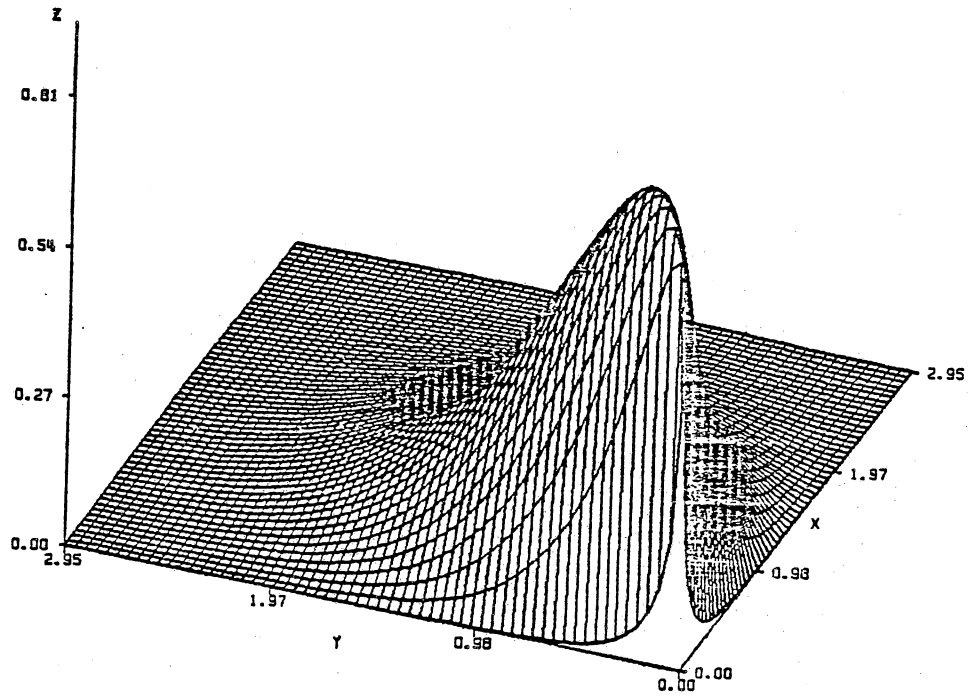

Figure 14. The Bi-variate Weibull Density Function ($\rho = 0.9$, $\alpha = 1.5$).

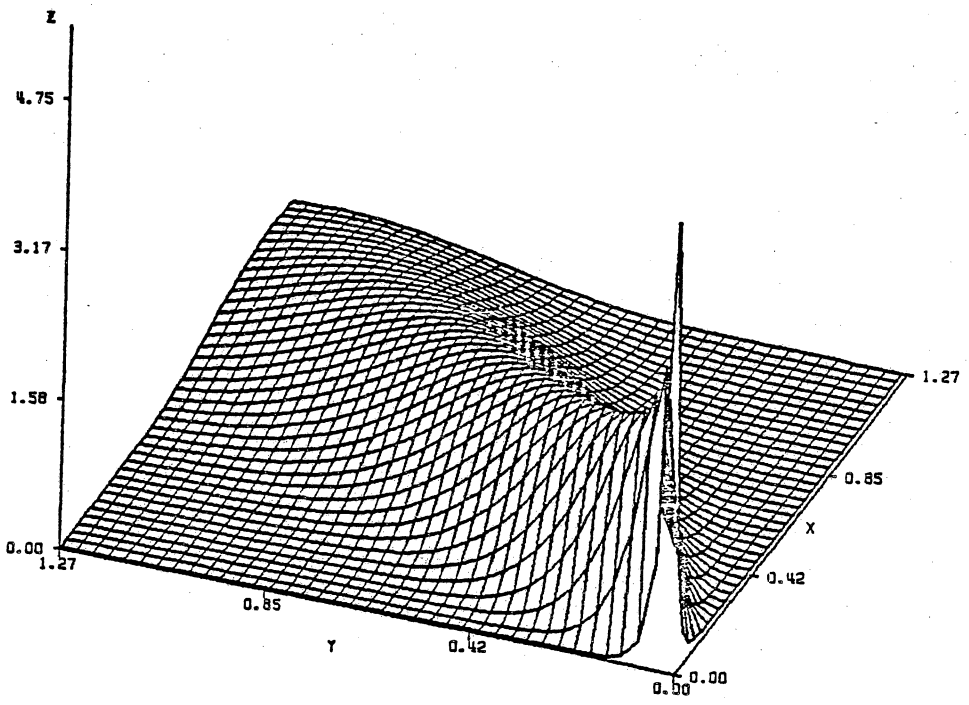

Figure 15. The Bi-variate Weibull Density Function ($\gamma = 0.5$, $\alpha = 1.5$).

2.6. Clutter Generation

This section is concerned with a brief review of clutter generation techniques, and an illustration of non-Gaussian clutter samples. The generation scheme is the numerical implementation of the complex multivariate non-Gaussian clutter Model (II).

For the purpose of clutter sample generation for simulation of radar systems, research has been continuous since the 1970's. In 1971, Peebles [33] generated correlated Log-Normal random variables, representing the amplitude of the clutter. Later, in 1976, Szjanowski [34,35] generated correlated Log-Normal and Weibull random variables possessing certain correlation structure. The model for Log-Normal samples, in both cases, was to transform a correlated Gaussian vector by an exponential non-linearity to correlated Log-Normal variables.

In the case of Weibull clutter generation [35], two independent Gaussian variables were used and the non-linearity consisted of summing the square of Gaussian amplitudes followed by taking a specific root of the sum.

In 1977, Schleher [36] generated the clutter as a vector-Markov process by introducing a dynamic model for the clutter. He also performed some experiments for Log-Normal clutter generation using the General Purpose System Identifier and Evaluator (GPSIE) program, referenced in [36].

In 1985, Farina, et al. [37,38] attempted to generalize the clutter generation model for any density function and correlation structure. This model consisted of driving a linear filter cascaded with a non-linear filter by white Gaussian noise.

However, due to structural simplicity, they only identified the Log-Normal generation model completely.

The Gaussian Transformation noise model of Figures (3) and (4), in sections (2.2) and (2.3), are general methods for clutter generation. For example, using Model (I), equations (2.2-14b) and (2.2-18) completely specify clutter generation with a specific covariance structure and marginal amplitude density function. As for Model (II), equations (2.3-1) through (2.3-7) specify complex clutter generation with given first-order in-phase, quadrature phase density, and complex correlation structure.

It should be emphasized that the validity of the multivariate non-Gaussian model depends on the solution of the mapping, expressed by (2.2-20). As mentioned in [23], not all the correlation structures can be mapped by the covariance mapping technique. This is an open problem that requires further investigation.

As an example of clutter generation, consider a complex multivariate clutter with Generalized Cauchy distribution as its first-order in-phase and quadrature phase component density. The Generalized Cauchy density function is given by:

$$p(x) = \frac{\Gamma[\nu + \frac{1}{2}]}{\sqrt{\pi}\,\beta\,\Gamma[\nu]} \; \frac{1}{\{\,1 + (\frac{x}{\beta})^2\,\}^{\nu+\frac{1}{2}}} \qquad (2.6-1)$$

With $\beta = \sqrt{2}$ and $\nu = 2$, one obtains unit variance Cauchy density (Var(x) = 1) as:

$$p(x) = \frac{3}{4\sqrt{2}} \frac{1}{\{\ 1 + (\frac{x}{\sqrt{2}})^2\ \}^{\frac{5}{2}}} \qquad (2.6-2)$$

This density is depicted in Figure (16) for comparison with unit variance Gaussian density. As observed, the tail section of the Cauchy density is heavier than Gaussian. This is one reason that this density has been cited as an example of in-phase and quadrature phase density in radar applications [11].

Suppose the input complex correlation structure is given by:

$$\underline{\tilde{R}} = 2 \begin{bmatrix} 1 & \rho + j\rho & \rho^2 + j\rho^2 & \dots & \rho^M + j\rho^M \\ \rho - j\rho & 1 & \rho + j\rho & \dots & \rho^{M-1} + j\rho^{M-1} \\ & & \dots\ \dots\ \dots\ \dots & & \\ & & \dots\ \dots\ \dots\ \dots & & \\ \rho^M - j\rho^M & \dots & \dots & \dots & \rho - j\rho\ \ 1 \end{bmatrix} \qquad (2.6-3)$$

This is the correlation structure associated with equations (2.3-7) and (2.3-8). The first step in clutter generation is to characterize the in-phase and quadrature phase ZMNL given by equations (2.3-1) and (2.3-2) for the Cauchy distribution. This non-linearity and its inverse are shown in Figures (17) and (18) respectively.

Next, applying the Hermitian Cholesky decomposition to the complex matrix $\underline{\tilde{R}}$, given by (2.3-6), one obtains the desired linear transformation associated with

the Gaussian transformation of Model (II). At this stage, all the elements of the block diagram of Figure (4) are known. Driving the system of Figure (4) by unit variance, zero mean, and (i.i.d) complex Gaussian vector results in the complex non-Gaussian vector with the desired non-Gaussian first-order density. Three 50-sample realizations of amplitude and phase are shown in Figures (19) and (20) respectively.

In the next chapter, the multivariate non-Gaussian noise Models (I) and (II) will be used in the development of Locally Optimal Detector (LOD) structures.

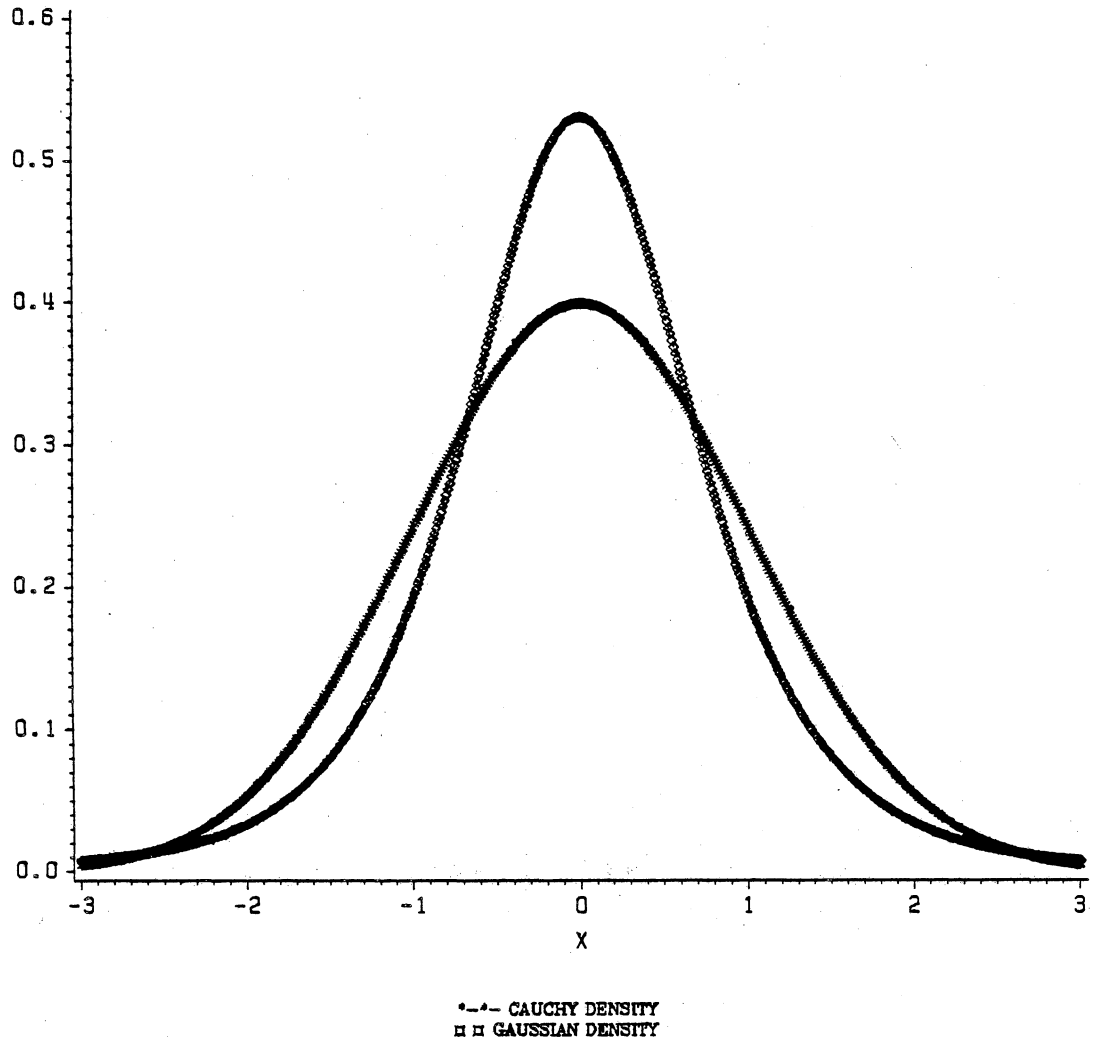

Figure 16. Unit Variance Generalized Cauchy and Gaussian Density Functions.

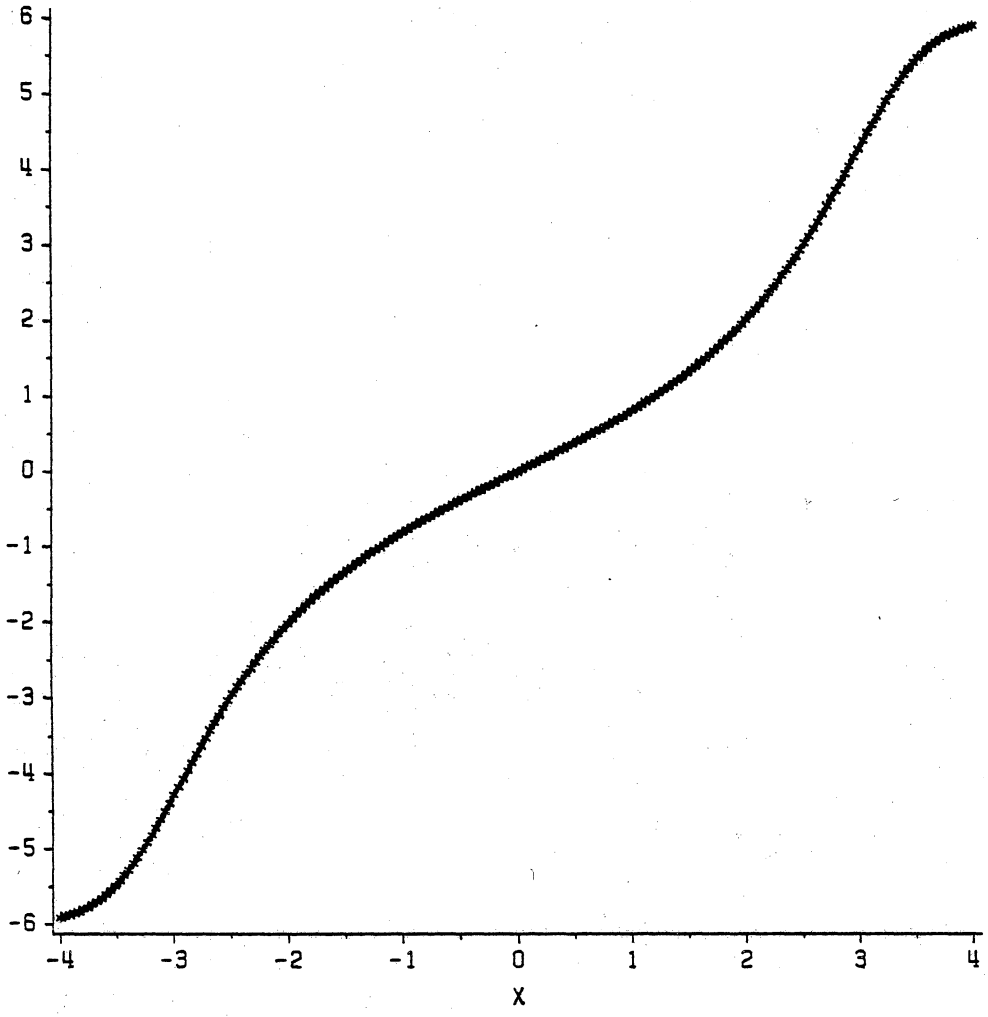

Figure 17. ZMNL associated with Unit Variance Generalized Cauchy Density.

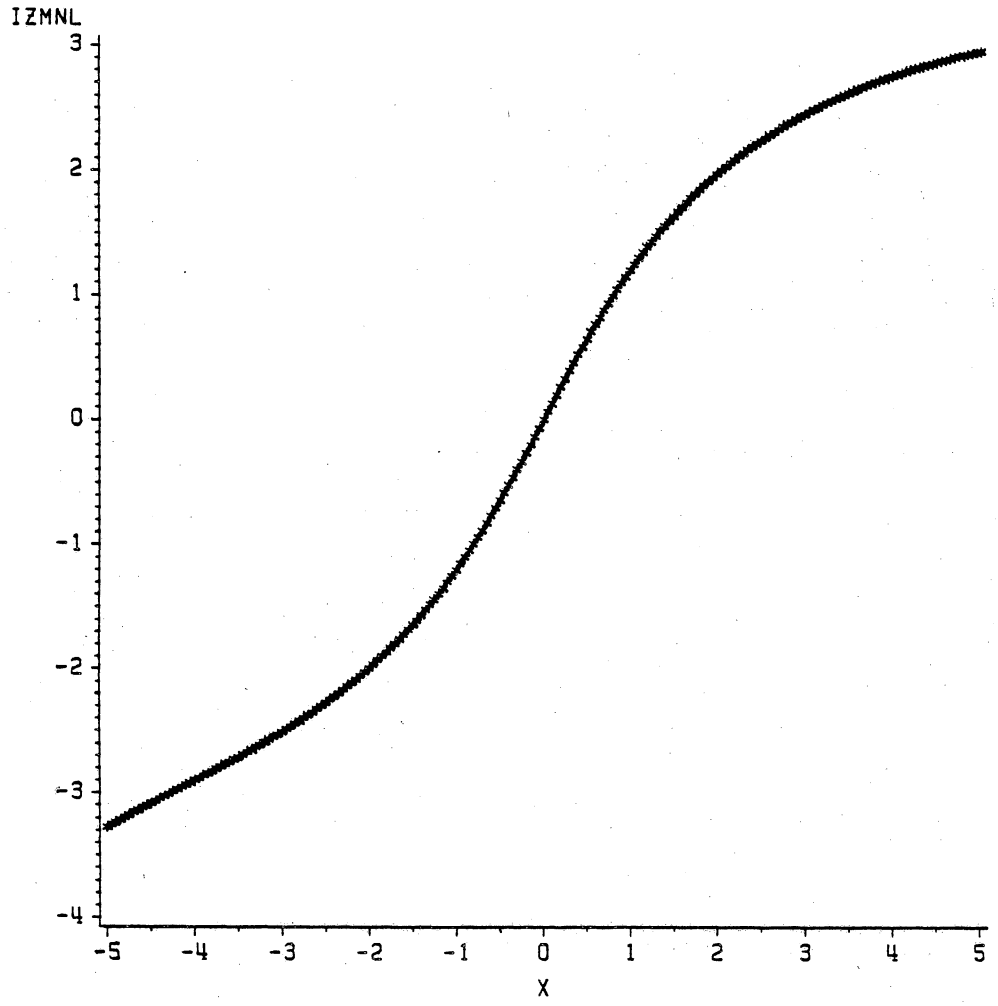

Figure 18. Inverse ZMNL associated with Unit Variance Generalized Cauchy Density.

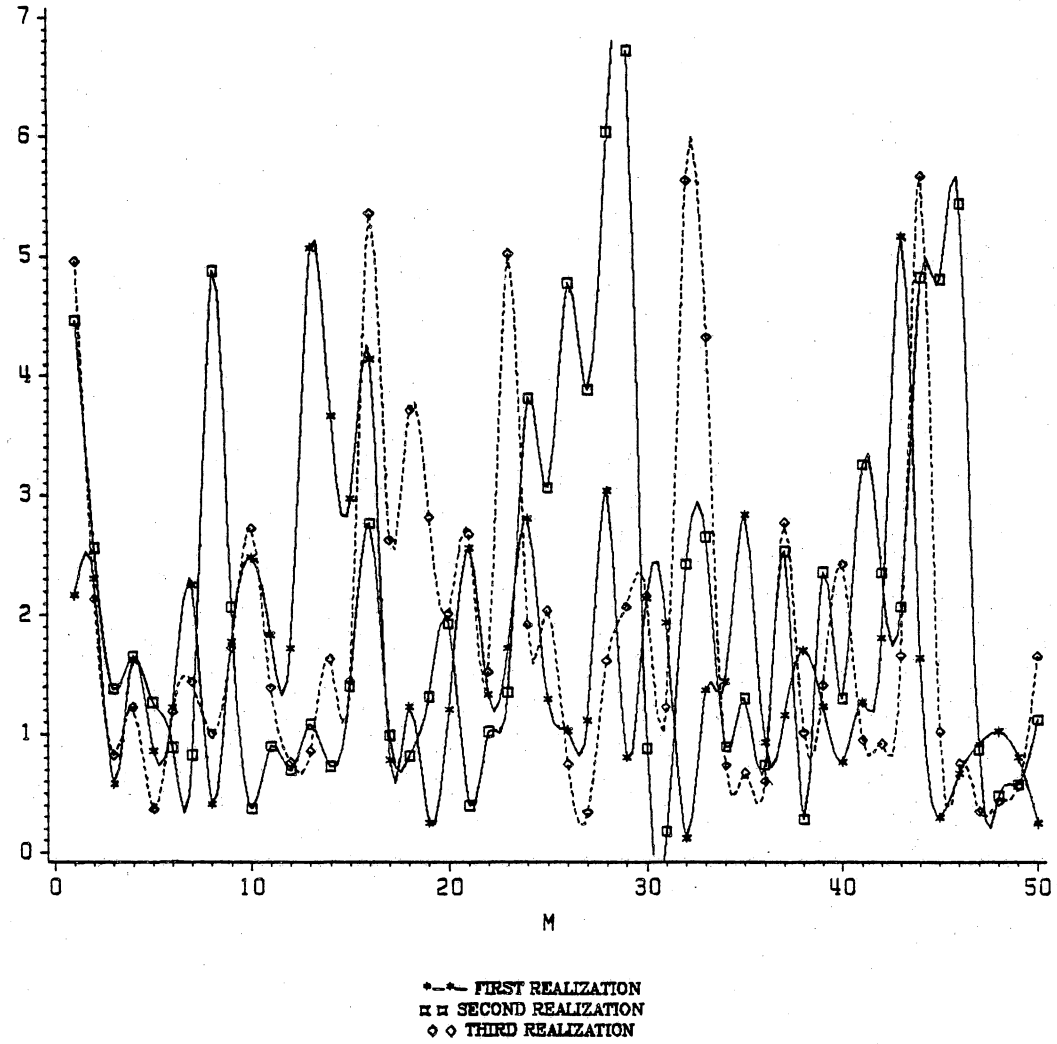

Figure 19. 50-Sample Amplitude Realizations of a Non-Gaussian Clutter.

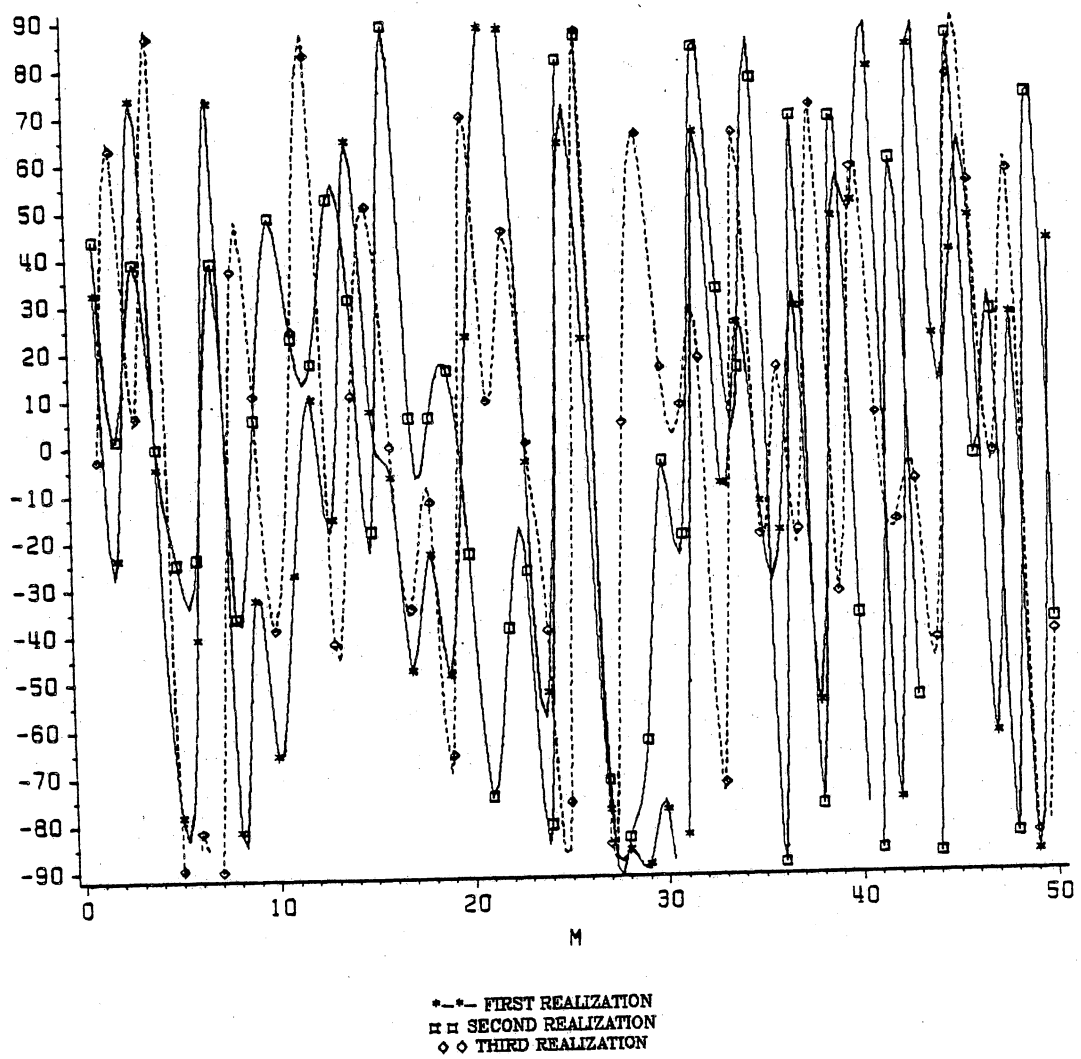

Figure 20. 50-Sample Phase Realizations of a Non-Gaussian Clutter.

III. Locally Optimum Detection in Multivariate Non-Gaussian Noise

3.1. Statement of the Problem

This chapter is concerned with the characterization of optimal non-linear structures, operating under non-Gaussian noise environment. In particular, the problem is specialized to optimal discrete-time detection of weak constant complex signal embedded in multivariate non-Gaussian noise.

Mathematically, the problem can be formulated in the general context of Hypothesis Testing for the presence or absence of the desired signal as:

$$H_0 : \underline{\tilde{r}} = \underline{\tilde{n}} \qquad (3.1-1)$$

$$H_1 : \underline{\tilde{r}} = \theta\underline{\tilde{s}} + \underline{\tilde{n}} \qquad (3.1-2)$$

where $\underline{\tilde{r}}$, $\underline{\tilde{n}}$, and $\underline{\tilde{s}}$ are the M-vector complex received , multivariate noise, and desired signal respectively. The real and imaginary parts of the components of these M-vector signals are obtained by sampling the in-phase and quadrature phase components of the " narrow-band " process $[\tilde{n}(t)]$ and $[\theta\tilde{s}(t) + \tilde{n}(t)]$ as:

$$\tilde{r}_i = r_I^i + jr_Q^i, \quad i = 1,...,M \qquad (3.1-3)$$

$$\tilde{n}_i = n_I^i + jn_Q^i, \quad i = 1,...,M \qquad (3.1-4)$$

$$\tilde{s}_i = s_I^i + js_Q^i, \quad i = 1,...,M \qquad (3.1-5)$$

where the subscripts (I) and (Q) denote the in-phase and quadrature phase components, and the superscript (i) represents the i-th sample.

The parameter (θ) in (3.1-2) is a real positive constant that is proportional to the signal amplitude. It is assumed that (θ) is vanishingly small ($\theta \rightarrow 0$). This is one of the major assumptions that is imposed in the development of the detector structures. As will be seen later, this assumption has a fundamental impact on the complexity of the detection scheme.

Another significant aspect, in the detection scheme, is the multivariate nature of the noise. In the past, most of the research on the weak narrow-band signal detection has been conducted under the assumption of independent and identically distributed noise samples. In the development presented here, the multivariate noise model, as discussed in Chapter II, is employed.

Also, the actual information for decision process, available from the received signal $\underline{r}$, depends on whether the receiver system (i.e., communication or radar) is coherent or non-coherent. In discrete-time coherent system, both the in-phase and quadrature phase samples are measurable(i.e., n_I^i, and n_Q^i). However, in non-coherent system, only the amplitude is available (i.e., $\sqrt{n_I^2 + n_Q^2}$). The performance of the receiver structures considered in this Chapter, will be affected by the coherency of the receiver.

In section (3.2), the Neyman-Pearson detector is discussed, and as its specialization, Locally Optimum Detector (LOD), is formulated. Sections (3.3) through (3.5) deal with various noise and measurement models , all under multivariate assumption. Finally, Section (3.6) is concerned with the special case of independent and identically distributed noise model.

3.2. Neyman-Pearson Optimum and Locally Optimum Detection Schemes

In this section, the underlying theory for optimum detection of weak signals is discussed, and a general canonical structure for detection in multivariate noise is developed.

It is well-known that, in a binary Hypothesis Testing, minimization of the total risk in making a decision, given a priori cost assignment and probability of occurrence of each alternative, leads to Bayesian Optimal Detector [40]. The total risk, (R), can be expressed as:

$$R = C_{00}P_0P(H_0/H_0) + C_{01}P_1P(H_0/H_1) + C_{10}P_0P(H_1/H_0) + C_{11}P_1P(H_1/H_1) \qquad (3.2-1)$$

where C_{ij} is the cost associated with each possible course of decision, P_0 and P_1 are a priori probabilities of each event, and $P(H_i/H_j)$ is the conditional probability of choosing (H_i) given that (H_j) is true. However, in some applications, such as radar system, the a priori knowledge of these probabilities are unknown, and assigning a realistic cost is impractical. In such cases, one can define the " False Alarm " and " Detection " probabilities as:

$$P_{fa} = \int_{R_{fa}} p(\underline{\tilde{r}}/H_0)\, d\underline{\tilde{r}} \qquad (3.2-2)$$

$$P_{\text{det}} = \int_{R_{\text{det}}} p(\tilde{\underline{r}}/H_1)\ d\tilde{\underline{r}} \qquad (3.2-3)$$

where $\tilde{\underline{r}}$ is the complex (or real) observation vector, and R_{fa} and R_{det} are appropriate regions of integration.

The Neyman-Pearson detector is based on fixing (constraining) the false-alarm probability and maximizing the probability of detection [40-42]. This type of criterion leads to a test structure based on the Likelihood Ratio Test (LRT) as:

$$\Lambda(\tilde{\underline{r}}) = \frac{p(\tilde{\underline{r}}/H_1)}{p(\tilde{\underline{r}}/H_0)} \begin{matrix} H_1 \\ > \\ < \\ H_0 \end{matrix} \textit{Threshold} \qquad (3.2-4)$$

where the Threshold is chosen, based on the statistic of the LRT function as:

$$P_{fa} = \int_{\textit{Threshold}}^{\infty} p(\Lambda/H_0)\ d\Lambda \qquad (3.2-5)$$

The Neyman-Pearson detector is optimum in the sense that the detection probability P_{det} is maximum for a given false alarm probability P_{fa}, Signal to Noise Ratio (SNR), and the number of samples. However, the implementation of this structure is usually quite complicated.

For example, consider the binary Hypothesis Testing problem for the real multivariate noise and the measurement model as:

$$H_0: \ \underline{y} = \underline{n} \qquad (3.2-6)$$

$$H_1: \ \underline{y} = \underline{n} + \theta \ \underline{s} \qquad (3.2-7)$$

where $\underline{y}$, $\underline{n}$, and $\underline{s}$ are the real M-vector of measurements, noise, and the signal respectively. The LRT function associated with this problem is:

$$\Lambda(\underline{y}) = \frac{p_{\underline{n}}(\underline{y}/H_1)}{p_{\underline{n}}(\underline{y}/H_0)} = \frac{p_{\underline{n}}(\underline{y} - \theta\underline{s})}{p_{\underline{n}}(\underline{y})} \qquad (3.2-8)$$

where $p_{\underline{n}}(.)$ denotes the multivariate density function of the noise. The numerator of equation (3.2-8) can be expanded in Taylor series around $\theta = 0$ as:

$$p_{\underline{n}}(\underline{y} - \theta\underline{s}) = p_{\underline{n}}(\underline{y}) + \sum_{k=1}^{\infty} \frac{(-1)^k}{k!} (\theta \underline{s}^T \nabla_{\underline{y}})^k \ p_{\underline{n}}(\underline{y}) \qquad (3.2-9)$$

and (3.2-9) can be written as:

$$p_{\underline{n}}(\underline{y} - \theta\underline{s}) = p_{\underline{n}}(\underline{y}) - \theta \underline{s}^T \nabla_{\underline{y}} \ p_{\underline{n}}(\underline{y}) + \frac{1}{2}\theta^2 \underline{s}^T \nabla_{\underline{y}}^2 \ p_{\underline{n}}(\underline{y})\underline{s} + O(\theta^3) \qquad (3.2-10)$$

where $\nabla_{\underline{y}} p_{\underline{n}}(\underline{y})$ is an M-vector Gradient vector of the density function defined as :

$$\nabla_{\underline{y}} p_{\underline{n}}(\underline{y}) = \begin{bmatrix} \frac{\partial p_{\underline{n}}(\underline{y})}{\partial y_1} \\ \cdots \\ \frac{\partial p_{\underline{n}}(\underline{y})}{\partial y_M} \end{bmatrix} \qquad (3.2-11)$$

and $\nabla^2_{\underline{y}} p_{\underline{n}}(\underline{y})$ is the Hessian matrix with (ij-th) element as:

$$\left\{ \nabla^2_{\underline{y}} p_{\underline{n}}(\underline{y}) \right\}_{ij} = \frac{\partial p_{\underline{n}}(\underline{y})}{\partial y_i \partial y_j}$$

Substitution of (3.2-10) into (3.2-8) yields:

$$\Lambda(\underline{y}) = 1 - \theta \underline{s}^T \left(\frac{\nabla_{\underline{y}} p_{\underline{n}}(\underline{y})}{p_{\underline{n}}(\underline{y})}\right) + \frac{1}{2}\theta^2 \underline{s}^T \left(\frac{\nabla^2_{\underline{y}} p_{\underline{n}}(\underline{y})}{p_{\underline{n}}(\underline{y})}\right) \underline{s} + O(\theta^3) \qquad (3.2-12)$$

As noticed from (3.2-12), the implementation of $\Lambda(\underline{y})$ is fairly complicated. However, in some practical situations of interest, where (θ) is vanishingly small, the complexity of the optimal detector can be reduced by compromising the optimality. This is precisely the underlying motivation for the development of " Locally Optimum Detectors ". Essentially, the idea is that if a detector is near-optimal for weak signal, then it will perform with reasonable accuracy for strong signal (high SNR), even if the detector is well below optimal level [43,44].

The LOD is a Generalized Neyman-Pearson Detector which maximizes the derivative of the Power Function at $\theta = 0$, subject to fixed false alarm rate (α) . Formally, consider the class of detectors D_α operating with probability of false alarm of $P_{fa} = \alpha$. The LOD, D_{LOD}, is a detector with $P_{fa} = \alpha$ which satisfies [45]:

$$\max_{D \in D_\alpha} \{ \frac{d}{d\theta} P_{\text{det}}(\theta/D)|_{\theta=0} \} = \frac{d}{d\theta} P_{\text{det}}(\theta/D_{LOD})|_{\theta=0} \qquad (3.2-13)$$

where P_{det} is the detection probability for the signal of amplitude θ. From the Generalized Neyman-Pearson Lemma [2,46], the decision strategy is equivalent to :

$$\Gamma(\underline{y}) = \frac{\partial \Lambda(\underline{y}, \theta)}{\partial \theta}|_{\theta=0} \underset{H_0}{\overset{H_1}{\gtrless}} \lambda \qquad (3.2-14)$$

where (λ) is defined by:

$$\alpha = P_{fa} = \int_\lambda^\infty p(\Gamma/H_0)\, d\Gamma \qquad (3.2-15)$$

Application of (3.2-14) to (3.2-12) results in:

$$\Gamma(\underline{y}) = -\frac{s^T \nabla_{\underline{y}} p_{\underline{n}}(\underline{y})}{p_{\underline{n}}(\underline{y})} \qquad (3.2-16)$$

Certainly, the implementation of (3.2-16) is quite simpler than (3.2-12). Also, as noticed, (3.2-16) is proportional to the second term of the Taylor series expansion in equation (3.2-12). That is, if the optimal detector is approximated by the first two terms of its Taylor series expansion as:

$$\Psi(\underline{y}) \cong 1 - \theta \underline{s}^T \left(\frac{\nabla_{\underline{y}} p_{\underline{n}}(\underline{y})}{p_{\underline{n}}(\underline{y})}\right) \begin{array}{c} H_1 \\ > \\ < \\ H_0 \end{array} \lambda_\Psi \qquad (3.2-17)$$

and is compared to the LOD :

$$\Gamma(\underline{y}) = \frac{\partial \Lambda(\underline{y})}{\partial \theta}\Big|_{\theta=0} = -\underline{s}^T \left(\frac{\nabla_{\underline{y}} p_{\underline{n}}(\underline{y})}{p_{\underline{n}}(\underline{y})}\right) \begin{array}{c} H_1 \\ > \\ < \\ H_0 \end{array} \lambda_\Gamma \qquad (3.2-18)$$

it is noticed that the two detectors are basically the same except for the level of the thresholds which are decided by (3.2-15) and:

$$\alpha = P_{fa} = \int_{\lambda_\Psi}^{\infty} p(\Psi/H_0)\, d\Psi \qquad (3.2-19)$$

Equations (3.2-14) and (3.2-15) are the general equations for the Locally Optimum Detector design. In the next three sections, they will be employed to characterize the structure of various detectors under complex and real Hypothesis Testing models.

3.3. Locally Optimum Detector for Complex Noise and Amplitude Density Model

In this section, the structure for the Locally Optimum Detection of weak signal in multivariate non-Gaussian noise is considered. In this structure the signal and noise are added in the complex domain (phasor addition), and the effect of this type of complex signal addition is significant in modeling of the joint density function.

The problem can be formally stated in a binary Hypothesis Test as:

$$H_0 : \underset{\sim}{\tilde{y}} = \underset{\sim}{\tilde{n}} \qquad (3.3-1)$$

$$H_1 : \underset{\sim}{\tilde{y}} = \underset{\sim}{\tilde{n}} + \theta \underset{\sim}{\tilde{s}} \qquad (3.3-2)$$

where $\underset{\sim}{\tilde{n}} \equiv [\tilde{n}_1, ..., \tilde{n}_M]^T$, $\underset{\sim}{\tilde{s}} \equiv [\tilde{s}_1, ..., \tilde{s}_M]^T$, and $\underset{\sim}{\tilde{y}} \equiv [\tilde{y}_1, ...\tilde{y}_M]^T$ are the M-vector complex noise, signal, and measured samples respectively. As before, the parameter (θ) is a real positive constant, representing the amplitude of the signal, and assumed to be vanishingly small ($\theta \to 0$) . As noticed, the hypothesis model is based on the complex measurements, thus requiring coherent detector structure. However, in the formulation of the Likelihood Ratio (Λ), one can either use the joint amplitude density or the joint complex density model of the noise. In the development of the first detector structure, only the joint amplitude density function is utilized. Using the Generalized Neyman-Pearson Lemma for weak signal, the optimum detection strategy yields:

$$\Gamma(\tilde{\underline{y}}) = \frac{\partial \Lambda(|\tilde{\underline{y}}|, \theta)}{\partial \theta} \Big|_{\theta=0} = \frac{\partial}{\partial \theta} \frac{p(|\tilde{\underline{y}}|/H_1)}{p(|\tilde{\underline{y}}|/H_0)} \Big|_{\theta=0} \qquad (3.3-3)$$

The numerator and denominator of the right hand side of (3.3-3) are the conditional probability density functions of the measurement signal, which can be expressed in terms of the multivariate noise amplitude density function as:

$$\Gamma(\tilde{\underline{y}}) = \frac{1}{p_{|\tilde{\underline{n}}|}(|\tilde{\underline{y}}|)} \frac{\partial}{\partial \theta} p_{|\tilde{\underline{n}}|}(|\tilde{y}_1 - \theta \tilde{s}_1|, \ \ldots \ , |\tilde{y}_M - \theta \tilde{s}_M|) \Big|_{\theta=0}$$

$$(3.3-4)$$

Carrying out the differentiation, equation (3.3-4) reduces to :

$$\Gamma(\tilde{\underline{y}}) = \sum_{i=1}^{M} \{\frac{\partial |\tilde{y}_i - \theta \tilde{s}_i|}{\partial \theta}\} \Big|_{\theta=0} \frac{1}{p_{|\tilde{\underline{n}}|}(|\tilde{\underline{y}}|)} \frac{\partial p_{|\tilde{\underline{n}}|}(|\tilde{\underline{y}}|)}{\partial |\tilde{y}_i|} \qquad (3.3-5)$$

where, as before the joint multivariate amplitude density function is defined as:

$$p_{|\tilde{\underline{n}}|}(|\tilde{\underline{y}}|) = p_{|\tilde{\underline{n}}|}(|\tilde{y}_1|, ..., |\tilde{y}_M|) \qquad (3.3-6)$$

The derivative in the summand of (3.3-5) can be simplified by noting that:

$$| \tilde{y}_i - \theta \tilde{s}_i | = \sqrt{(y_{I_i} - \theta s_{I_i})^2 + (y_{Q_i} - \theta s_{Q_i})^2} \qquad (3.3-7)$$

where y_{I_i}, y_{Q_i}, s_{I_i}, and s_{Q_i} are the i-th inphase and quadrature phase components of the measured sample and the desired signal respectively. Then, one can obtain:

$$\{\frac{\partial |\tilde{y}_i - \theta \tilde{s}_i|}{\partial \theta}\} |_{\theta=0} = \frac{-(y_{I_i} - \theta s_{I_i}) s_{I_i} - (y_{Q_i} - \theta s_{Q_i}) s_{Q_i}}{| \tilde{y}_i - \theta \tilde{s}_i |} |_{\theta=0}$$

$$= - \frac{Real\ (\tilde{y}_i \tilde{s}_i^*)}{|\tilde{y}_i|} \qquad (3.3-8)$$

where (*) denotes complex conjugate. Thus, (3.3-5) can be written as:

$$\Gamma(\underline{\tilde{y}}) = \sum_{i=1}^{M} - \frac{Real\ (\tilde{y}_i \tilde{s}_i^*)}{\tilde{y}_i} \frac{1}{p_{|\underline{\tilde{n}}|}(|\underline{\tilde{y}}|)} \frac{\partial p_{|\underline{\tilde{n}}|}(|\underline{\tilde{y}}|)}{\partial |\tilde{y}_i|} \qquad (3.3-9)$$

Now, by the noise Model (I) of Chapter II, and using the following equations:

$$p_{|\underline{\tilde{n}}|}(|\underline{\tilde{y}}|) = p_G(g(|\tilde{y}_1|), ..., g(|\tilde{y}_M|)) \prod_{i=1}^{M} |g'(|\tilde{y}_i|)| \qquad (3.3-10)$$

and

$$p_G(g(|\tilde{y}_1|), \ ... \ , g(|\tilde{y}_M|)) = \frac{1}{(2\pi)^{\frac{M}{2}} |\underline{R}_{|\underline{\tilde{y}}|}|^{\frac{1}{2}}}$$

$$\exp\ \{ -\frac{1}{2} \sum_{i=1}^{M} \sum_{j=1}^{M} \alpha_{ij}\ g(|\tilde{y}_i|)\ \ g(|\tilde{y}_j|) \} \qquad (3.3-11)$$

one obtains the first (LOD) structure as:

$$(LOD)_I = \sum_{i=1}^{M} \sum_{j=1}^{M} \alpha_{ij} \frac{Real(\tilde{y}_i\ \tilde{s}_i^*)}{|\tilde{y}_i|} g'(|\tilde{y}_i|)\ \ g(|\tilde{y}_j|)$$

$$- \sum_{i=1}^{M} \frac{Real(\tilde{y}_i\ \tilde{s}_i^*)}{|\tilde{y}_i|}\ \frac{g''(|\tilde{y}_i|)}{g'(|\tilde{y}_i|)} \qquad (3.3-12)$$

where, as before:

$$g(|\tilde{y}_i|) = \Phi^{-1}\ [\ F_{|\tilde{n}_i|}(|\tilde{y}_i|)\ ] \qquad (3.3-13)$$

$$\alpha_{ij} = \{\underline{R}_{|\underline{\tilde{y}}|}^{-1}\}_{ij} \qquad (3.3-14)$$

and

$$g'(|\tilde{y}_i|) = \frac{p_{|\tilde{n}_i|}(|\tilde{y}_i|)}{p_G(\ g(|\tilde{y}_i|)\ )} \qquad (3.3-15)$$

where (Φ^{-1}) denotes the inverse error function, $F_{|\tilde{n}_i|}$ is the non-Gaussian marginal cumulative distribution function, $p_{|\tilde{n}_i|}$ is the non-Gaussian marginal density function, and p_G is the Gaussian density with mean zero and unit variance.

The $(LOD)_I$ from (3.3-12) is the first detector whose structure is based on the noise Model (I). The block diagram of this detector is illustrated in Figure (21). In this diagram, the double line indicates the transfer of information for all the samples, and the single line indicates the flow of a single sample.

As noticed from the diagram, this is a detector whose operation requires memory (all the samples are required before processing the data). The detector structure has certain similarities with the matched filter. That is, after non-linear processing of the measurement amplitudes, the matched filtering is implemented by " matching " every sample with a function of measurement and signal as:

$$h(\tilde{y}_i, \tilde{s}_i) = \frac{Real\ (\tilde{y}_i\ \tilde{s}_i^*)}{|\tilde{y}_i|} \qquad (3.3-16)$$

The (α_{ij}), elements of the inverse of the correlation matrix of the Gaussian density, can be estimated directly from the data. In the next section, a more general detector structure using the complex multivariate noise density is developed.

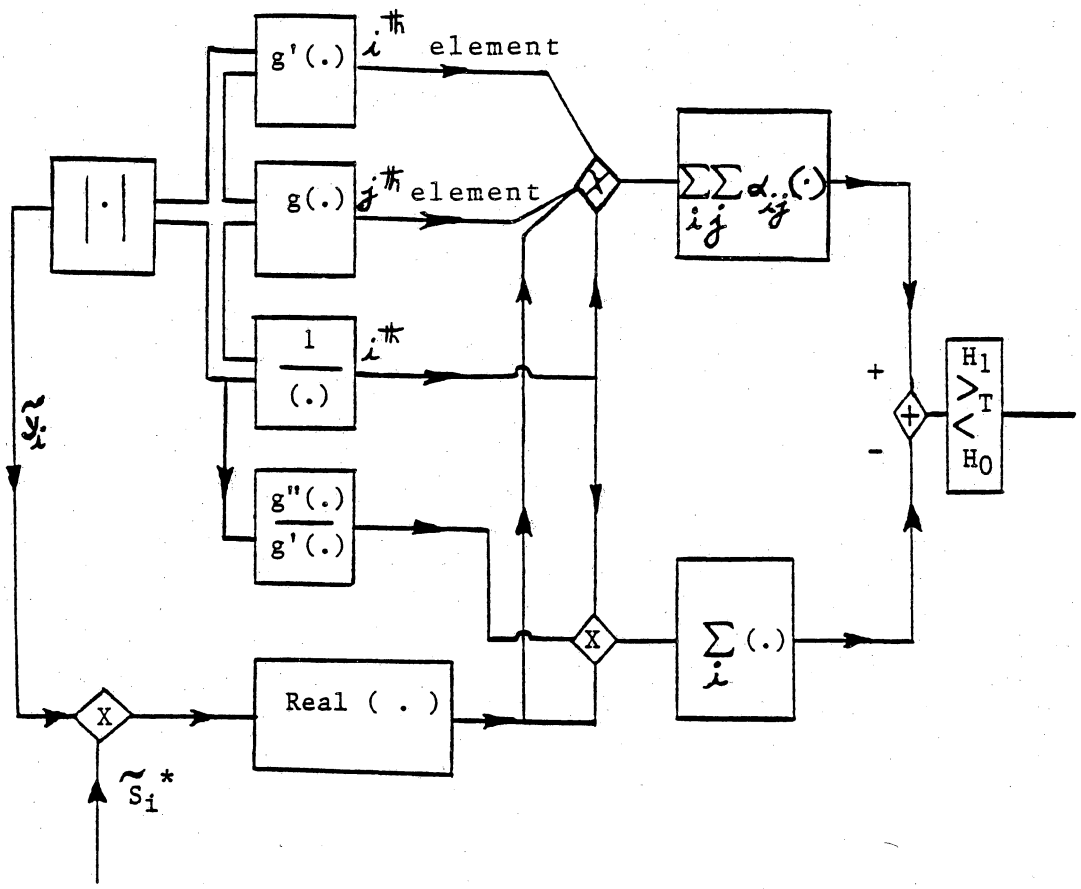

Figure 21. Block Diagram of the LOD for Complex Noise and Amplitude Density Model.

3.4. Locally Optimum Detector for Complex Noise and Multivariate Density Model (I)

In this section, the most general Locally Optimum Detector structure under the multivariate non-Gaussian noise density, characterized by Model (I), is derived. The generality of the model is due to both the utilization of the complex measurement of the signal and noise, and the complex modeling of the noise density.

The Hypothesis Testing model is:

$$H_0 : \underset{\sim}{y} = \underset{\sim}{n} \qquad (3.4-1)$$

$$H_1 : \underset{\sim}{y} = \underset{\sim}{n} + \theta \underset{\sim}{s} \qquad (3.4-2)$$

where $\underset{\sim}{n} \equiv [n_1, ..., n_M]^T$, $\underset{\sim}{s} \equiv [s_1, ..., s_M]^T$, and $\underset{\sim}{y} \equiv [y_1, ...y_M]^T$ are the M-vector complex noise, signal, and measured samples respectively. As before, the parameter (θ) is a real positive constant, representing the amplitude of the signal, and assumed to be vanishingly small ($\theta \to 0$) .

In this section, the most general expression for the Likelihood Ratio Test function (LRT) is considered as follows:

$$\Lambda(\underset{\sim}{y}, \theta) =$$

$$\frac{p_{n_{I_1}, n_{Q_1}, ..., n_{I_M}, n_{Q_M}}(y_{I_1} - \theta s_{I_1}, y_{Q_1} - \theta s_{Q_1}, \ \cdots \ , y_{I_M} - \theta s_{I_M}, y_{Q_M} - \theta s_{Q_M})}{p_{n_{I_1}, n_{Q_1}, ..., n_{I_M}, n_{Q_M}}(y_{I_1}, y_{Q_1}, \ \cdots \ , y_{I_M}, y_{Q_M})}$$

(3.4 − 3)

where

$$p_{n_{I_1}, n_{Q_1}, ..., n_{I_M}, n_{Q_M}} (n_{I_1}, n_{Q_1}, \ \cdots \ , n_{I_M}, n_{Q_M}) \tag{3.4 - 4}$$

is the complex multivariate non-Gaussian noise density function, and (I) and (Q) represent the in-phase and quadrature phase components respectively.

Since, the signal is weak, the optimum detection strategy is to use the Generalized Neyman-Pearson Lemma, which leads to the following form as:

$$\Gamma(\underset{\sim}{y}) = \frac{\partial \Lambda(\underset{\sim}{y}, \theta)}{\partial \theta} \Big|_{\theta=0} = \frac{\partial}{\partial \theta} \frac{p(\underset{\sim}{y}/H_1)}{p(\underset{\sim}{y}/H_0)} \Big|_{\theta=0} \tag{3.4 - 5}$$

Now, taking the derivative of the LRT function, yields:

$$\frac{\partial \Lambda(\underset{\sim}{y}, \theta)}{\partial \theta} = \frac{1}{p_{n_{I_1}, n_{Q_1}, ..., n_{I_M}, n_{Q_M}} (y_{I_1}, y_{Q_1}, \ \cdots \ , y_{I_M}, y_{Q_M})} \sum_{i=1}^{M}$$

$$- s_{I_i} \frac{\partial p_{n_{I_1}, n_{Q_1}, ..., n_{I_M}, n_{Q_M}} (y_{I_1} - \theta s_{I_1}, y_{Q_1} - \theta s_{Q_1}, ..., y_{I_M} - \theta s_{I_M}, y_{Q_M} - \theta s_{Q_M})}{\partial \ (y_{I_i} - \theta s_{I_i})}$$

$$- s_{Q_i} \frac{\partial p_{n_{I_1}, n_{Q_1}, ..., n_{I_M}, n_{Q_M}} (y_{I_1} - \theta s_{I_1}, y_{Q_1} - \theta s_{Q_1}, ..., y_{I_M} - \theta s_{I_M}, y_{Q_M} - \theta s_{Q_M})}{\partial \ (y_{Q_i} - \theta s_{Q_i})}$$

(3.4 − 6)

Setting ($\theta = 0$) in (3.4-6) results in :

$$(LOD)_{II} = \frac{1}{p_{n_{I_1}, n_{Q_1}, ..., n_{I_M}, n_{Q_M}}(y_{I_1}, y_{Q_1}, \cdots, y_{I_M}, y_{Q_M})} \sum_{i=1}^{M}$$

$$- s_{I_i} \frac{\partial\, p_{n_{I_1}, n_{Q_1}, ..., n_{I_M}, n_{Q_M}}(y_{I_1}, y_{Q_1}, \cdots, y_{I_M}, y_{Q_M})}{\partial\,(y_{I_i})}$$

$$- s_{Q_i} \frac{\partial\, p_{n_{I_1}, n_{Q_1}, ..., n_{I_M}, n_{Q_M}}(y_{I_1}, y_{Q_1}, \cdots, y_{I_M}, y_{Q_M})}{\partial\,(y_{Q_i})} \qquad (3.4-7)$$

At this stage, it is assumed that the complex joint multivariate density function possesses " circular symmetry " property, defined by equation (2.2-1) as:

$$p_{n_{I_1}, n_{Q_1}, ..., n_{I_M}, n_{Q_M}}(n_{I_1}, n_{Q_1}, \cdots, n_{I_M}, n_{Q_M}) =$$

$$f(\sqrt{n_{I_1}^2 + n_{Q_1}^2}, ..., \sqrt{n_{I_M}^2 + n_{Q_M}^2}) \qquad (3.4-8)$$

Following the procedure that was developed in section (2) of Chapter II, one can obtain:

$$p_{n_{I_1}, n_{Q_1}, \ldots, n_{I_M}, n_{Q_M}}\left(n_{I_1}, n_{Q_1}, \cdots, n_{I_M}, n_{Q_M}\right) = \frac{1}{(2\pi)^M}$$

$$\frac{p_{|\tilde{\underline{n}}|}\left(\sqrt{n_{I_1}^2 + n_{Q_1}^2}, \ldots, \sqrt{n_{I_M}^2 + n_{Q_M}^2}\right)}{\prod_{i=1}^{M}\left(\sqrt{n_{I_i}^2 + n_{Q_i}^2}\right)} \qquad (3.4-9)$$

Thus:

$$p_{n_{I_1}, n_{Q_1}, \ldots, n_{I_M}, n_{Q_M}}\left(y_{I_1}, y_{Q_1}, \cdots, y_{I_M}, y_{Q_M}\right) = \frac{1}{(2\pi)^M}$$

$$\frac{p_{|\tilde{\underline{n}}|}\left(\sqrt{y_{I_1}^2 + y_{Q_1}^2}, \ldots, \sqrt{y_{I_M}^2 + y_{Q_M}^2}\right)}{\prod_{i=1}^{M}\left(\sqrt{y_{I_i}^2 + y_{Q_i}^2}\right)}$$

$$= \frac{1}{(2\pi)^M} \frac{p_{|\tilde{\underline{n}}|}(|\tilde{y}_1|, \ldots, |\tilde{y}_M|)}{\prod_{i=1}^{M}|\tilde{y}_i|} \qquad (3.4-10)$$

Carrying out the differentiation in (3.4-7) results in:

$$\frac{\partial p_{n_{I_1}, n_{Q_1}, \ldots, n_{I_M}, n_{Q_M}}\left(y_{I_1}, y_{Q_1}, \cdots, y_{I_M}, y_{Q_M}\right)}{\partial\left(y_{I_i}\right)} = \frac{y_{I_i}}{|\tilde{y}_i|}$$

$$\frac{\partial p_{n_{I_1}, n_{Q_1}, \ldots, n_{I_M}, n_{Q_M}}\left(y_{I_1}, y_{Q_1}, \cdots, y_{I_M}, y_{Q_M}\right)}{\partial\left(|\tilde{y}_i|\right)} \qquad (3.4-11)$$

and

$$\frac{\partial p_{n_{I_1}, n_{Q_1}, \ldots, n_{I_M}, n_{Q_M}}(y_{I_1}, y_{Q_1}, \cdots, y_{I_M}, y_{Q_M})}{\partial (y_{Q_i})} = \frac{y_{Q_i}}{|\tilde{y}_i|}$$

$$\frac{\partial p_{n_{I_1}, n_{Q_1}, \ldots, n_{I_M}, n_{Q_M}}(y_{I_1}, y_{Q_1}, \cdots, y_{I_M}, y_{Q_M})}{\partial (|\tilde{y}_i|)} \qquad (3.4-12)$$

Substitution of (3.4-11) and (3.4-12) into (3.4-7) yields:

$$(LOD)_{II} = \sum_{i=1}^{M} - \frac{Real(\tilde{y}_i \tilde{s}_i^*)}{|\tilde{y}_i|} \frac{1}{p_{n_{I_1}, n_{Q_1}, \ldots, n_{I_M}, n_{Q_M}}(y_{I_1}, y_{Q_1}, \cdots, y_{I_M}, y_{Q_M})}$$

$$\frac{\partial p_{n_{I_1}, n_{Q_1}, \ldots, n_{I_M}, n_{Q_M}}(y_{I_1}, y_{Q_1}, \cdots, y_{I_M}, y_{Q_M})}{\partial (|\tilde{y}_i|)} \qquad (3.4-13)$$

Now, using (3.4-10), one can easily obtain:

$$\frac{1}{p_{n_{I_1}, n_{Q_1}, \ldots, n_{I_M}, n_{Q_M}}(y_{I_1}, y_{Q_1}, \ldots, y_{I_M}, y_{Q_M})} \frac{\partial p_{n_{I_1}, n_{Q_1}, \ldots, n_{I_M}, n_{Q_M}}(y_{I_1}, y_{Q_1}, \ldots, y_{I_M}, y_{Q_M})}{\partial (|\tilde{y}_i|)}$$

$$= - \frac{1}{|\tilde{y}_i|} + \frac{1}{p_{|\underline{\tilde{n}}|}(|\tilde{y}_1|, \ldots, |\tilde{y}_M|)} \frac{\partial p_{|\underline{\tilde{n}}|}(|\tilde{y}_1|, \ldots, |\tilde{y}_M|)}{\partial |\tilde{y}_i|} \qquad (3.4-14)$$

Finally, substitution of (3.4-14) into (3.4-7) yields:

$$(LOD)_{II} = \sum_{i=1}^{M} \frac{Real(\tilde{y}_i \tilde{s}_i^*)}{|\tilde{y}_i|}$$

$$[\frac{1}{|\tilde{y}_i|} - \frac{1}{p_{|\underline{\tilde{n}}|}(|\tilde{y}_1|, ..., |\tilde{y}_M|)} \frac{\partial p_{|\underline{\tilde{n}}|}(|\tilde{y}_1|, ..., |\tilde{y}_M|)}{\partial |\tilde{y}_i|}] \qquad (3.4-15)$$

Now, by application of the noise model, developed in Chapter II as Model (I), one obtains:

$$p_{|\underline{\tilde{n}}|}(|\underline{\tilde{y}}|) = p_G(g(|\tilde{y}_1|), ..., g(|\tilde{y}_M|)) \prod_{i=1}^{M} |g'(|\tilde{y}_i|)| \qquad (3.4-16)$$

equation (3.4-15) yields:

$$(LOD)_{II} = \sum_{i=1}^{M} \sum_{j=1}^{M} \alpha_{ij} \frac{Real(\tilde{y}_i \tilde{s}_i^*)}{|\tilde{y}_i|} g'(|\tilde{y}_i|) \; g(|\tilde{y}_j|)$$

$$- \sum_{i=1}^{M} \frac{Real(\tilde{y}_i \tilde{s}_i^*)}{|\tilde{y}_i|} [\frac{g''(|\tilde{y}_i|)}{g'(|\tilde{y}_i|)} - \frac{1}{|\tilde{y}_i|}] \qquad (3.4-17)$$

The block diagram of this detector is shown in Figure (22). As before, the double line indicates the transfer of all the samples, and the single line indicates the flow of a single sample. This is the most general detector that can be obtained

by utilizing all the available information from the amplitude and phase of the measurements and density Model (I).

As noticed, comparing $(LOD)_I$ from (3.3-12) with $(LOD)_{II}$ from (3.4-17) shows an additional non-linearity present in $(LOD)_{II}$. This is due to " circular symmetry " assumption that has been employed in the multivariate density modeling.

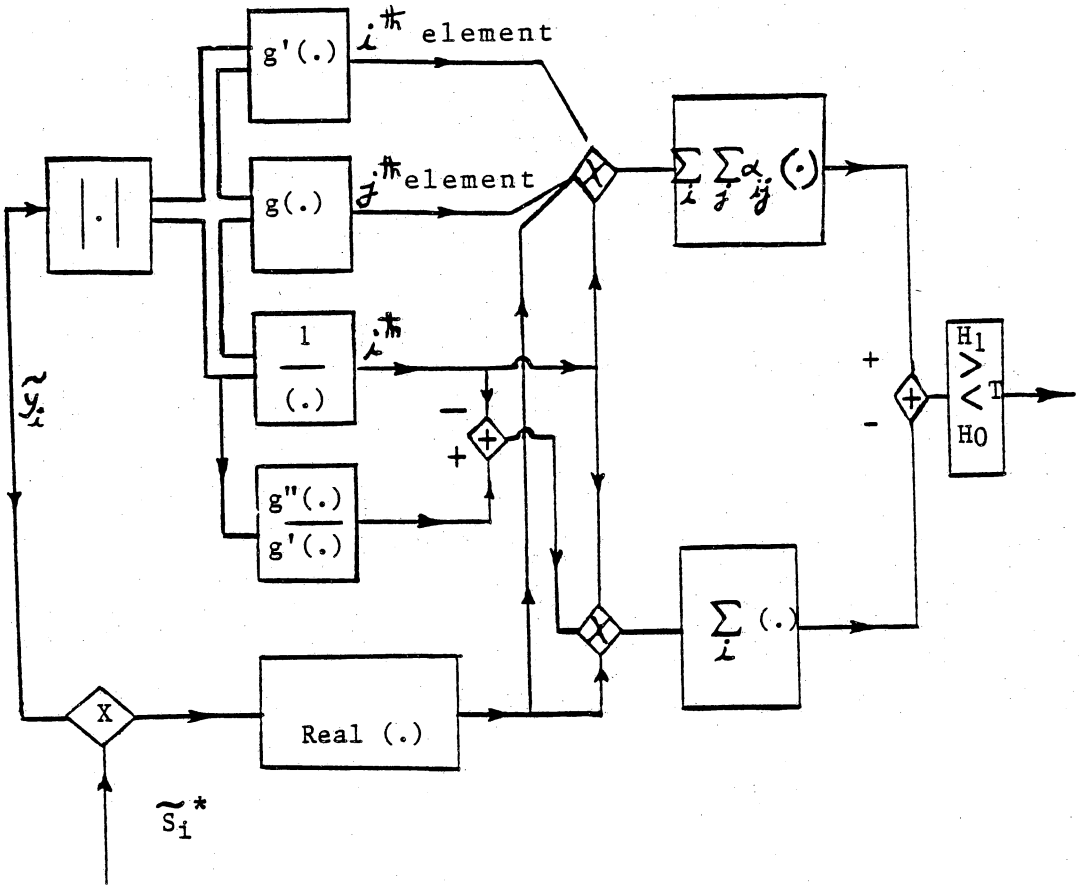

Figure 22. Block Diagram of the LOD for Complex Noise and Complex Multivariate Density Model(I).

3.5. Locally Optimum Detector for Complex Noise and Multivariate Density Model (II)

In this section, the most general Locally Optimum Detector structure under the multivariate non-Gaussian noise density, characterized by Model (II), is derived. The generality of the model is due to both the complex (phasor) addition of the signal and noise, the complex modeling of the noise density, and the use of complex correlation structure.

The Hypothesis Testing model is:

$$H_0 : \underset{\sim}{y} = \underset{\sim}{n} \qquad (3.5-1)$$

$$H_1 : \underset{\sim}{y} = \underset{\sim}{n} + \theta \underset{\sim}{s} \qquad (3.5-2)$$

where $\underset{\sim}{n} \equiv [n_1, ..., n_M]^T$, $\underset{\sim}{s} \equiv [s_1, ..., s_M]^T$, and $\underset{\sim}{y} \equiv [y_1, ...y_M]^T$ are the M-vector complex noise, signal, and measured samples respectively. As before, the parameter (θ) is a real positive constant, representing the amplitude of the signal, and assumed to be vanishingly small ($\theta \to 0$) .

As in the previous section, the most general expression for the Likelihood Ratio Test function (LRT) is considered as follows:

$$\Lambda(\underset{\sim}{y}, \theta) =$$

$$\frac{p_{n_{I_1}, n_{Q_1}, ..., n_{I_M}, n_{Q_M}}(y_{I_1} - \theta s_{I_1}, y_{Q_1} - \theta s_{Q_1}, \cdots, y_{I_M} - \theta s_{I_M}, y_{Q_M} - \theta s_{Q_M})}{p_{n_{I_1}, n_{Q_1}, ..., n_{I_M}, n_{Q_M}}(y_{I_1}, y_{Q_1}, \cdots, y_{I_M}, y_{Q_M})}$$

(3.5 − 3)

where

$$p_{n_{I_1}, n_{Q_1}, ..., n_{I_M}, n_{Q_M}} (n_{I_1}, n_{Q_1}, \ \cdots \ , n_{I_M}, n_{Q_M}) \qquad (3.5 - 4)$$

is the complex multivariate non-Gaussian noise density function, and (I) and (Q) represent the in-phase and quadrature phase components respectively.

Since, the signal is weak, the optimum detection strategy is to use the Generalized Neyman-Pearson Lemma, which leads to the following form as:

$$\Gamma(\tilde{y}) = \frac{\partial \Lambda(\tilde{y}, \theta)}{\partial \theta} \Big|_{\theta=0} = \frac{\partial}{\partial \theta} \frac{p(\tilde{y}/H_1)}{p(\tilde{y}/H_0)} \Big|_{\theta=0} \qquad (3.5 - 5)$$

Now, taking the derivative of the LRT function, yields:

$$\frac{\partial \Lambda(\tilde{y}, \theta)}{\partial \theta} = \frac{1}{p_{n_{I_1}, n_{Q_1}, ..., n_{I_M}, n_{Q_M}} (y_{I_1}, y_{Q_1}, \ \cdots \ , y_{I_M}, y_{Q_M})} \sum_{i=1}^{M}$$

$$- s_{I_i} \frac{\partial p_{n_{I_1}, n_{Q_1}, ..., n_{I_M}, n_{Q_M}} (y_{I_1} - \theta s_{I_1}, y_{Q_1} - \theta s_{Q_1}, ..., y_{I_M} - \theta s_{I_M}, y_{Q_M} - \theta s_{Q_M})}{\partial \ (y_{I_i} - \theta s_{I_i})}$$

$$- s_{Q_i} \frac{\partial p_{n_{I_1}, n_{Q_1}, ..., n_{I_M}, n_{Q_M}} (y_{I_1} - \theta s_{I_1}, y_{Q_1} - \theta s_{Q_1}, ..., y_{I_M} - \theta s_{I_M}, y_{Q_M} - \theta s_{Q_M})}{\partial \ (y_{Q_i} - \theta s_{Q_i})}$$

Setting ($\theta = 0$) in (3.5-6) results in :

$$(LOD)_{III} = \frac{1}{p_{n_{I_1}, n_{Q_1}, ..., n_{I_M}, n_{Q_M}}(y_{I_1}, y_{Q_1}, \cdots, y_{I_M}, y_{Q_M})} \sum_{i=1}^{M}$$

$$- s_{I_i} \frac{\partial\, p_{n_{I_1}, n_{Q_1}, ..., n_{I_M}, n_{Q_M}}(y_{I_1}, y_{Q_1}, \cdots, y_{I_M}, y_{Q_M})}{\partial\,(y_{I_i})}$$

$$- s_{Q_i} \frac{\partial\, p_{n_{I_1}, n_{Q_1}, ..., n_{I_M}, n_{Q_M}}(y_{I_1}, y_{Q_1}, \cdots, y_{I_M}, y_{Q_M})}{\partial\,(y_{Q_i})} \qquad (3.5-7)$$

At this stage, one can invoke the complex multivariate non-Gaussian density function, characterized by Model (II) as:

$$p_{n_{I_1}, n_{Q_1}, ..., n_{I_M}, n_{Q_M}}(y_{I_1}, y_{Q_1}, \cdots, y_{I_M}, y_{Q_M}) =$$

$$P_G[\, g_I(y_{I_1}), , g_Q(y_{Q_1}), ..., g_I(y_{I_M}), , g_Q(y_{Q_M})\,] \mid \prod_{i=1}^{M} g'_I(y_{I_i})\, g'_Q(y_{Q_i}) \mid$$

$$(3.5-8)$$

where the multivariate Gaussian density is given by:

$$P_G[\, g_I(y_{I_1}), , g_Q(y_{Q_1}), ..., g_I(y_{I_M}), , g_Q(y_{Q_M})\,] = \frac{1}{(2\pi)^M \mid \underline{R} \mid^{\frac{1}{2}}}$$

$$\left\{ - \frac{1}{2}[\, g_I^T(\underline{y}_I)\, \underline{A}\, g_I(\underline{y}_I) + g_Q^T(\underline{y}_Q)\, \underline{D}\, g_Q(\underline{y}_Q) + g_I^T(\underline{y}_I)\, (\underline{B} + \underline{C}^T)\, g_Q(\underline{y}_Q)\,] \right\}$$

(3.5 − 9)

and the Gaussian correlation structure is denoted as:

$$\underline{R} = \begin{bmatrix} \underline{R}_{II} & \underline{R}_{IQ} \\ \\ \underline{R}_{QI} & \underline{R}_{QQ} \end{bmatrix} \qquad (3.5 - 10)$$

with its inverse expressed as:

$$\underline{R}^{-1} = \begin{bmatrix} \underline{A} & \underline{B} \\ \\ \underline{C} & \underline{D} \end{bmatrix} \qquad (3.5 - 11)$$

Then, using the following two relations:

$$\frac{\partial}{\partial y_{I_i}} \left| \prod_{m=1}^{M} g_I'(y_{I_m})\, g_Q'(y_{Q_m}) \right| = \left| \prod_{m=1}^{M} g_I'(y_{I_m})\, g_Q'(y_{Q_m}) \right| \frac{g_I''(y_{I_i})}{g_I'(y_{I_i})}$$

(3.5 − 12)

$$\frac{\partial}{\partial y_{Q_i}} \left| \prod_{m=1}^{M} g_I'(y_{I_m})\, g_Q'(y_{Q_m}) \right| = \left| \prod_{m=1}^{M} g_I'(y_{I_m})\, g_Q'(y_{Q_m}) \right| \frac{g_Q''(y_{Q_i})}{g_Q'(y_{Q_i})}$$

(3.5 − 13)

one can obtain:

$$\frac{1}{p_{n_{I_1}, n_{Q_1}, \ldots, n_{I_M}, n_{Q_M}}(y_{I_1}, y_{Q_1}, \ldots, y_{I_M}, y_{Q_M})} \frac{\partial p_{n_{I_1}, n_{Q_1}, \ldots, n_{I_M}, n_{Q_M}}(y_{I_1}, y_{Q_1}, \ldots, y_{I_M}, y_{Q_M})}{\partial (y_{Q_i})}$$

$$= \frac{g_Q''(y_{Q_i})}{g_Q'(y_{Q_i})} - \frac{1}{2} g_Q'(y_{Q_i}) \sum_{j=1}^{M} (d_{ij} + d_{ji}) g_Q(y_{Q_j}) + (b_{ji} + c_{ij}) g_I(y_{I_j}) \qquad (3.5 - 14)$$

and

$$\frac{1}{p_{n_{I_1}, n_{Q_1}, \ldots, n_{I_M}, n_{Q_M}}(y_{I_1}, y_{Q_1}, \ldots, y_{I_M}, y_{Q_M})} \frac{\partial p_{n_{I_1}, n_{Q_1}, \ldots, n_{I_M}, n_{Q_M}}(y_{I_1}, y_{Q_1}, \ldots, y_{I_M}, y_{Q_M})}{\partial (y_{I_i})}$$

$$= \frac{g_I''(y_{I_i})}{g_I'(y_{I_i})} - \frac{1}{2} g_I'(y_{I_i}) \sum_{j=1}^{M} (a_{ij} + a_{ji}) g_I(y_{I_j}) + (b_{ij} + c_{ji}) g_Q(y_{Q_j}) \qquad (3.5 - 15)$$

where $a_{ij}, b_{ij}, c_{ij}, d_{ij}$ are the elements of the matrices: $\underline{A}, \underline{B}, \underline{C}, and \underline{D}$ respectively. Substituting (3.5-14) and (3.5-15) into (3.5-7), one obtains:

$$(LOD)_{III} = \frac{1}{2} \sum_{i=1}^{M} \sum_{j=1}^{M} S_{I_i} g_I'(y_{I_i}) [(a_{ij} + a_{ji}) g_I(y_{I_j}) + (b_{ij} + c_{ji}) g_Q(y_{Q_j})]$$

$$+ \frac{1}{2} \sum_{i=1}^{M} \sum_{j=1}^{M} S_{Q_i} g_Q'(y_{Q_i}) [(b_{ji} + c_{ij}) g_I(y_{I_j}) + (d_{ij} + d_{ji}) g_Q(y_{Q_j})]$$

$$- \sum_{i=1}^{M} S_{I_i} \frac{g_I''(y_{I_i})}{g_I'(y_{I_i})} - \sum_{i=1}^{M} S_{Q_i} \frac{g_Q''(y_{Q_i})}{g_Q'(y_{Q_i})} \qquad (3.5-16)$$

This is the structure of the (LOD) under the noise Model (II). The block diagram of this detector is shown in Figure (23). As before, the double line indicates the transfer of all the samples, and the single line indicates the flow of a single sample. This is the most general detector that can be obtained by utilizing all the available information from the in-phase and quadrature phase components separately and the given complex correlation structure. As noticed from Figure (23), the detector structure can be decomposed into three parts. The upper part is the in-phase component processing, identified by:

$$(LOD)_{In-Phase} = \frac{1}{2} \sum_{i=1}^{M} \sum_{j=1}^{M} S_{I_i} (a_{ij} + a_{ji}) g_I'(y_{I_i}) g_I(y_{I_j}) -$$

$$\sum_{i=1}^{M} S_{I_i} \frac{g_I''(y_{I_i})}{g_I'(y_{I_i})} \qquad (3.5-17)$$

The lower part is the quadrature phase component processing, given by:

$$(LOD)_{Quadrature} = \frac{1}{2} \sum_{i=1}^{M} \sum_{j=1}^{M} S_{Q_i} (d_{ij} + d_{ji})\, g_Q'(y_{Q_i})\, g_Q(y_{Q_j}) -$$

$$\sum_{i=1}^{M} S_{Q_i} \frac{g_Q''(y_{Q_i})}{g_Q'(y_{Q_i})} \qquad (3.5 - 18)$$

and the middle part is the joint in-phase and quadrature phase processing, given by:

$$\frac{1}{2} \sum_{i=1}^{M} \sum_{j=1}^{M} S_{I_i} (b_{ij} + c_{ji})\, g_I'(y_{I_i})\, g_Q(y_{Q_j}) + S_{Q_i} (b_{ji} + c_{ij})\, g_Q'(y_{Q_i})\, g_I(y_{I_j})$$

$$(3.5 - 19)$$

As observed, the structure of Figure (23) is more complex than Figure (22). This is due to the fact that the phase information of the clutter is not assumed to be uniform, and the true measured phase is used. In the next section, the first two detector structures will be specialized to the case of independent and identically distributed (i.i.d) noise.

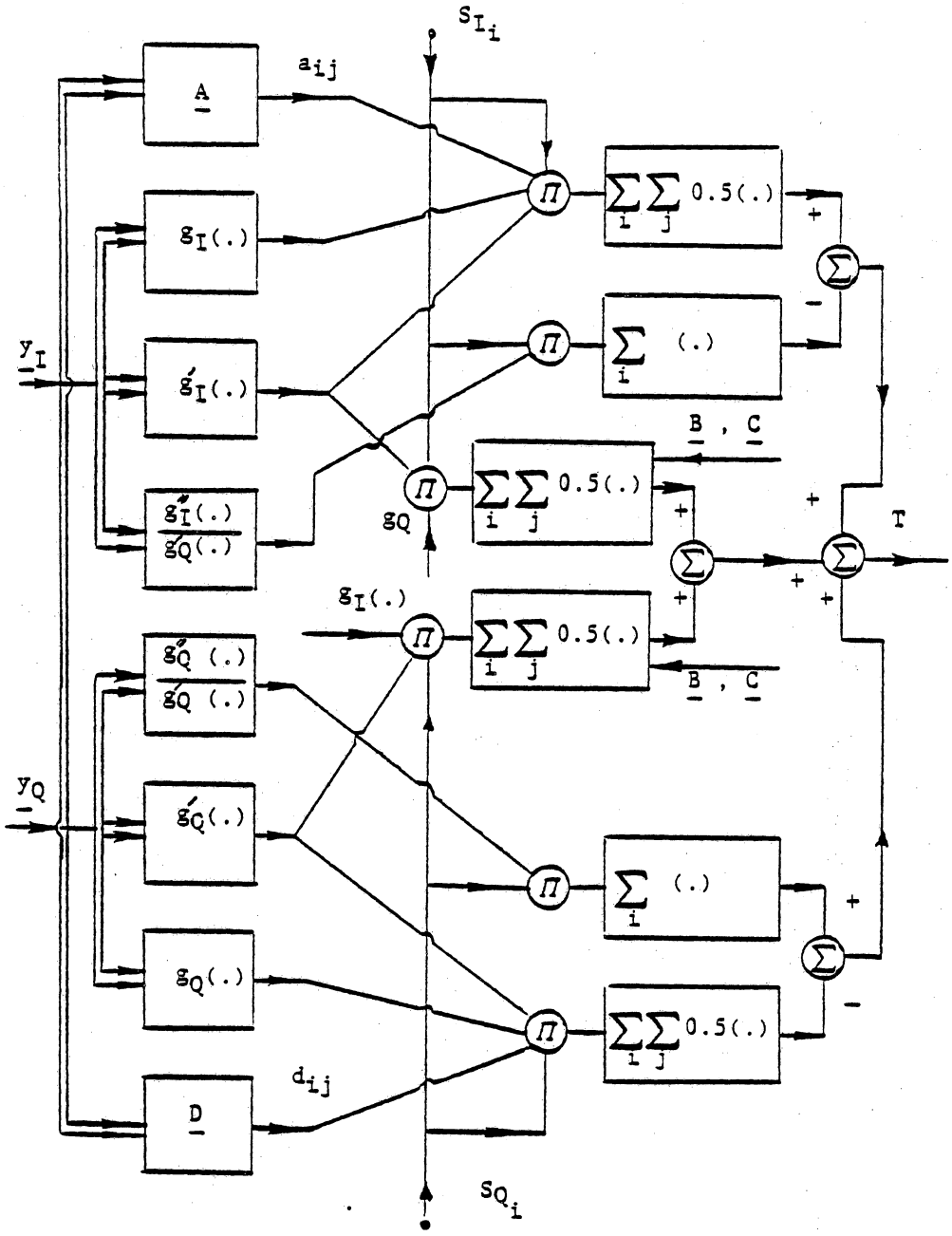

Figure 23. Block Diagram of the LOD for Complex Noise and Complex Multivariate Density Model (II).

3.6. Locally Optimum Detector for Independent and Identically Distributed Noise

In this section, the special case of independent and identically distributed noise (i.i.d) is considered. The underlying idea is to derive the detector structures under each of the density function models, so that they can be compared for their performances. The (i.i.d) assumption is very appealing, since the resulting detector structures are less complicated and the analysis is easier. However, as will be seen in Chapter IV, under the dependent noise environment, the performance is severely degraded.

First, consider the basic structure of $(LOD)_I$ from (3.3-9) as:

$$(LOD)_I = \sum_{i=1}^{M} - \frac{Real\ (\tilde{y}_i\ \tilde{s}_i^*)}{|\tilde{y}_i|} \frac{1}{p_{|\underline{\tilde{n}}|}(|\underline{\tilde{y}}|)} \frac{\partial p_{|\underline{\tilde{n}}|}(|\underline{\tilde{y}}|)}{\partial |\tilde{y}_i|} \qquad (3.6-1)$$

Under independent and identically distributed assumption, the multivariate density function is reduced to the product of univariate density functions as:

$$p_{|\underline{\tilde{n}}|}(|\underline{\tilde{y}}|) = p_{|\underline{\tilde{n}}|}(|\tilde{y}_1|, ..., |\tilde{y}_M|) = \prod_{k=1}^{M} p_{|\tilde{n}|}(|\tilde{y}_k|) \qquad (3.6-2)$$

where $p_{|\tilde{n}|}(.)$ is the non-Gaussian univariate density function of the noise amplitude. Substituting (3.6-2) into (3.6-1), and carrying out the differentiation, results in:

$$(LOD)_{I,(i.i.d)} = \sum_{i=1}^{M} - \frac{Real\ (\tilde{y}_i\ \tilde{s}_i^*)}{|\tilde{y}_i|} \frac{1}{p_{|\tilde{n}|}(|\tilde{y}_i|)} \frac{\partial p_{|\tilde{n}|}(|\tilde{y}_i|)}{(\partial |\tilde{y}_i|)} \qquad (3.6-3)$$

This structure depends only on the functional form of the univariate density function, which in practice, is usually known. As noticed, this detector is less complicated than $(LOD)_I$ in (3.3-12). Also, since the samples are assumed to be independent, the task of estimating α_{ij} from the data is eliminated. This helps reduce the signal processing and decision process time. Also, as stated before, due to simplicity of analysis and implementation, the (i.i.d) detector for weak narrow-band signal has been investigated previously. In fact, the structure of equation (3.6-3) is identical to equation (9) of Modestino [11].

Second, consider the fundamental structure of $(LOD)_{II}$ given by (3.4-7) as:

$$(LOD)_{II} = \frac{1}{p_{n_{I_1}, n_{Q_1}, ..., n_{I_M}, n_{Q_M}}(y_{I_1}, y_{Q_1}, \cdots, y_{I_M}, y_{Q_M})} \sum_{i=1}^{M}$$

$$- s_{I_i} \frac{\partial\, p_{n_{I_1}, n_{Q_1}, ..., n_{I_M}, n_{Q_M}}(y_{I_1}, y_{Q_1}, \cdots, y_{I_M}, y_{Q_M})}{\partial\,(y_{I_i})}$$

$$- s_{Q_i} \frac{\partial\, p_{n_{I_1}, n_{Q_1}, ..., n_{I_M}, n_{Q_M}}(y_{I_1}, y_{Q_1}, \cdots, y_{I_M}, y_{Q_M})}{\partial\,(y_{Q_i})} \qquad (3.6-4)$$

In this case, the joint complex multivariate density function reduces to the product of the complex univariate density functions as:

$$p_{n_{I_1}, n_{Q_1}, \ldots, n_{I_M}, n_{Q_M}}(y_{I_1}, y_{Q_1}, \cdots, y_{I_M}, y_{Q_M}) = \prod_{k=1}^{M} p_{n_I, n_Q}(y_{I_k}, y_{Q_k}) \qquad (3.6-5)$$

Substituting (3.6-5) into (3.6-4), and carrying out the differentiation, results in :

$$(LOD)_{II,(i.i.d)} = \sum_{i=1}^{M} \frac{Real(\tilde{y}_i \tilde{s}_i^*)}{|\tilde{y}_i|} \left[\frac{1}{|\tilde{y}_i|} - \frac{1}{p_{|\tilde{n}|}(|\tilde{y}_i|)} \frac{\partial p_{|\tilde{n}|}(|\tilde{y}_i|)}{\partial(|\tilde{y}_i|)} \right]$$

$$(3.6-6)$$

Comparison of (3.6-6) with (3.4-17) clearly indicates the difference between the complexity of the two structures.

Now, if $p_{|\tilde{n}|}(|\tilde{y}_i|)$ is replaced with the corresponding " circular symmetry " representation as introduced in (2.2-1), one obtains:

$$p_{|\tilde{n}|}(|\tilde{y}_i|) = 2\pi |\tilde{y}_i| f(|\tilde{y}_i|) \qquad (3.6-7)$$

Substitution of (3.6-7) into (3.6-6), results in:

$$(LOD)_{II,(i.i.d)} = \sum_{i=1}^{M} \frac{Real(\tilde{y}_i \tilde{s}_i^*)}{|\tilde{y}_i|} \left\{ - \frac{d \ln f(|\tilde{y}_i|)}{d(|\tilde{y}_i|)} \right\} \qquad (3.6-8)$$

Equation (3.6-8) is identical to equation (17) of Modestino [11].

In summary, the structure of three non-linear detectors, for detection of weak signal embedded in multivariate non-Gaussian noise, have been developed. The

structures have various levels of complexity, based on the use of available information and the modeling of the underlying noise density function. The next task is to evaluate the performance of the developed detectors.

IV. Performance Evaluation

4.1. Statement of the Problem

This chapter is concerned with the performance evaluation of the Locally Optimum Detector structures, $(LOD)_I$ and $(LOD)_{II}$, that have been developed in Chapter III. The performance evaluation of any non-linear receiver (i.e., detector) is, analytically, a difficult problem. Furthermore, non-Gaussianity of the noise and dependence between samples increase the difficulty.

In general, as in the case of Neyman-Pearson detector and radar terminology, one can define the probability of detection and false alarm as:

$$P_{\text{det}} = \int_{\lambda}^{\infty} p(\mathrm{T}(\underset{\sim}{y}) / H_1)\, d\mathrm{T} \qquad (4.1-1)$$

$$P_{fa} \doteq \int_{\lambda}^{\infty} p(\mathrm{T}(\underline{\tilde{y}}) / H_0)\, d\mathrm{T} \qquad (4.1-2)$$

where $\mathrm{T}(\underline{\tilde{y}})$ is the test statistic (i.e., detector structure) with decision threshold of λ :

$$\mathrm{T}(\underline{\tilde{y}}) \underset{H_0}{\overset{H_1}{\gtrless}} \lambda \qquad (4.1-3)$$

Equations (4.1-1) and (4.1-2) require a priori knowledge of the density function of the test statistic $\mathrm{T}(\underline{\tilde{y}})$.

If the test statistic can be expressed, in terms of signal $\tilde{s}_i$ and measurement $\tilde{y}_i$, in a canonical form as:

$$\mathrm{T}(\underline{\tilde{y}}) = \sum_{i=1}^{M} G(\tilde{y}_i, \tilde{s}_i) \qquad (4.1-4)$$

and if the $G(\tilde{y}_i, \tilde{s}_i)$'s are statistically independent, then one can invoke the Central Limit Theorem. That is, asymptotically, as $(M \to \infty)$, $\mathrm{T}(\underline{\tilde{y}})$ has Gaussian distribution, and its mean and variance completely specify its density. In this case, equations (4.1-1) and (4.1-2) are reduced to :

$$P_{\mathrm{det}} = 1 - \Phi\{ \frac{\lambda - E(\mathrm{T}/H_1)}{\sqrt{Var(\mathrm{T}/H_1)}} \} \qquad (4.1-5)$$

$$P_{fa} = 1 - \Phi\{ \frac{\lambda - E(\mathrm{T}/H_0)}{\sqrt{Var(\mathrm{T}/H_0)}} \} \qquad (4.1-6)$$

where Φ is the Error function defined as:

$$\Phi(x) = \int_{-\infty}^{x} \frac{1}{\sqrt{2\pi}} e^{-\frac{1}{2}u^2} du \qquad (4.1-7)$$

If the noise samples are strongly dependent, the asymptotic normality of the test statistic can not be invoked. However, in the special case of weak dependence, under certain regularity conditions on the mean and variance, it can be shown that $\mathrm{T}(\underline{y})$ is asymptotically Normal [47]. In general, the threshold level, and P_{fa} can be evaluated by extensive simulation.

Although, the performance evaluation of a non-linear detector in terms of P_{fa} and P_{det} is difficult, there exists asymptotic technique to compare the performance of the two detectors. This is the main objective of this Chapter.

Since, the non-linear detectors under independent noise assumption have been investigated extensively, they will be compared with the detectors that have been developed in Chapter III. In Section (4.2), the criterion for performance measure is introduced. In Section (4.3), the $(LOD)_{II}$ is rederived by maximizing the performance measure. This is to show that, indeed, the LOD derived under Neyman-Pearson Lemma has optimal property under the performance measure. Sections (4.4) through (4.6) are devoted to the analytic evaluation of performance measures for the $(LOD)_I$ and $(LOD)_{II}$. Finally, numerical results concerning Weibull distribution are presented.

4.2. Efficacy, Pitman-Noether Theorem, and Asymptotic Relative Efficiency

This section is concerned with a brief introduction to the concepts of Efficacy and Asymptotic Relative Efficiency (ARE). As stated in the previous section, in general, knowledge of the density function of the non-linear test statistic is not available. In order to partially remedy the problem, and gain some insight into the characteristic of the test statistic, it is always possible to resort to the mean and variance of the test statistic. This idea has been used extensively, in classification and pattern recognition. A very general discussion of second-order measure of quality is given by Gardner [48].

For weak signal detection, embedded in noise, with a test statistic (T), a modified version of Signal to Noise Ratio, called " Differential SNR" (DSNR) has been introduced [48,49] as:

$$DSNR \equiv \frac{[\frac{\partial E(\mathrm{T}/H_1)}{\partial \theta}]^2_{\theta=0}}{Var(\mathrm{T}/H_1)|_{\theta=0}} \qquad (4.2-1)$$

This second-order measure is similar to the general definition of

" Efficacy " [11] as:

$$Efficacy(T_N) = \underset{\substack{\theta \to 0 \\ N \to \infty}}{Limit} \frac{\left[\frac{\partial E(T_N/H_1)}{\partial \theta}\right]^2}{N \; Var(T_N/H_0)} \qquad (4.2-2)$$

where T_N is the test statistics using (N) samples. Also, Martinez, et al.[17] define Efficacy for any test statistic by:

$$Efficacy(T) = \underset{\theta \to 0}{Limit} \frac{\left[\frac{\partial E_\theta(T)}{\partial \theta}\right]^2}{Var_\theta(T)} \qquad (4.2-3)$$

As noticed, equations (4.2-1),(4.2-2), and (4.2-3) convey the same information.

These three definitions are also very close to the "Contrast" or "Deflection" criterion [48,50] defined as:

$$C[T] = \frac{[E(T/H_1) - E(T/H_0)]^2}{Var[T/H_0]} \qquad (4.2-4)$$

which is proportional to the measure of separation between the centers of the two conditional probability density functions $p(T/H_1)$ and $p(T/H_0)$ (shift in mean). In the sequel, the definition of Martinez, et al.[17] for Efficacy , given by (4.2-3), will be adopted, and its relation with Contrast (Deflection) will be pointed out.

Next, to measure the relative performance of two detectors, the concept of Asymptotic Relative Efficiency (ARE) due to Pitman is required [51,52]. For weak signal condition and large sample-size data, the Asymptotic Efficiency of detector (T_1) relative to another detector (T_2) is defined as:

$$ARE^{\theta}_{T_1, T_2} = \underset{\substack{N_1 \to \infty \\ \theta \to 0}}{Limit}\ e(P_{fa}, \theta, N_1) = \underset{\substack{N_1 \to \infty \\ \theta \to 0}}{Limit}\ \left(\frac{N_2}{N_1}\right) \qquad (4.2-5)$$

where $e(P_{fa}, \theta, N_1)$ is the relative number of samples that detector T_2 requires to achieve the same P_{det} that T_1 achieves for sample size (N_1), when both T_1 and T_2 are operating with fixed (constant) probability of false alarm and the signal strength (θ). The limiting operation of ($\theta \to 0$) is carried out in such a manner that as ($N_1 \to \infty$) , the P_{det} converges to a number β such that: $P_{fa} < \beta < 1$.

Now, by Pitman-Noether Theorem [51,52], within certain regularity conditions, the ARE is given by the ratio of their Efficacies:

$$(ARE)_{T_1, T_2} = \frac{Efficacy(T_1)}{Efficacy(T_2)} \qquad (4.2-6)$$

Equations (4.2-3) and (4.2-6) are the required definitions for the performance evaluation and comparison of two detectors.

To motivate the concept of ARE and its relation with Efficacy, and obtain some insight into the problem, consider the special case of Gaussian distributed test statistic. Let (T) be the test statistic of a detector which is operating with the probability of false alarm, $P_{fa} = \alpha$, and the probability of detection, $P_{\text{det}} = \beta$. That is:

$$\beta = 1 - \Phi\{ \frac{\alpha - E(\mathrm{T}/H_1)}{\sqrt{Var(\mathrm{T}/H_1)}} \} \qquad (4.2 - 7)$$

$$\alpha = 1 - \Phi\{ \frac{\alpha - E(\mathrm{T}/H_0)}{\sqrt{Var(\mathrm{T}/H_0)}} \} \qquad (4.2 - 8)$$

where Φ is the Error function defined as:

$$\Phi(x) = \int_{-\infty}^{x} \frac{1}{\sqrt{2\pi}} e^{-\frac{1}{2}u^2} du \qquad (4.2 - 9)$$

Equations (4.2-7) and (4.2-8) can be combined to obtain:

$$\beta = 1 - \Phi\{ \frac{\sqrt{Var(T/H_0)}\,\Phi^{-1}(1 - \alpha) + E(T/H_0) - E(T/H_1)}{\sqrt{Var(T/H_1)}} \} \qquad (4.2 - 10)$$

Now, consider two detectors with test statistics T_1 and T_2 , with corresponding sample sizes N_1 and N_2 , such that they achieve the same $P_{\text{det}} = \beta$ under $P_{fa} = \alpha$. After some algebraic manipulation, it can be shown [53] that the following relation holds:

$$\frac{\overline{N_2}}{\sqrt{N_1}} = \left[\frac{(\mu_1/H_1) - (\mu_1/H_0)}{(\mu_2/H_1) - (\mu_2/H_0)}\right]\left[\frac{(\sigma_2/H_1)}{(\sigma_1/H_1)}\right] - \frac{\Phi^{-1}(1-\alpha)}{\sqrt{N_1}} \frac{(\sigma_2/H_1)}{(\mu_2/H_1) - (\mu_2/H_0)}$$

$$\left[\frac{(\sigma_1/H_0)}{(\sigma_1/H_1)} - \frac{(\sigma_2/H_0)}{(\sigma_2/H_1)}\right] \qquad (4.2-11)$$

where (μ_i) and (σ_i) are the mean and the standard deviation of the samples of the test statistic under (H_i) hypothesis. This implicitly assumes that the test statistic is the sum of independent random variables with equal mean and variance. Now, consider equation (4.2-11), and let $N_1 \to \infty$:

$$\underset{N_1 \to \infty}{Limit} \left(\frac{N_2}{N_1}\right) = \left[\frac{(\mu_1/H_1) - (\mu_1/H_0)}{(\mu_2/H_1) - (\mu_2/H_0)}\right]^2 \frac{(\sigma_2^2/H_1)}{(\sigma_1^2/H_1)} \qquad (4.2-12)$$

If, $\theta \to 0$, then equation (4.2-12) can be written as:

$$\underset{\substack{N_1 \to \infty \\ \theta \to 0}}{Limit} \left(\frac{N_2}{N_1}\right) = \frac{\dfrac{[(\mu_1/H_1) - (\mu_1/H_0)]^2}{(\sigma_1^2/H_0)}}{\dfrac{[(\mu_2/H_1) - (\mu_2/H_0)]^2}{(\sigma_2^2/H_0)}} \qquad (4.2-13)$$

which is identical to the ratio of their Contrasts (Deflections).

In order to relate the ratio of Contrasts of two detectors to the ratio of Efficacies, consider the following truncated Taylor series expansion:

$$E\{T/H_1\} \cong E\{T/H_0\} + \theta \frac{d}{d\theta} E\{T/H_1\}|_{\theta=0} \qquad (4.2-14)$$

where (θ) is assumed to be small (weak signal), and (T) is the test statistic of the operating detector. By definition of Contrast, given by (4.2-4), equation (4.2-14) can be written as:

$$\frac{[E(T/H_1) - E(T/H_0)]^2}{Var[T/H_0]} \cong \theta^2 \frac{[\frac{d}{d\theta} E\{T/H_1\}|_{\theta=0}]^2}{Var\{T/H_0\}} \qquad (4.2-15)$$

Substitution of (4.2-15) into (4.2-13) results in:

$$\underset{\substack{N_1 \to \infty \\ \theta \to 0}}{Limit} \left(\frac{N_2}{N_1}\right) = \frac{\frac{[\frac{d}{d\theta} E\{T_1/H_1\}|_{\theta=0}]^2}{Var\{T_1/H_0\}}}{\frac{[\frac{d}{d\theta} E\{T_2/H_1\}|_{\theta=0}]^2}{Var\{T_2/H_0\}}} \qquad (4.2-16)$$

The right hand side of equation (4.2-16) is the ratio of Efficacy of two detectors. Thus, assuming that the approximation in (4.2-14) is justified, the ratio of Contrasts is identical to the ratio of Efficacies. This type of reasoning gives some mathematical framework and intuitive justification to use the ARE for performance evaluation.

It should be noted that, by application of (4.2-13), two types of error are incurred. First, the test statistic is, in general, non-Gaussian, and second, the sample size (N_1) is finite. Although, this is a special case of Gaussian test statistic, the

underlying idea of performance measure as the ratio of their Efficacies has been applied to the case of non-Gaussian test statistic.

In the next section, $(LOD)_{II}$ will be rederived by maximizing Efficacy, and thus proving that the Generalized Neyman-Pearson Lemma and Maximum Efficacy Detector yield the same non-linear detector structure.

4.3. Locally Optimum Detector with Maximum Efficacy

In this section, the Locally Optimum Detector structure, for complex multivariate noise and complex density model, $(LOD)_{II}$, is developed by maximum Efficacy criteria. This is important, since it gives a unifying view of the optimality of the Generalized Neyman-Pearson Lemma and Efficacy.

The detection problem can be formulated as:

$$H_0 : \underline{\tilde{y}} = \underline{\tilde{n}} \qquad (4.3-1)$$

$$H_1 : \underline{\tilde{y}} = \underline{\tilde{n}} + \theta\,\underline{\tilde{s}} \qquad (4.3-2)$$

where $\underline{\tilde{n}} \equiv [\tilde{n}_1, ..., \tilde{n}_M]^T$, $\underline{\tilde{s}} \equiv [\tilde{s}_1, ..., \tilde{s}_M]^T$, and $\underline{\tilde{y}} \equiv [\tilde{y}_1, ...\tilde{y}_M]^T$ are the M-vector complex noise, signal, and measured samples respectively. As before, the parameter (θ) is a real positive constant, representing the amplitude of the signal, and assumed to be vanishingly small ($\theta \rightarrow 0$) .

It is assumed that there exist a non-linear detector $T(\underline{\tilde{y}})$, operating on $(\underline{\tilde{y}})$. The scalar-valued test statistic is compared to a threshold level (λ) , to decide between H_0 and H_1 . The Efficacy of $T(\underline{\tilde{y}})$ is defined from (4.2-3) to be:

$$Efficacy(\,T(\underline{\tilde{y}})\,) = \underset{\theta \rightarrow 0}{Limit} \frac{[\,\frac{\partial\, E_\theta(T(\underline{\tilde{y}}))}{\partial\,\theta}\,]^2}{Var_\theta(T(\underline{\tilde{y}}))} \qquad (4.3-3)$$

It is desired to obtain a $T(\underline{\tilde{y}})$ which maximizes this quantity.

Since $T(\underline{\tilde{y}})$ is independent of (θ) , one can express (4.3-3) as:

$$Efficacy(\,T(\underline{\tilde{y}})\,) \;=\; \frac{[\,\int\, T(\underline{\tilde{y}})\;\{\;\frac{\partial\, p_{\underline{n}}(\underline{\tilde{y}}\;-\;\theta\underline{\tilde{s}})}{\partial\,\theta}\;\}_{\theta=0}\;d\underline{\tilde{y}}\;]^2}{Var[\,T(\underline{\tilde{y}})\,/H_0\,]} \qquad (4.3-4)$$

where $p_{\underline{n}}(\underline{\tilde{y}}\;-\;\theta\underline{\tilde{s}}) \;=\; p(\underline{\tilde{y}}/H_1)$ and is defined to be the joint multivariate in-phase and quadrature phase components density as:

$$p_{\underline{n}}(\underline{\tilde{y}}\;-\;\theta\underline{\tilde{s}}) \;=\; p_{\underline{n}}(\underline{y}_I\;-\;\theta\underline{s}_I, \underline{y}_Q\;-\;\theta\underline{s}_Q) \qquad (4.3-5)$$

Then, using (4.3-5), one can easily obtain:

$$\{\;\frac{\partial\, p_{\underline{n}}(\underline{\tilde{y}}\;-\;\theta\underline{\tilde{s}})}{\partial\,\theta}\;\}_{\theta=0} \;=\; \sum_{i=1}^{M} -\,s_{I_i}\,\frac{\partial\, p_{\underline{n}}(\underline{y}_I, \underline{y}_Q)}{\partial\, y_{I_i}} \;-\; s_{Q_i}\,\frac{\partial\, p_{\underline{n}}(\underline{y}_I, \underline{y}_Q)}{\partial\, y_{Q_i}}$$

$$=\;\; -\,\underline{s}_I^T\;\nabla_{\underline{y}_I}\;p_{\underline{n}}(\underline{\tilde{y}}) \;-\; \underline{s}_Q^T\;\nabla_{\underline{y}_Q}\;p_{\underline{n}}(\underline{\tilde{y}}) \qquad (4.3-6)$$

where $\nabla_{\underline{y}_I}$ and $\nabla_{\underline{y}_Q}$ are Gradient of the noise density function with respect to the in-phase and quadrature phase components. Thus, (4.3-4) can be expressed as:

$$Efficacy(\,T(\underline{\tilde{y}})\,) \;=\; \frac{[\,E\;\{\;T(\underline{\tilde{y}})\;(\;-\,\underline{s}_I^T\;\frac{\nabla_{\underline{y}_I}\;p_{\underline{n}}(\underline{\tilde{y}})}{p_{\underline{n}}(\underline{\tilde{y}})} \;-\; \underline{s}_Q^T\;\frac{\nabla_{\underline{y}_Q}\;p_{\underline{n}}(\underline{\tilde{y}})}{p_{\underline{n}}(\underline{\tilde{y}})}\;)\;\}\;]^2}{Var[\,T(\underline{\tilde{y}})\,/H_0\,]}$$

$$(4.3-7)$$

At this point, one can apply the correlation inequality [54] to the numerator of equation (4.3-7) as:

$$[\, E\{\, T(\tilde{\underline{y}})\, (\, -\underline{s}_I^T \frac{\nabla_{\underline{y}_I}\, p_{\underline{n}}^{-}(\tilde{\underline{y}})}{p_{\underline{n}}^{-}(\tilde{\underline{y}})} - \underline{s}_Q^T \frac{\nabla_{\underline{y}_Q}\, p_{\underline{n}}^{-}(\tilde{\underline{y}})}{p_{\underline{n}}^{-}(\tilde{\underline{y}})}\,)\, \}\,]^2 \leq E[\, T^2(\tilde{\underline{y}})\,]$$

$$E\, [\, \{\, -\underline{s}_I^T \frac{\nabla_{\underline{y}_I}\, p_{\underline{n}}^{-}(\tilde{\underline{y}})}{p_{\underline{n}}^{-}(\tilde{\underline{y}})} - \underline{s}_Q^T \frac{\nabla_{\underline{y}_Q}\, p_{\underline{n}}^{-}(\tilde{\underline{y}})}{p_{\underline{n}}^{-}(\tilde{\underline{y}})}\, \}^2\,] \qquad (4.3-8)$$

with equality if:

$$T(\tilde{\underline{y}}) = k\, \{\, -\underline{s}_I^T \frac{\nabla_{\underline{y}_I}\, p_{\underline{n}}^{-}(\tilde{\underline{y}})}{p_{\underline{n}}^{-}(\tilde{\underline{y}})} - \underline{s}_Q^T \frac{\nabla_{\underline{y}_Q}\, p_{\underline{n}}^{-}(\tilde{\underline{y}})}{p_{\underline{n}}^{-}(\tilde{\underline{y}})}\, \} \qquad (4.3-9)$$

where (k) is a constant. Now, the value of the mean of (4.3-6) is:

$$E\, \{\, -\underline{s}_I^T \frac{\nabla_{\underline{y}_I}\, p_{\underline{n}}^{-}(\tilde{\underline{y}})}{p_{\underline{n}}^{-}(\tilde{\underline{y}})} - \underline{s}_Q^T \frac{\nabla_{\underline{y}_Q}\, p_{\underline{n}}^{-}(\tilde{\underline{y}})}{p_{\underline{n}}^{-}(\tilde{\underline{y}})}\, \} =$$

$$-\underline{s}_I^T \int \nabla_{\underline{y}_I} p_{\underline{n}}^{-}(\tilde{\underline{y}})\, d\tilde{\underline{y}} - \underline{s}_Q^T \int \nabla_{\underline{y}_Q} p_{\underline{n}}^{-}(\tilde{\underline{y}})\, d\tilde{\underline{y}} = 0 \qquad (4.3-10)$$

since:

$$\int \nabla_{\underline{y}_I} p_{\underline{n}}(\tilde{\underline{y}})\, d\tilde{\underline{y}} = 0 \qquad (4.3-11)$$

$$\int \nabla_{\underline{y}_Q} p_{\underline{n}}(\tilde{\underline{y}})\, d\tilde{\underline{y}} = 0 \qquad (4.3-12)$$

Therefore, equation (4.3-7) reduces to :

$$Efficacy(\,T(\tilde{\underline{y}})\,) = \frac{Cov\,\{\,T(\tilde{\underline{y}})\,(\,-\underline{s}_I^T \frac{\nabla_{\underline{y}_I} p_{\underline{n}}(\tilde{\underline{y}})}{p_{\underline{n}}(\tilde{\underline{y}})} - \underline{s}_Q^T \frac{\nabla_{\underline{y}_Q} p_{\underline{n}}(\tilde{\underline{y}})}{p_{\underline{n}}(\tilde{\underline{y}})}\,)\,\}}{E[\,T^2(\tilde{\underline{y}})\,/H_0\,]}$$

$$\leq E\left[\,\{\,-\underline{s}_I^T \frac{\nabla_{\underline{y}_I} p_{\underline{n}}(\tilde{\underline{y}})}{p_{\underline{n}}(\tilde{\underline{y}})} - \underline{s}_Q^T \frac{\nabla_{\underline{y}_Q} p_{\underline{n}}(\tilde{\underline{y}})}{p_{\underline{n}}(\tilde{\underline{y}})}\,\}^2\,\right] \qquad (4.3-13)$$

With the condition of equality from (4.3-9), and the fact that $E\{T(\tilde{\underline{y}})\}$ is zero, one obtains the maximum Efficacy (k = 1) as:

$$T(\tilde{\underline{y}}) = \{\,-\underline{s}_I^T \frac{\nabla_{\underline{y}_I} p_{\underline{n}}(\tilde{\underline{y}})}{p_{\underline{n}}(\tilde{\underline{y}})} - \underline{s}_Q^T \frac{\nabla_{\underline{y}_Q} p_{\underline{n}}(\tilde{\underline{y}})}{p_{\underline{n}}(\tilde{\underline{y}})}\,\} \qquad (4.3-14)$$

which is the same as equation (3.4-7). Thus maximizing Efficacy leads to the same non-linear structure as the Generalized Neyman-Pearson Lemma. Intuitively, this means that maximizing SNR is the same as maximizing P_{det} .

Although, in this section, only $(LOD)_{II}$ has been considered, one can apply the same method to other Hypothesis Testing models, and obtain the corre-

sponding structure for $(LOD)_I$. In the next two sections, Efficacy of $(LOD)_I$ and $(LOD)_{II}$ will be derived.

4.4. Efficacy for LOD with Complex Noise and Amplitude Density Model

This section is concerned with the derivation of an analytic expression for the Efficacy of the $(LOD)_I$. Later, this expression will be applied to evaluate the relative performance of $(LOD)_I$ with other types of detectors. The expression for $(LOD)_I$, from (3.3-12), written as the test statistic, T_I , is:

$$(\mathrm{T})_I = \sum_{i=1}^{M}\sum_{j=1}^{M} \alpha_{ij} \frac{Real(\tilde{y}_i\ \tilde{s}_i^*)}{|\tilde{y}_i|} g'(|\tilde{y}_i|)\ g(|\tilde{y}_j|)$$

$$- \sum_{i=1}^{M} \frac{Real(\tilde{y}_i\ \tilde{s}_i^*)}{|\tilde{y}_i|}\ \frac{g''(|\tilde{y}_i|)}{g'(|\tilde{y}_i|)} \qquad (4.4-1)$$

and the expression for the calculation of Efficacy from (4.2-3) can be written as:

$$Efficacy(\mathrm{T}_I) = \underset{\theta \to 0}{Limit} \frac{[\frac{\partial E(\mathrm{T}_I/H_1)}{\partial \theta}]^2}{Var(\mathrm{T}_I/H_0)} \qquad (4.4-2)$$

First, the numerator of the Efficacy expression is evaluated by defining E_i and E_s as a measure of signal energy as:

$$E_i \equiv s_{I_i}^2 + s_{Q_i}^2 \qquad (4.4-3)$$

$$E_s \equiv \sum_{i=1}^{M} E_i \qquad (4.4-4)$$

Under the hypothesis H_1, one can express:

$$Real(\tilde{y}_i \tilde{s}_i^*) = \theta E_i + R_i(s_{I_i} \cos \varphi_i + s_{Q_i} \sin \varphi_i) \qquad (4.4-5)$$

where R_i and φ_i are the amplitude and phase of the complex noise sample defined as:

$$\tilde{n}_i = n_{I_i} + j n_{Q_i} = R_i e^{j\varphi_i} \qquad (4.4-6)$$

Using the notations E_i , R_i , φ_i , and after some algebraic manipulation, one can show:

$$\frac{\partial T_I}{\partial \theta}\Big|_{\theta=0} = \sum_{i=1}^{M}\sum_{j=1}^{M} \alpha_{ij}\, g'(R_i)\; g'(R_j)\; (s_{I_i} \cos \varphi_i + s_{Q_i} \sin \varphi_i)$$

$$(s_{I_j} \cos \varphi_j + s_{Q_j} \sin \varphi_j) + \sum_{i=1}^{M}\sum_{j=1}^{M} \alpha_{ij}\, g(R_i)\; (s_{I_j} \cos \varphi_j + s_{Q_j} \sin \varphi_j)^2$$

$$[g''(R_j) - \frac{g'(R_j)}{R_j}] + \sum_{i=1}^{M}\sum_{j=1}^{M} \alpha_{ij} E_j [\frac{g(R_i)\, g'(R_j)}{R_j}] - \sum_{i=1}^{M} E_i [\frac{g''(R_i)}{g'(R_i)} \frac{1}{R_i}]$$

$$+ \sum_{i=1}^{M} (s_{I_i} \cos \varphi_i + s_{Q_i} \sin \varphi_i)^2 [\frac{g''^2(R_i)}{g'^2(R_i)} + \frac{g''(R_i)}{g'(R_i)} - \frac{g^{(3)}(R_i)}{g'(R_i)}] \qquad (4.4-7)$$

The first step in calculation of the expectation of the test statistic is to integrate the phase. Since, the phase is assumed to be uniformly distributed, one obtains:

$$\frac{1}{(2\pi)^2}\int_0^{2\pi} d\varphi_i \int_0^{2\pi} d\varphi_j \left\{ \frac{\partial T_I}{\partial\theta}\Big|_{\theta=0} \right\} = \frac{1}{2}\left\{ \sum_{i=1}^{M} E_i\, \alpha_{ii}\, g'^2(R_i) \right.$$

$$+ \sum_{i=1}^{M} E_i \left[\frac{g''^2(R_i)}{g'^2(R_i)} - \frac{g''(R_i)}{R_i\, g'(R_i)} - \frac{g^{(3)}(R_i)}{g'(R_i)} \right]$$

$$\left. + \sum_{i=1}^{M}\sum_{j=1}^{M} E_j\, \alpha_{ij} \left[g(R_i)\, g''(R_j) + \frac{g(R_i)\, g'(R_j)}{R_j} \right] \right\} \qquad (4.4-8)$$

Now, integrating the random variables R_i and R_j with joint density function $p(R_i, R_j)$, one obtains:

$$E\left\{ \frac{\partial T_I}{\partial\theta}\Big|_{\theta=0} \right\} = \frac{1}{2}\left\{ \sum_{i=1}^{M} E_i\, \alpha_{ii} \int_0^{\infty} dR_i\, g'^2(R_i)\, p(R_i) \right.$$

$$+ \sum_{i=1}^{M} E_i \int_0^{\infty} dR_i \left[\frac{g''^2(R_i)}{g'^2(R_i)} - \frac{g''(R_i)}{R_i\, g'(R_i)} - \frac{g^{(3)}(R_i)}{g'(R_i)} \right] p(R_i)$$

$$\left. + \sum_{i=1}^{M}\sum_{j=1}^{M} E_j\, \alpha_{ij} \int_0^{\infty} dR_i \int_0^{\infty} dR_j \left[g(R_i)\, g''(R_j) + \frac{g(R_i)\, g'(R_j)}{R_j} \right] p(R_i, R_j) \right\}$$

$$(4.4-9)$$

Since, the expression in (4.4-9) consists of double sum expression, care is required to distinguish between $(i \neq j)$ and $(i = j)$. In the case, when $(i = j)$, $p(R_i, R_j)$ collapses to $p(R_i)$. Taking this case into consideration, one obtains:

$$E \{ \frac{\partial T_I}{\partial \theta} |_{\theta=0} \} =$$

$$\frac{1}{2} \{ \sum_{i=1}^{M} \sum_{\substack{j=1 \\ j \neq i}}^{M} \alpha_{ij} E_j \int_0^\infty dx \int_0^\infty dy \left[g(x)\, g''(y) + \frac{g(x)g'(y)}{y} \right] p_{ij}(x,y) \}$$

$$+ \frac{1}{2} \{ \sum_{i=1}^{M} \alpha_{ii} E_i \int_0^\infty dx \left[g(x)\, g''(x) + \frac{g(x)\, g'(x)}{x} \right] p(x) \}$$

$$+ \frac{1}{2} \{ \sum_{i=1}^{M} E_i \int_0^\infty dx \left[\frac{g''^2(x)}{g'^2(x)} - \frac{g''(x)}{x\, g'(x)} - \frac{g^{(3)}(x)}{g'(x)} \right] p(x) \}$$

$$+ \frac{1}{2} \sum_{i=1}^{M} \alpha_{ii} E_i \int_0^\infty dx\, g'^2(x)\, p(x)\, dx \qquad (4.4-10)$$

Next, the denominator of (4.4-2) should be evaluated. By integrating the phase, it can be easily shown:

$$E \{ T_I / H_0 \} = 0$$

Thus, variance of the test statistic is identical to its second order moment: $E(T_I^2/H_0)$. The square of the test statistic is given by:

$$(T_I^2/H_0) = \sum_{i=1}^{M}\sum_{j=1}^{M}\sum_{k=1}^{M}\sum_{l=1}^{M} \alpha_{ij}\ \alpha_{kl}\ g(R_j)\ g'(R_i)\ g(R_l)\ g'(R_k)$$

$$(s_{I_i}\cos\varphi_i + s_{Q_i}\sin\varphi_i)\ (s_{I_k}\cos\varphi_k + s_{Q_k}\sin\varphi_k) + \sum_{i=1}^{M}\sum_{j=1}^{M}$$

$$(s_{I_i}\cos\varphi_i + s_{Q_i}\sin\varphi_i)\ (s_{I_j}\cos\varphi_j + s_{Q_j}\sin\varphi_j)\ \left[\frac{g''(R_i)\ g''(R_j)}{g'(R_i)\ g'(R_j)}\right]$$

$$-2\sum_{i=1}^{M}\sum_{j=1}^{M}\sum_{k=1}^{M} \alpha_{ij}\ (s_{I_i}\cos\varphi_i + s_{Q_i}\sin\varphi_i)\ (s_{I_k}\cos\varphi_k + s_{Q_k}\sin\varphi_k)$$

$$\left[\ g(R_j)\ g'(R_i)\frac{g''(R_k)}{g'(R_k)}\ \right] \qquad (4.4-11)$$

After some careful algebraic manipulation, one can integrate the phase in (4.4-11) and obtain:

$$\frac{1}{(2\pi)^4}\int_0^{2\pi} d\varphi_i\ \int_0^{2\pi} d\varphi_j\ \int_0^{2\pi} d\varphi_k\ \int_0^{2\pi} d\varphi_l\ (T_I^2/H_0) =$$

$$\frac{1}{2}\sum_{i=1}^{M}\sum_{j=1}^{M}\sum_{k=1}^{M} E_i\ (\alpha_{ij}\ \alpha_{ik})\ g'^2(R_i)\ g(R_j)\ g(R_k)$$

$$-\sum_{i=1}^{M}\sum_{j=1}^{M} E_i\ (\alpha_{ij})\ g''(R_i)\ g(R_j) + \frac{1}{2}\sum_{i=1}^{M} E_i\left[\frac{g''^2(R_i)}{g'^2(R_i)}\right]$$

$$(4.4-12)$$

Integrating the random variables R_i, R_j, and R_k in (4.4-12), one obtains:

$$Var\{(T_I^2 / H_0)\} =$$

$$\frac{1}{2} \sum_{i=1}^{M} \sum_{j=1}^{M} \sum_{k=1}^{M} E_i \, \alpha_{ij} \, \alpha_{ik} \int_0^\infty dx \int_0^\infty dy \int_0^\infty dz \; g'^2(x) \; g(y) \; g(z) \; p_{ijk}(x, y, z)$$

$$- \sum_{i=1}^{M} \sum_{j=1}^{M} E_i \, \alpha_{ij} \int_0^\infty dx \int_0^\infty dy \; g''(x) \; g(y) \; p_{ij}(x, y)$$

$$+ \frac{1}{2} \sum_{i=1}^{M} E_i \int_0^\infty dx \; \frac{g''^2(x)}{g'^2(x)} \; p(x) \qquad (4.4 - 13)$$

where $p_{ij}(x, y)$ and $p_{ijk}(x, y, z)$ are ordered bivariate and trivariate non-Gaussian density functions. However, as before, special care is required to treat the triple sum and double sum cases. That is, $p_{ijk}(x, y, z)$ reduces to $p_{ij}(x, y)$, $p_{ik}(x, z)$, $p_{jk}(y, z)$, and $p(x)$ if (j=k), (j=i), (i=k), and (i=j=k) respectively. After taking the special cases into consideration, equation (4.4-13) reduces to:

$$Var\{T_I^2/H_0\} =$$

$$+ \frac{1}{2} \sum_{i=1}^{M} \sum_{\substack{j=1 \\ j \neq i}}^{M} \sum_{\substack{k=1 \\ k \neq j \\ k \neq i}}^{M} E_i \, (\alpha_{ij} \alpha_{ik}) \int_0^\infty dx \int_0^\infty dy \int_0^\infty dz \; g'^2(x) \; g(y) \; g(z) \; p_{ijk}(x, y, z)$$

$$+ \frac{1}{2} \sum_{i=1}^{M} \sum_{\substack{j=1 \\ j \neq i}}^{M} E_i \, (\alpha_{ij})^2 \int_0^\infty dx \int_0^\infty dy \; g'^2(x) \; g^2(y) \; p_{ij}(x,y)$$

$$+ \sum_{i=1}^{M} \sum_{\substack{j=1 \\ j \neq i}}^{M} E_i \, \alpha_{ii} \, \alpha_{ij} \int_0^\infty dx \int_0^\infty dy \; g'^2(x) \; g(x) \; g(y) \; p_{ij}(x,y)$$

$$- \sum_{i=1}^{M} \sum_{\substack{j=1 \\ j \neq i}}^{M} E_i \alpha_{ij} \int_0^\infty dx \int_0^\infty dy \; g''(x) \; g(y) \; p_{ij}(x,y)$$

$$+ \frac{1}{2} \sum_{i=1}^{M} E_i \, (\alpha_{ii})^2 \int_0^\infty dx \; g'^2(x) \; g^2(x) \; p(x)$$

$$- \sum_{i=1}^{M} E_i \, \alpha_{ii} \int_0^\infty dx \; g''(x) g(x) \; p(x) \; + \; \frac{1}{2} \sum_{i=1}^{M} E_i \int_0^\infty dx \; \frac{g''^2(x)}{g'^2(x)} \; p(x)$$

(4.4 − 14)

Equations (4.4-10) and (4.4-14) are the required equations for the calculation of Efficacy. These two equations will be used in section (4.7) with specific density function for numerical evaluation. As noticed, the required information is the measure of signal energy, E_i , the covariance structure of the samples (related to α_{ij}), and the non-linearities g(.), g′(.), and g″(.), which are Gaussian random variables. Finally, $p_{ijk}(x,y,z)$ is obtained from the modeling of the joint multivariate non-Gaussian density, Model (I), as discussed in Chapter II.

4.5. Efficacy for LOD with Complex Noise and Complex Density Model

This section deals with the derivation of an analytic expression for the Efficacy of the $(LOD)_{II}$. The expression for $(LOD)_{II}$, from (3.4-17) written as the test statistic, T_{II} , is:

$$(T)_{II} = \sum_{i=1}^{M}\sum_{j=1}^{M} \alpha_{ij} \frac{Real(\tilde{y}_i \tilde{s}_i^*)}{|\tilde{y}_i|} g'(|\tilde{y}_i|)\ g(|\tilde{y}_j|)$$

$$- \sum_{i=1}^{M} \frac{Real(\tilde{y}_i \tilde{s}_i^*)}{|\tilde{y}_i|} \left[\frac{g''(|\tilde{y}_i|)}{g'(|\tilde{y}_i|)} - \frac{1}{|\tilde{y}_i|}\right] \qquad (4.5-1)$$

and, as before, the expression for the calculation of Efficacy from (4.2-3) can be written as:

$$Efficacy(T_{II}) = \underset{\theta \to 0}{Limit} \frac{\left[\frac{\partial E(T_{II}/H_1)}{\partial \theta}\right]^2}{Var(T_{II}/H_0)} \qquad (4.5-2)$$

As in section (4.4), the measure of signal energy is defined as:

$$E_i \equiv s_{I_i}^2 + s_{Q_i}^2 \qquad (4.5-3)$$

and

$$E_s \equiv \sum_{i=1}^{M} E_i \qquad (4.5-4)$$

Also, the complex noise sample is defined as:

$$\tilde{n}_i = n_{I_i} + j n_{Q_i} = R_i e^{j\varphi_i} \qquad (4.5-5)$$

In order to calculate the Efficacy, first the numerator is evaluated. Using, E_i , R_i , and φ_i as defined in (4.5-3) and (4.5-5), one can obtain:

$$\frac{\partial T_{II}}{\partial\theta}|_{\theta=0} = \sum_{i=1}^{M}\sum_{j=1}^{M} \alpha_{ij}\, g'(R_i)\; g'(R_j)\; (s_{I_i}\cos\varphi_i + s_{Q_i}\sin\varphi_i)$$

$$(s_{I_j}\cos\varphi_j + s_{Q_j}\sin\varphi_j) + \sum_{i=1}^{M}\sum_{j=1}^{M} \alpha_{ij}\, g(R_i)\; (s_{I_j}\cos\varphi_j + s_{Q_j}\sin\varphi_j)^2$$

$$[g''(R_j) - \frac{g'(R_j)}{R_j}] + \sum_{i=1}^{M}\sum_{j=1}^{M} \alpha_{ij}\, E_j[\frac{g(R_i)\, g'(R_j)}{R_j}] - \sum_{i=1}^{M} E_i[\frac{g''(R_i)}{g'(R_i)}\frac{1}{R_i}]$$

$$+ \sum_{i=1}^{M} (s_{I_i}\cos\varphi_i + s_{Q_i}\sin\varphi_i)^2\, [\frac{g''^2(R_i)}{g'^2(R_i)} + \frac{g''(R_i)}{g'(R_i)} - \frac{g^{(3)}(R_i)}{g'(R_i)}] \qquad (4.5-6)$$

Integrating the uniformly distributed phase, and the amplitude of the multivariate non-Gaussian noise, one obtains:

$$E\{\frac{\partial T_{II}}{\partial\theta}|_{\theta=0}\} =$$

$$\frac{1}{2}\{\sum_{\substack{i=1\\ j\neq i}}^{M}\sum_{j=1}^{M} \alpha_{ij}\, E_j \int_0^\infty dx \int_0^\infty dy\, [\, g(x)\, g''(y) + \frac{g(x)g'(y)}{y}\,]\, p_{ij}(x,y)\}$$

$$+\frac{1}{2}\{\sum_{i=1}^{M}\alpha_{ii}E_i\int_0^{\infty}dx\ [\ g(x)\,g''(x)\ +\ \frac{g(x)\,g'(x)}{x}\ ]\ p(x)\ \}$$

$$+\frac{1}{2}\{\sum_{i=1}^{M}E_i\int_0^{\infty}dx\ \ [\frac{g''^2(x)}{g'^2(x)}\ -\ \frac{g''(x)}{x\,g'(x)}\ -\ \frac{g^{(3)}(x)}{g'(x)}]\ p(x)\ \}$$

$$+\ \frac{1}{2}\sum_{i=1}^{M}\alpha_{ii}\ E_i\int_0^{\infty}dx\ g'^2(x)\ p(x)\ dx \qquad (4.5-7)$$

Next, the denominator of the Efficacy should be calculated. By integrating the uniformly distributed phase, it can be easily shown:

$$E\ \{\ T_{II}/H_0\ \}\ =\ 0$$

Thus, the variance of the test statistic is identical to its second-order moment $E(T_{II}^2/H_0)$. To calculate the second-order moment, first consider:

$$(T_{II}^2/H_0)\ =\ \sum_{i=1}^{M}\sum_{j=1}^{M}\sum_{k=1}^{M}\sum_{l=1}^{M}\alpha_{ij}\ \alpha_{kl}\ g(R_j)\ g'(R_i)\ g(R_l)\ g'(R_k)$$

$$(s_{I_i}\cos\varphi_i\ +\ s_{Q_i}\sin\varphi_i)\ (s_{I_k}\cos\varphi_k\ +\ s_{Q_k}\sin\varphi_k)\ +\ \sum_{i=1}^{M}\sum_{j=1}^{M}$$

$$(s_{I_i}\cos\varphi_i\ +\ s_{Q_i}\sin\varphi_i)\ (s_{I_j}\cos\varphi_j\ +\ s_{Q_j}\sin\varphi_j)$$

$$[\ \frac{1}{R_i}\ -\ \frac{g''(R_i)}{g'(R_i)}\ ]\ [\ \frac{1}{R_j}\ -\ \frac{g''(R_j)}{g'(R_j)}\ ]$$

$$- 2 \sum_{i=1}^{M} \sum_{j=1}^{M} \sum_{k=1}^{M} \alpha_{ij} \, (s_{I_i} \cos \varphi_i + s_{Q_i} \sin \varphi_i) \, (s_{I_k} \cos \varphi_k + s_{Q_k} \sin \varphi_k)$$

$$[\; g(R_j) \, g'(R_i) \;] \; [\; \frac{1}{R_k} - \frac{g''(R_k)}{g'(R_k)} \;] \qquad (4.5 - 8)$$

After some careful algebraic manipulation, one can integrate the phase in (4.5-8) and obtain:

$$\frac{1}{(2\pi)^4} \int_0^{2\pi} d\varphi_i \int_0^{2\pi} d\varphi_j \int_0^{2\pi} d\varphi_k \int_0^{2\pi} d\varphi_l \, (T_{II}^2 / H_0) \; =$$

$$\frac{1}{2} \sum_{i=1}^{M} \sum_{j=1}^{M} \sum_{k=1}^{M} E_i \, (\alpha_{ij} \, \alpha_{ik}) \, g'^2(R_i) \, g(R_j) \, g(R_k)$$

$$- \sum_{i=1}^{M} \sum_{j=1}^{M} E_i \, (\alpha_{ij}) \, g'(R_i) \, g(R_j) \, [\; \frac{1}{R_i} - \frac{g''(R_i)}{g'(R_i)} \;]$$

$$+ \frac{1}{2} \sum_{i=1}^{M} E_i \, [\; \frac{1}{R_i} - \frac{g''(R_i)}{g'(R_i)} \;]^2 \qquad (4.5 - 9)$$

Integrating the random variables R_i, R_j , and R_k in (4.5-9), one obtains:

$$Var \{ (T_{II}^2 / H_0) \} \; =$$

$$\frac{1}{2} \sum_{i=1}^{M} \sum_{j=1}^{M} \sum_{k=1}^{M} E_i \, \alpha_{ij} \, \alpha_{ik} \int_0^{\infty} dx \int_0^{\infty} dy \int_0^{\infty} dz \; g'^2(x) \, g(y) \, g(z) \; p_{ijk}(x, y, z)$$

$$- \sum_{i=1}^{M} \sum_{j=1}^{M} E_i \, \alpha_{ij} \int_0^\infty dx \int_0^\infty dy \left[\frac{1}{x} - \frac{g''(x)}{g'(x)} \right] p_{ij}(x,y)$$

$$+ \frac{1}{2} \sum_{i=1}^{M} E_i \int_0^\infty dx \left[\frac{1}{x} - \frac{g''(x)}{g'(x)} \right]^2 p(x) \qquad (4.5-10)$$

where $p_{ij}(x,y)$ and $p_{ijk}(x,y,z)$ are ordered bivariate and trivariate non-Gaussian density functions. Following the procedures of section (4.4) for treatment of double and triple sums, equation (4.5-10) reduces to:

$$Var \{ T_{II}^2 / H_0 \} =$$

$$+ \frac{1}{2} \sum_{i=1}^{M} \sum_{\substack{j=1 \\ j \neq i}}^{M} \sum_{\substack{k=1 \\ k \neq j \\ k \neq i}}^{M} E_i \, (\alpha_{ij} \alpha_{ik}) \int_0^\infty dx \int_0^\infty dy \int_0^\infty dz \; g'^2(x) \; g(y) \; g(z) \; p_{ijk}(x,y,z)$$

$$+ \frac{1}{2} \sum_{i=1}^{M} \sum_{\substack{j=1 \\ j \neq i}}^{M} E_i \, (\alpha_{ij})^2 \int_0^\infty dx \int_0^\infty dy \; g'^2(x) \; g^2(y) \; p_{ij}(x,y)$$

$$+ \sum_{i=1}^{M} \sum_{\substack{j=1 \\ j \neq i}}^{M} E_i \, \alpha_{ii} \, \alpha_{ij} \int_0^\infty dx \int_0^\infty dy \; g'^2(x) \; g(x) \; g(y) \; p_{ij}(x,y)$$

$$- \sum_{i=1}^{M} \sum_{\substack{j=1 \\ j \neq i}}^{M} E_i \alpha_{ij} \int_0^\infty dx \int_0^\infty dy \left[g''(x) \, g(y) - \frac{g'(x) \, g(y)}{x} \right] p_{ij}(x,y)$$

$$+ \frac{1}{2} \sum_{i=1}^{M} E_i \, (\alpha_{ii})^2 \int_0^{\infty} dx \; g'^2(x) \; g^2(x) \; p(x)$$

$$- \sum_{i=1}^{M} E_i \, \alpha_{ii} \int_0^{\infty} dx \; [\; g''(x) \, g(x) \; - \; \frac{g'(x) \, g(x)}{x} \;] \; p(x)$$

$$+ \frac{1}{2} \sum_{i=1}^{M} E_i \int_0^{\infty} dx \; [\; \frac{g''^2(x)}{g'^2(x)} \; - \; \frac{g''(x)}{x \, g'(x)} \; + \; \frac{1}{x^2} \;] \; p(x)$$

(4.5 − 11)

Equations (4.5-7) and (4.5-11) are the required equations for calculation of Efficacy. These two equations will be used in section (4.7) with specific density function for numerical evaluation. As noticed, the required information is the measure of signal energy, E_i , the covariance structure of the samples (related to α_{ij}), and the non-linearities g(.), g′(.), and g″(.), which are Gaussian random variables. Finally, $p_{ijk}(x, y, z)$ is obtained from the modeling of the joint multivariate non-Gaussian density, Model (I), as discussed in Chapter II. The next section specializes the Efficacy calculation to the case of independent and identically distributed noise.

4.6. Efficacy for LOD with Independent and Identically Distributed Noise

In this section, the Efficacy for $(LOD)_I$ and $(LOD)_{II}$ under the assumption of independent and identically distributed noise are derived. The objective is that, in conjunction with the Efficacy for the developed detectors under dependent noise, one can formulate the Asymptotic Relative Efficiency and compare their relative performances.

As before, the expression for Efficacy is given by :

$$Efficacy(\mathrm{T}) = \underset{\theta \to 0}{Limit} \frac{[\frac{\partial E_\theta(\mathrm{T})}{\partial \theta}]^2}{Var_\theta(\mathrm{T})} \qquad (4.6-1)$$

The expressions for $(LOD)_{I,(i.i.d)}$ and $(LOD)_{II,(i.i.d)}$ are given from (3.6-3) and (3.6-8) as:

$$(LOD)_{I,(i.i.d)} = \sum_{i=1}^{M} - \frac{Real\,(\tilde{y}_i\,\tilde{s}_i^*)}{|\tilde{y}_i|} \frac{1}{p_{|\tilde{n}|}(|\tilde{y}_i|)} \frac{\partial p_{|\tilde{n}|}(|\tilde{y}_i|)}{(\partial |\tilde{y}_i|)} \qquad (4.6-2)$$

$$(LOD)_{II,(i.i.d)} = \sum_{i=1}^{M} \frac{Real\,(\tilde{y}_i\,\tilde{s}_i^*)}{|\tilde{y}_i|} [\frac{1}{|\tilde{y}_i|} - \frac{1}{p_{|\tilde{n}|}(|\tilde{y}_i|)} \frac{\partial p_{|\tilde{n}|}(|\tilde{y}_i|)}{\partial(|\tilde{y}_i|)}]$$

$$(4.6-3)$$

First, the Efficacy for $(LOD)_{I,(i.i.d)}$ is calculated. As in section (4.5), the measure of signal energy and complex noise are defined as:

$$E_i \equiv s_{I_i}^2 + s_{Q_i}^2 \qquad (4.6-4)$$

$$E_s \equiv \sum_{i=1}^{M} E_i \qquad (4.6-5)$$

and

$$\tilde{n}_i = n_{I_i} + j\, n_{Q_i} = R_i\, e^{j\varphi_i} \qquad (4.6-6)$$

After some algebraic manipulation, one can obtain:

$$\{ \frac{\partial}{\partial \theta} [\, E\, (\, (LOD)_{I,(i.i.d)} / H_1\,)\,]\, |_{\theta=0}\, \} =$$

$$\frac{1}{2}[\, \sum_{i=1}^{M} E_i\,]\, \int_0^{\infty} dx\, (\, -\, \frac{p'(x)}{x} + \frac{p'^2(x)}{p(x)}) \qquad (4.6-7)$$

where p(x) is the univariate non-Gaussian amplitude density function.

Also, by integrating the phase variable, it is easy to show that:

$$E\{\, (LOD)_{I,(i.i.d)} / H_0\, \} = 0$$

and:

$$E\, \{\, (LOD)^2_{I,(i.i.d)} / H_0\, \} = Var\, \{ (LOD)_{I,(i.i.d)} / H_0\, \} =$$

$$[\, \sum_{i=1}^{M} E_i\,]\, \int_0^{\infty} dx\, \frac{p'^2(x)}{p(x)} \qquad (4.6-8)$$

Thus, Efficacy can be written explicitly as:

$$Efficacy(LOD)_{I,(i.i.d)} = \frac{\frac{E_s}{2}\left[\int_0^\infty dx \left(-\frac{p'(x)}{x} + \frac{p'^2(x)}{p(x)}\right)\right]^2}{\int_0^\infty dx \frac{p'^2(x)}{p(x)}} \qquad (4.6-9)$$

In the special case, when circular symmetry assumption is imposed:

$$p(x) = 2\pi x f(x) \qquad (4.6-10)$$

one can obtain:

$$Efficacy(LOD)_{I,(i.i.d)} = \frac{\pi E_s\left[\int_0^\infty dx\, x^2 f'(x)\, G(x)\right]^2}{\left[\int_0^\infty dx\, x^3 f(x)\, G^2(x)\right]} \qquad (4.6-11)$$

where

$$G(x) = \frac{-p'(x)}{x\, p(x)} \qquad (4.6-12)$$

Equation (4.6-11) is identical to Equation (44) of Modestino [11].

Next, Efficacy for the $(LOD)_{II,(i.i.d)}$ is derived. Again, after some algebraic manipulation, one can obtain:

$$\left\{ \frac{\partial}{\partial \theta} \left[E\left((LOD)_{II,(i.i.d)} / H_1 \right) \right] \Big|_{\theta=0} \right\} =$$

$$\sum_{i=1}^{M} E_i \int_0^\infty dx \left(\frac{p'^2(x)}{p(x)} + \frac{p(x)}{x^2} - \frac{2\,p'(x)}{x} \right) \qquad (4.6-13)$$

and

$$E\ \{\ (LOD)^2_{II,(i.i.d)} / H_0\ \}\ =\ Var\ \{\ (LOD)_{II,(i.i.d)} / H_0\ \}\ =$$

$$\sum_{i=1}^{M} E_i \int_0^\infty dx\ p(x)\, x^2 \left(\frac{1}{x^2} - \frac{p'(x)}{xP(x)}\right)^2 \qquad (4.6-14)$$

Thus, Efficacy can be written as:

$$Efficacy(LOD)_{II,(i.i.d)}\ =$$

$$\frac{\frac{E_s}{2}\left[\ \int_0^\infty dx\ \left(\frac{p'^2(x)}{p(x)} + \frac{p(x)}{x^2} - \frac{2\,p'(x)}{x}\right)\ \right]^2}{\int_0^\infty dx\ p(x)\, x^2 \left(\frac{1}{x^2} - \frac{p'(x)}{xP(x)}\right)^2} \qquad (4.6-15)$$

where p(x) is the univariate non-Gaussian density function.

Equations (4.6-9) and (4.6-15) will be used in the next section for performance evaluation of various detectors under a specific univariate density function.

4.7. Simulation Results for Weibull Distribution

This section is primarily for presenting the numerical results of performance evaluation of various detector structures. The criteria of Asymptotic Relative Efficiency is used for comparing the performance of two detectors. From equation (4.2-6), the ARE between two detectors, with test statistic T_1 and T_2, is given by the ratio of their Efficacies as:

$$(ARE)_{T_1, T_2} = \frac{Efficacy(T_1)}{Efficacy(T_2)} \qquad (4.7-1)$$

where T_2 is the reference detector test statistic. With this definition, the value of $ARE > 1$ implies that the detector T_1 is superior to the reference detector T_2.

Since, the main theme of this research, is to advocate the " non-Gaussian " and " multivariate " noise model, the advantages of the $(LOD)_I$ and $(LOD)_{II}$ and their performance superiority should be demonstrated with respect to valid benchmarks.

Three non-linear detector structures $(LOD)_I$, $(LOD)_{II}$, and $(LOD)_{II,(i.i.d)}$ are compared, first with respect to the reference detector, $(LOD)_{I,(i.i.d)}$, and second, with respect to each other in various combinations. Also, $(LOD)_I$ and $(LOD)_{II}$ are compared with respect to complex and real matched filters.

The $(LOD)_{I,i.i.d}$ detector is chosen as one of the reference detectors to point out the multivariate nature of the problem. The matched filter, optimum in

Gaussian noise environment, is selected to show the performance degradation under non-Gaussian noise condition.

The specific non-Gaussian noise density function is Weibull distribution. This density is chosen, since not only it is one of the well-established amplitude density functions of the sea-clutter, but also it has certain mathematical tractabilities. The univariate Weibull density function, written in terms of the in-phase and quadrature phase components, with unity scale parameter is:

$$p_{NG}(\sqrt{I_i^2 + Q_i^2}) = \alpha(\sqrt{I_i^2 + Q_i^2})^{\alpha-1} \exp(-\sqrt{I_i^2 + Q_i^2})^{\alpha} \quad \alpha > 0 \tag{4.7 - 2}$$

Defining $x_i = \sqrt{I_i^2 + Q_i^2}$, and using (2.2-14) and (2.2-19), one can show:

$$g(x_i) = \Phi^{-1}[F_{NG}(x_i)] \tag{4.7 - 3}$$

$$g'(x_i) = \sqrt{2\pi}\, p_{NG}(x_i) \exp\{\frac{g^2(x_i)}{2}\} \tag{4.7 - 4}$$

$$g''(x_i) = \sqrt{2\pi}[p'_{NG}(x_i) + g'(x_i)\, g(x_i)\, p_{NG}(x_i)] \exp\{\frac{g^2(x_i)}{2}\} \tag{4.7 - 5}$$

$$g^{(3)}(x_i) = \sqrt{2\pi}[p''_{NG}(x_i) + g''(x_i)\, g(x_i)\, p_{NG}(x_i) + g'^2(x_i)\, p_{NG}(x_i) +$$

$$2\, g(x_i)\, g'(x_i)\, p'_{NG}(x_i) + g'^2(x_i)\, g^2(x_i)\, p_{NG}(x_i)] \exp\{\frac{g^2(x_i)}{2}\} \tag{4.7 - 6}$$

where Φ^{-1} is the inverse Error function and $F_{NG}(x_i)$ is the Weibull Cumulative Distribution Function (CDF):

$$F_{NG}(x_i) = 1 - e^{-x_i^{\alpha}} \qquad (4.7-7)$$

Next, in calculating the Efficacies, the required joint non-Gaussian density functions are the trivariate and bivariate densities $p_{ijk}(x, y, z)$ and $p_{ij}(x, y)$. From the complex noise modeling of Chapter II, by employing equation (2.2-18), one can obtain:

$$p_{ijk}(x, y, z) = p_{G,ijk}(g(x), g(y), g(z)) \mid g'(x) \mid \mid g'(y) \mid \mid g'(z) \mid \qquad (4.7-8)$$

and

$$p_{ij}(x, y) = p_{G,ij}(g(x), g(y)) \mid g'(x) \mid \mid g'(y) \mid \qquad (4.7-9)$$

where $p_{G,ijk}$ and $p_{G,ij}$ are the trivariate and bivariate zero-mean Gaussian density functions as:

$$p_{G,ijk}(x, y, z) = \frac{1}{(\sqrt{2\pi})^3 \mid \underline{R}_{ijk} \mid^{\frac{1}{2}}}$$

$$\exp\{ -\frac{1}{2}[g(x)\ g(y)\ g(z)]\ \underline{R}_{ijk}^{-1}\ [g(x)\ g(y)\ g(z)]^T \} \qquad (4.7-10)$$

and

$$p_{G,ij}(x,y) = \frac{1}{(\sqrt{2\pi})^2 \mid \underline{R}_{ij} \mid^{\frac{1}{2}}}$$

$$\exp\ \{\ -\ \frac{1}{2}[\,g(x)\ g(y)\,]\ \underline{R}_{ij}^{-1}\ [\,g(x)\ g(y)\,]^T\ \} \qquad (4.7-11)$$

with covariance matrices $\underline{R}_{ijk}$ and $\underline{R}_{ij}$.

The specific structure of the covariance matrices are determined from the covariance structure of the non-Gaussian noise by solution of a system of non-linear equation as described in Chapter II. For the example under consideration, it is assumed that the covariance structure of the amplitude of the non-Gaussian noise maps into a Gaussian covariance structure which is Markovian with $\{\underline{R}_{M\times M}\}_{ij} = a_{ij} = \rho^{|i-j|}$ as:

$$\underline{R}_{M\times M} = \begin{bmatrix} 1 & \rho & \rho^2 & \rho^3 & \dots & \rho^{M-1} \\ \rho & 1 & \rho & \rho^2 & \dots & \rho^{M-2} \\ & & \dots\dots & & & \\ \rho^{M-1} & \rho^{M-2} & & \dots & \rho & 1 \end{bmatrix} \qquad (4.7-12)$$

where (M) is the dimension of total samples under consideration. Now, $\underline{R}_{ijk}$ and $\underline{R}_{ij}$ are any combination of 3 × 3 and 2 × 2 matrices that are required from the ($M \times M$) matrix:

$$\underline{R}_{ijk} = \begin{bmatrix} a_{ii} & a_{ij} & a_{ik} \\ a_{ji} & a_{jj} & a_{jk} \\ a_{ki} & a_{kj} & a_{kk} \end{bmatrix}, \quad \underline{R}_{ij} = \begin{bmatrix} a_{ii} & a_{ij} \\ a_{ji} & a_{jj} \end{bmatrix} \qquad (4.7-13)$$

Given a specific value of correlation (ρ) , dimension (M) , Weibull density parameter (α) , and the measure of signal energy E_i , and the employment of equations (4.7-3) through (4.7-13), one can calculate the Efficacy of $(LOD)_I$ and $(LOD)_{II}$.

The Efficacy of $(LOD)_{I,(i.i.d)}$ and $(LOD)_{II,(i.i.d)}$, from (3.6-3) and (3.6-6), can be explicitly found to be:

$$Efficacy(T_{I,(i.i.d)}) =$$

$$\frac{(\frac{E_s}{2})[\,\alpha(\alpha-1)(\alpha-2)I - \alpha(2\alpha-3)\Gamma(2-\frac{2}{\alpha}) + \alpha^2\Gamma(3-\frac{2}{\alpha})\,]^2}{\alpha(\alpha-1)^2 I + \alpha^2\Gamma(3-\frac{2}{\alpha}) - 2\alpha(\alpha-1)\Gamma(2-\frac{2}{\alpha})} \qquad (4.7-14)$$

and

$$Efficacy(T_{II,(i.i.d)}) =$$

$$(\frac{E_s}{2})\frac{[\,(\alpha^3-4\alpha^2+4\alpha)I + (4\alpha-2\alpha^2)\Gamma(2-\frac{2}{\alpha}) + \alpha^2\Gamma(3-\frac{2}{\alpha})}{\alpha(\alpha-2)^2 I + \alpha^2\Gamma(3-\frac{2}{\alpha}) + (4\alpha-2\alpha^2)\Gamma(2-\frac{2}{\alpha})} \qquad (4.7-15)$$

where

$$I = \int_0^{\infty} x^{\alpha-3} e^{-x^{\alpha}} dx \qquad (4.7-16)$$

Since, there is no closed form solution for this integral, it should be performed numerically. Also, the Gamma functions are the result of the following type of integration:

$$\int_0^{\infty} dx\, x^{\beta-1} e^{-\gamma x^{p}} = \frac{1}{p} \gamma^{-\frac{\beta}{p}} \Gamma(\beta/p)$$

$$\gamma > 0,\ \beta > 0,\ p > 0 \qquad (4.7-17)$$

For the computer simulation under consideration, it is assumed that $E_i = 1$ for all (i), and ($\alpha = 1.5$) . Three values for correlation are considered: $\rho = 0.7$, $\rho = 0.8$, and $\rho = 0.9$. For each value of (ρ) , two different cases are considered. In the first case, the ARE of $(LOD)_{II}$, $(LOD)_{I}$, and $(LOD)_{II,(i.i.d)}$ are evaluated with respect to the reference detector $(LOD)_{I,(i.i.d)}$. In the second case, the ARE of $(LOD)_{II}$ with respect to $(LOD)_{II,(i.i.d)}$, the $(LOD)_{II}$ with respect to $(LOD)_{I}$, and $(LOD)_{II,(i.i.d)}$ with respect to $(LOD)_{I,(i.i.d)}$ are considered.

Figures (24) and (25) illustrate the ARE versus (M), the dimension of measurement vector, for $\rho = 0.7$. As noticed, the value of all the ARE's are greater than one, and non-decreasing function of (M). That is, taking the dependence into consideration enhances the detection capability. Figure (25) also illustrates the same phenomenon. Specifically, the increasing behaviour of the ARE for $(LOD)_{II}$ with respect to $(LOD)_{II,(i.i.d)}$ is clearly evident. Figures (26) and (27) are for ($\rho = 0.8$) . Also, as noticed, consistently, the complex model outperforms the

amplitude or independent model in terms of ARE. Finally, Figures (28) and (29) are for $\rho = 0.9$.

It should be mentioned that, as shown in Figures (24) and (27), where the reference detectors are the same, there is a threshold sample number (M) below which the ARE measure shows degradation. Thus, care should be exercised in specific applications in terms of the reference detector.

Next, the performance of $(LOD)_I$ and $(LOD)_{II}$ are compared with respect to complex and real matched filters. For the problem under consideration, the Efficacy for the complex matched filter is $\underline{\tilde{S}}^{\times T}\underline{\tilde{R}}_n^{-1}\underline{\tilde{S}}$, and for real matched filter is $|\underline{\tilde{S}}^{\times T}|\ \underline{R}_n^{-1}\ |\underline{\tilde{S}}|$. The matrix $\underline{\tilde{R}}_n$ is the covariance matrix associated with the complex signal, and $\underline{R}_n$ is the covariance matrix associated with the amplitude of the complex signal. In the case of complex matched filter the covariance matrix can be expressed as [55]:

$$\underline{\tilde{R}}_n = \begin{bmatrix} R_{II} & R_{IQ} \\ R_{QI} & R_{QQ} \end{bmatrix} \qquad (4.7-18)$$

where R_{II} and R_{QQ} are the auto-covariance matrices of in-phase and quadrature phase components, and R_{IQ} and R_{QI} are the cross-covariance matrices. For the problem under consideration, this matrix becomes the identity matrix, and thus the Efficacy reduces to $\underline{\tilde{S}}^{\times T}\underline{\tilde{S}}$.

Figures (30) through (32) show the results of the ARE versus (M) for the complex matched filter, and Figures (33) through (35) illustrate the results for the

real matched filter. The correlation coefficient is assumed to be $\rho = 0.7$, and three values for the Weibull density parameter are considered as: $\alpha = 1.5, 1.6, 1.7$. As noticed, in all cases, the ARE is consistently greater than one.

In summary, the results indicate that when there exist intersample dependence, it is definitely advantageous to use a detector structure which takes the correlation structure into consideration. Also, increase in information processing (i.e., amplitude and phase) enhances the performance capability, however, at the cost of increased structural complexity.

Since, the parameters of the underlying non-Gaussian density function change (i.e., due to non-stationarity of the sea-clutter), the non-linearities of the detector structure also change. It is proposed that by operating at a sub-optimum level, one can fix the non-linearities for a certain value of the density parameter. This is the topic of the next Chapter, where various approximations are introduced.

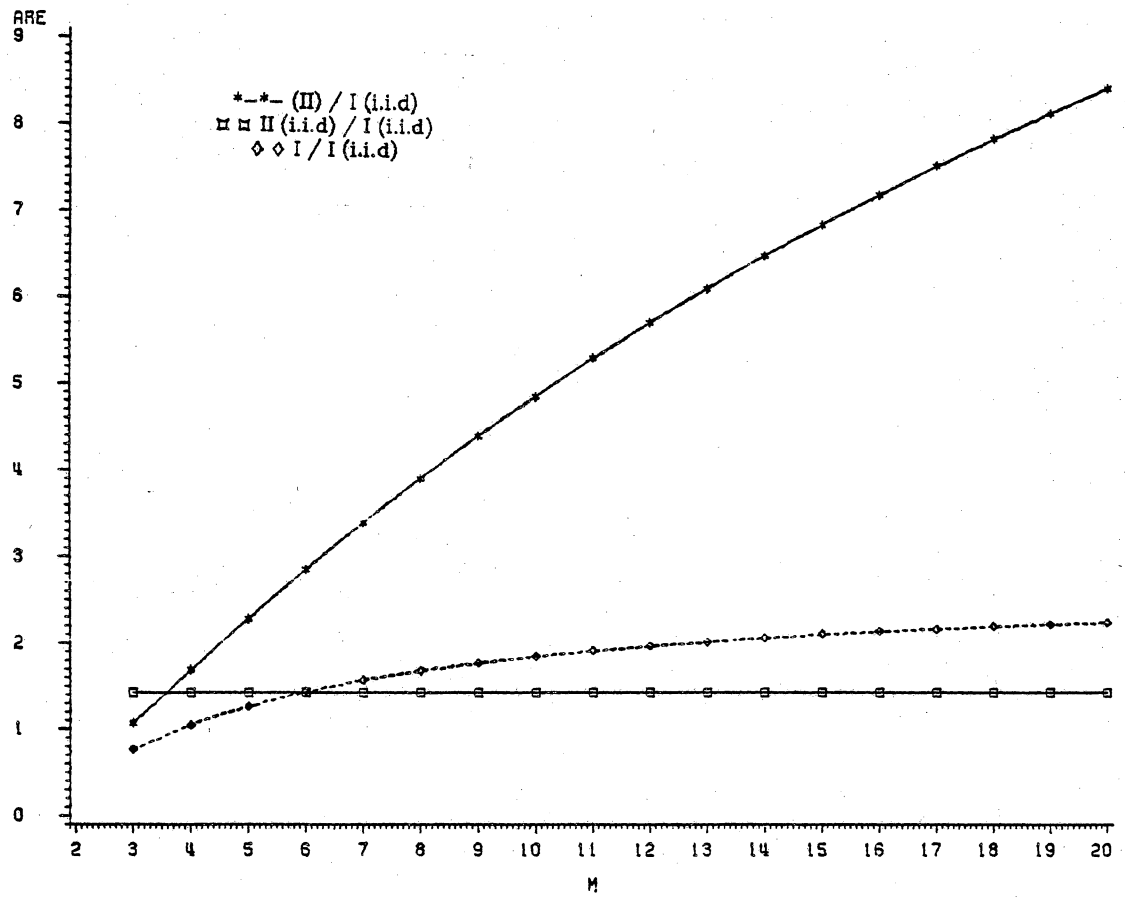

Figure 24. ARE versus (M) for Fixed Reference Detector and Correlation Coefficient of (0.7) and $\alpha = (1.5)$.

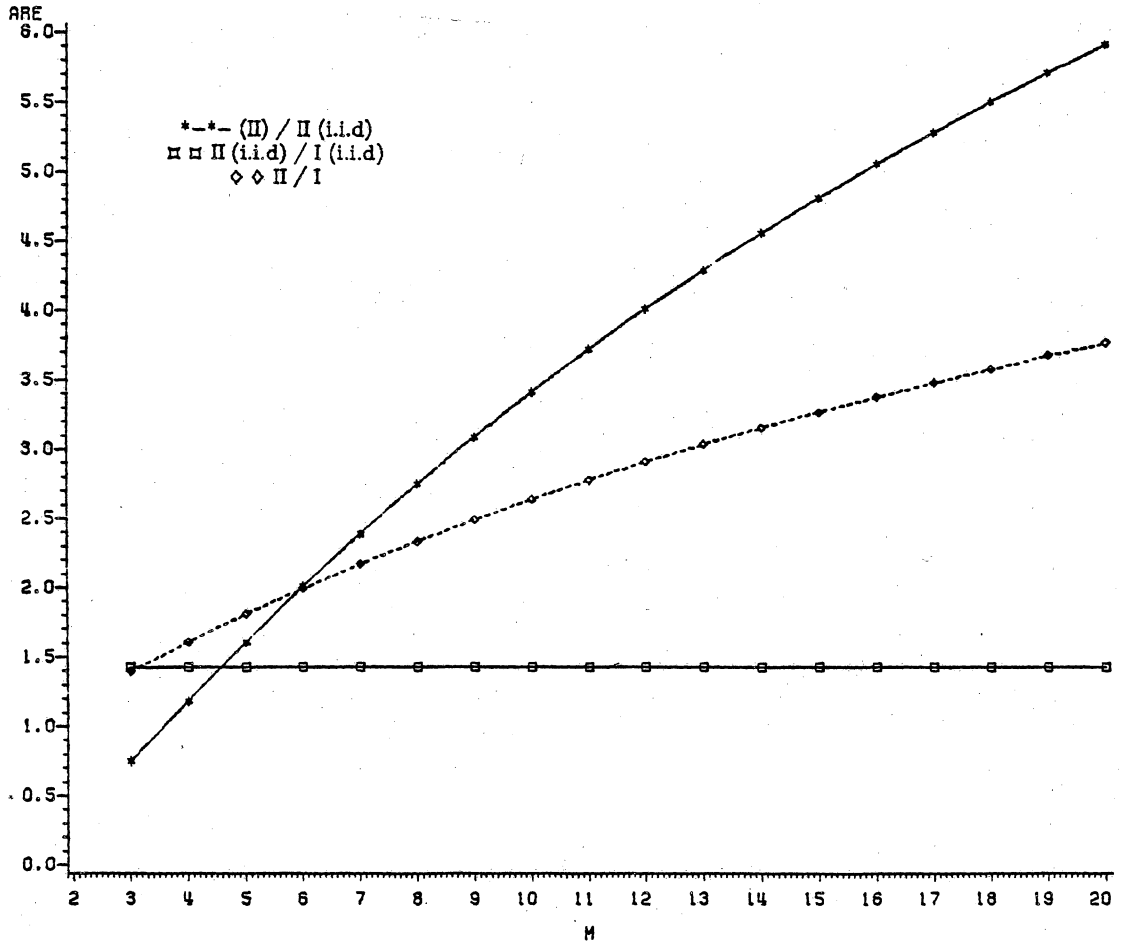

Figure 25. ARE versus (M) for Various Reference Detectors and Correlation Coefficient of (0.7) and α = (1.5).

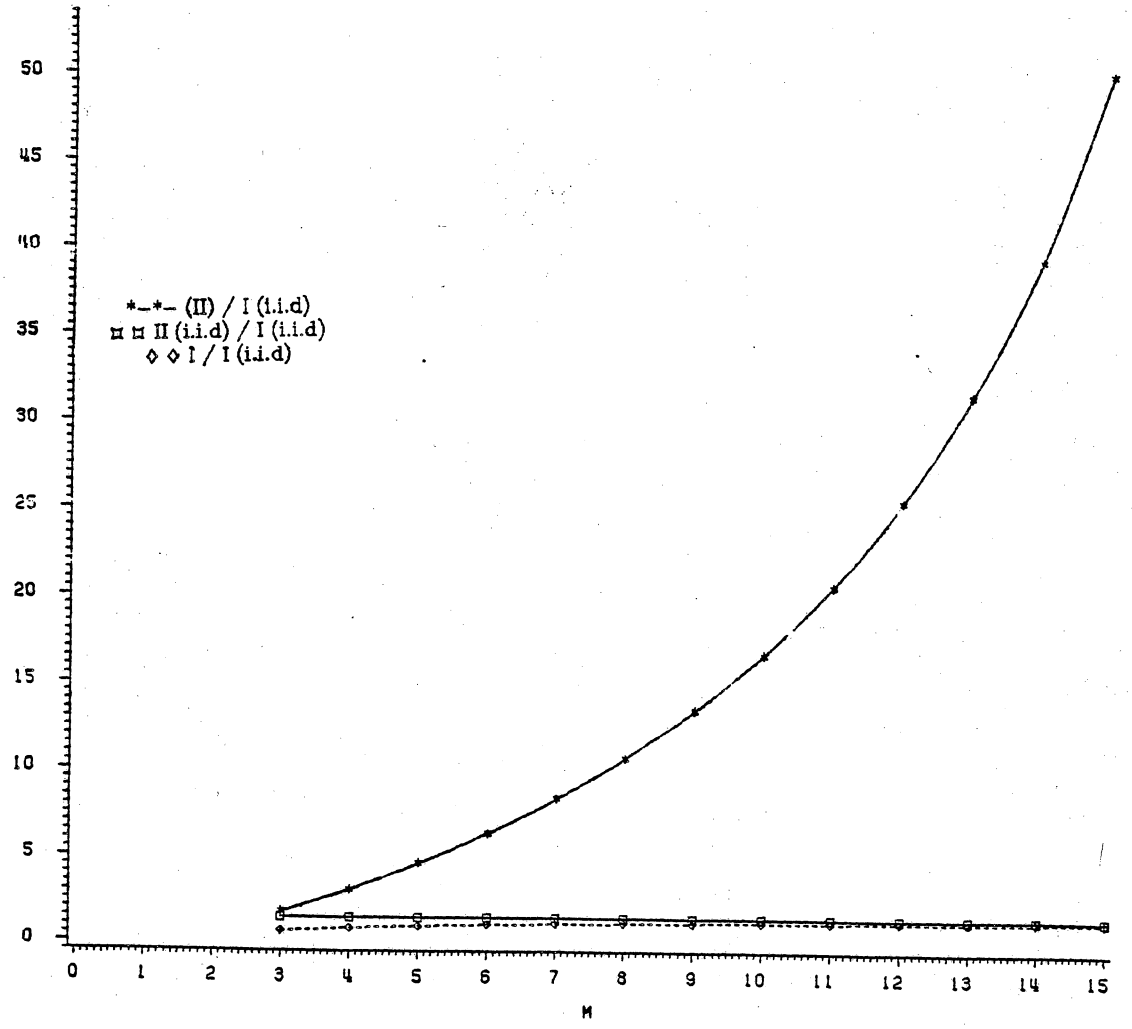

Figure 26. ARE versus (M) for Fixed Reference Detector and Correlation Coefficient of (0.8) and α=(1.5).

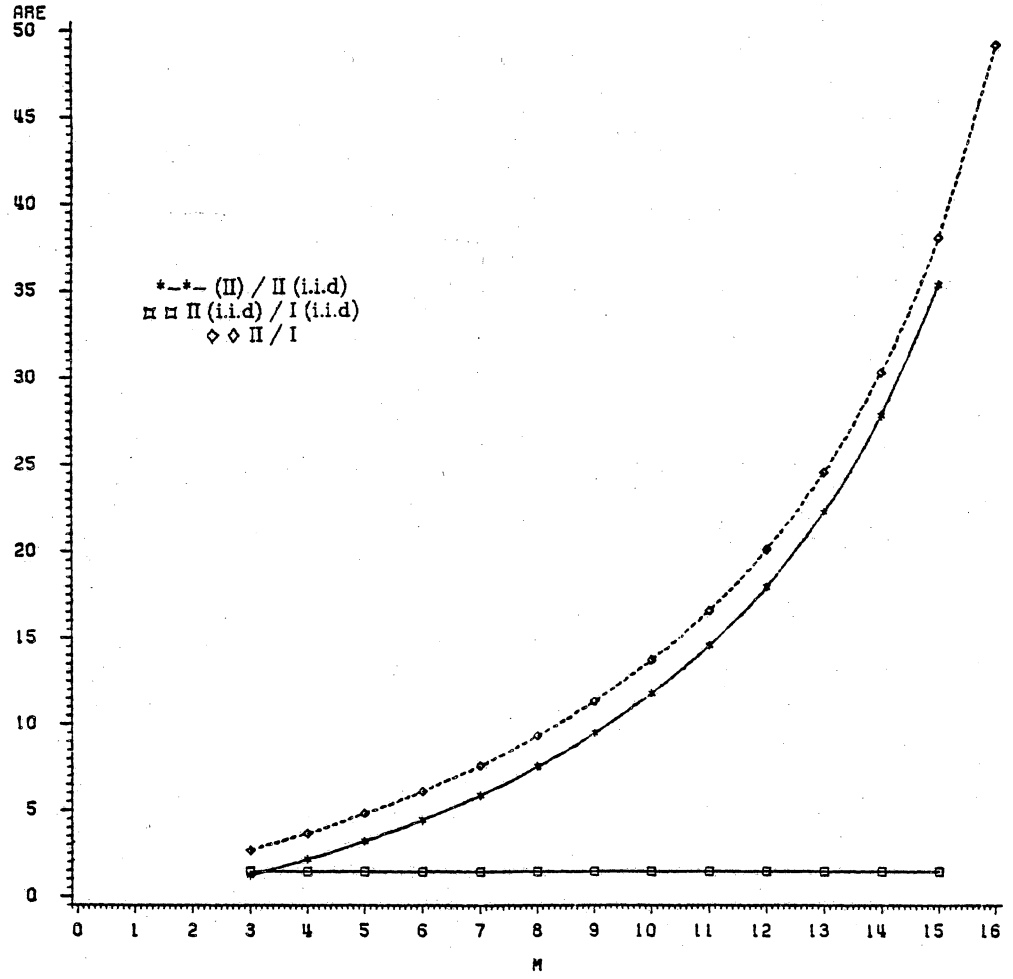

Figure 27. ARE versus (M) for Various Reference Detectors and Correlation Coefficient of (0.8) and $\alpha = (1.5)$.

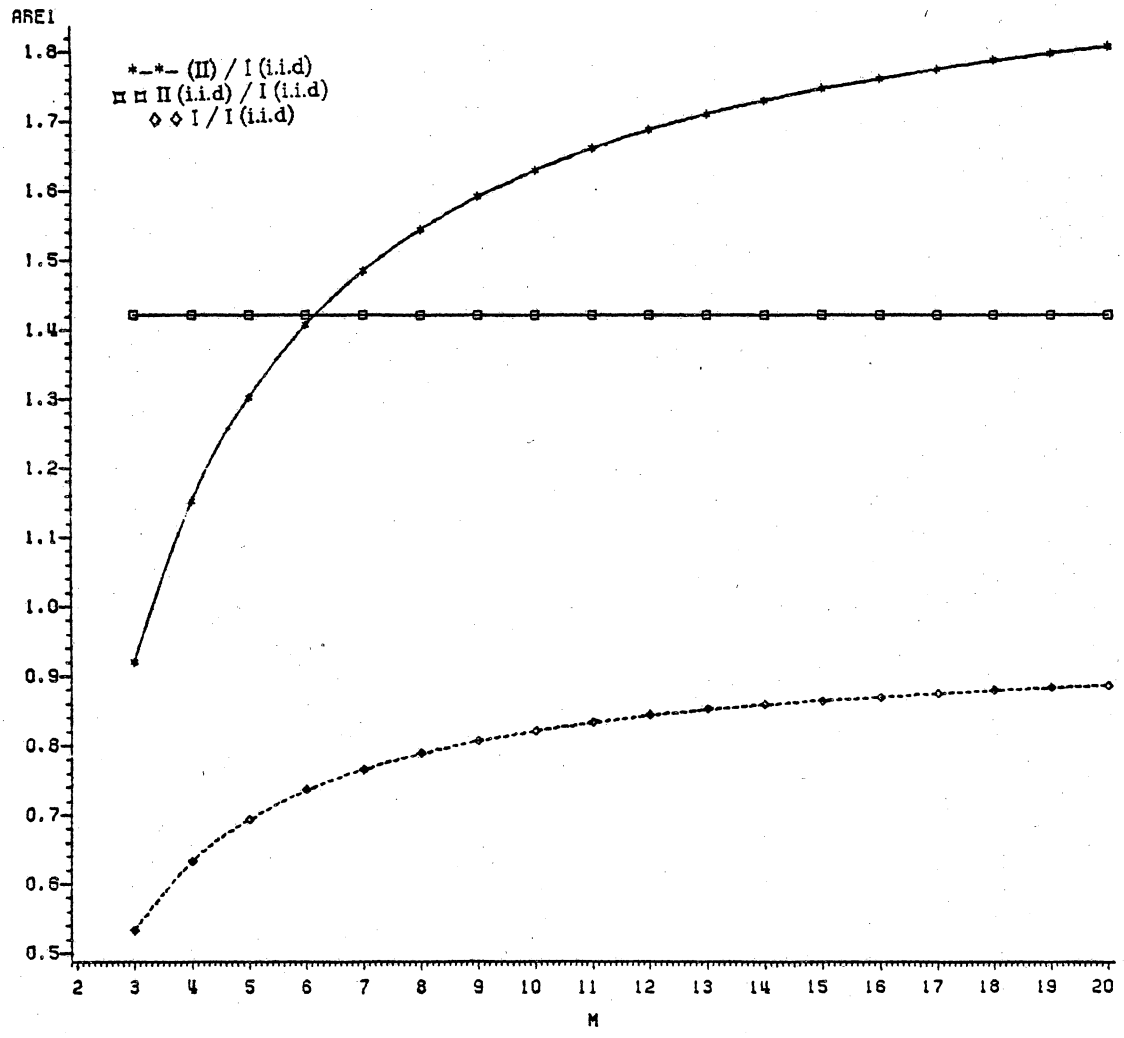

Figure 28. ARE versus (M) for Fixed Reference Detector and Correlation Coefficient of (0.9) and $\alpha = (1.5)$.

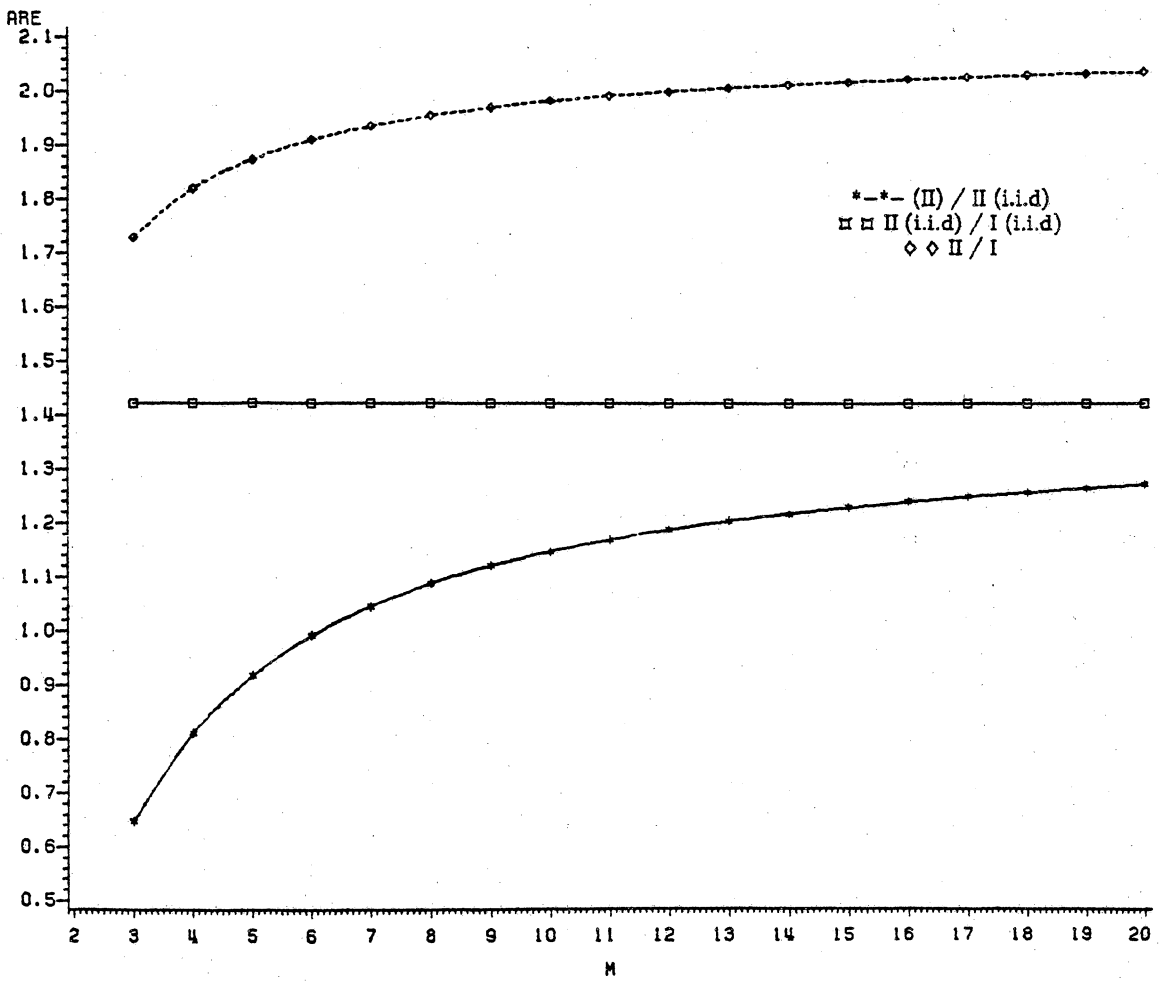

Figure 29. ARE versus (M) for Various Reference Detectors and Correlation Coefficient of (0.9) and $\alpha = (1.5)$.

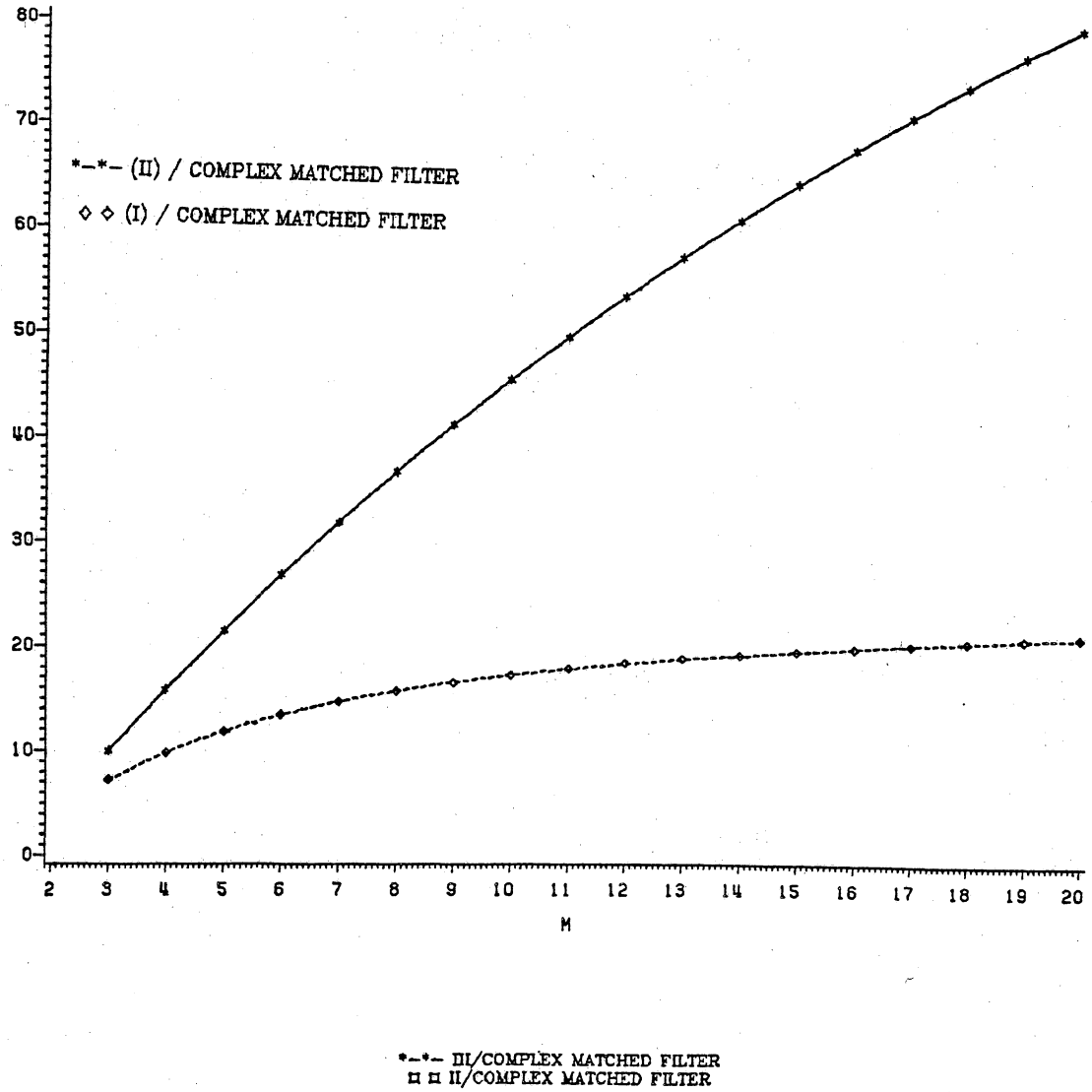

Figure 30. ARE versus (M) for Complex Matched Filter as Reference Detector and Correlation of $\rho = 0.7$, and $\alpha = 1.5$.

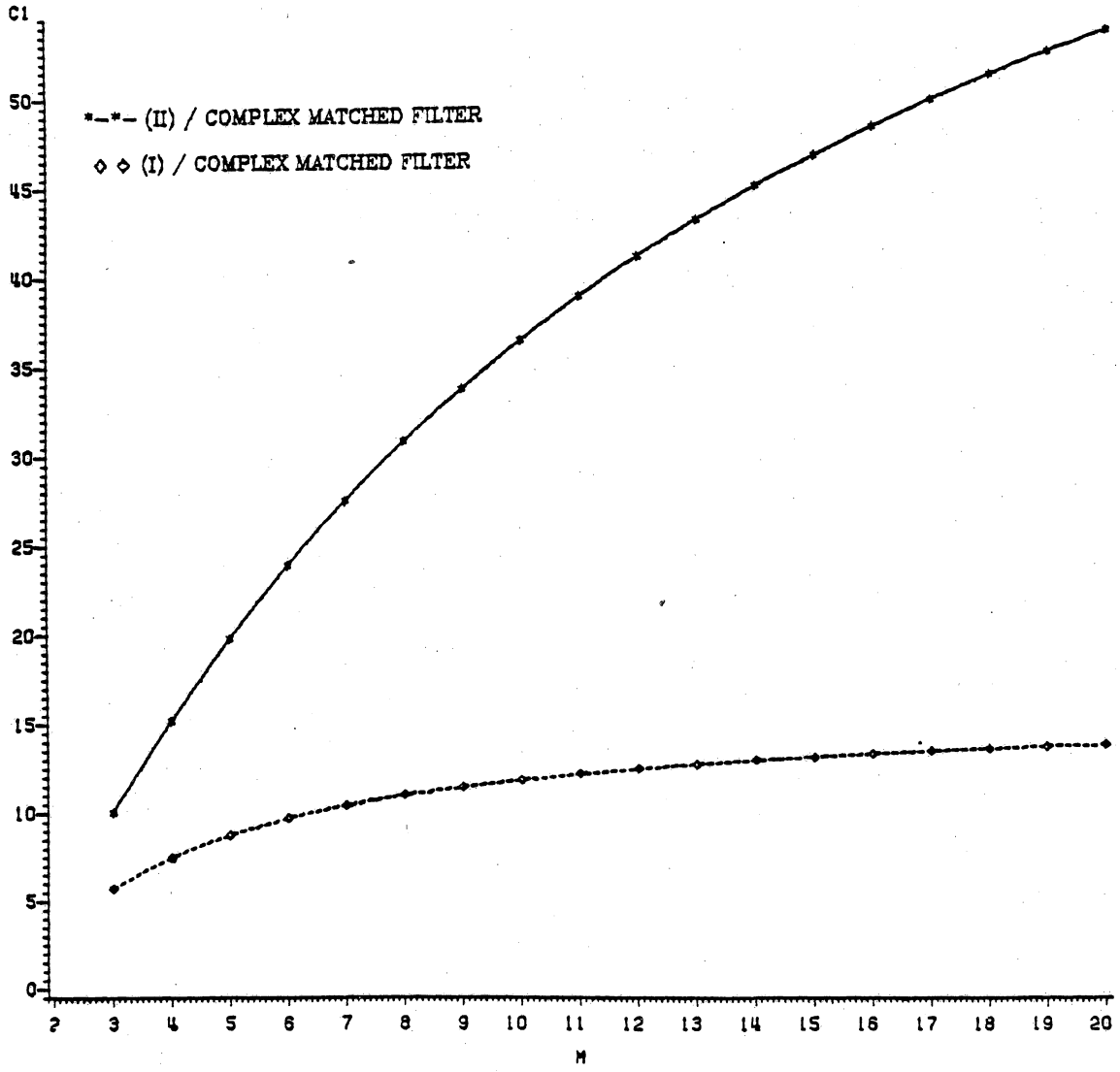

Figure 31. ARE versus (M) for Complex Matched Filter as Reference Detector and Correlation of $\rho = 0.7$, and $\alpha = 1.6$.

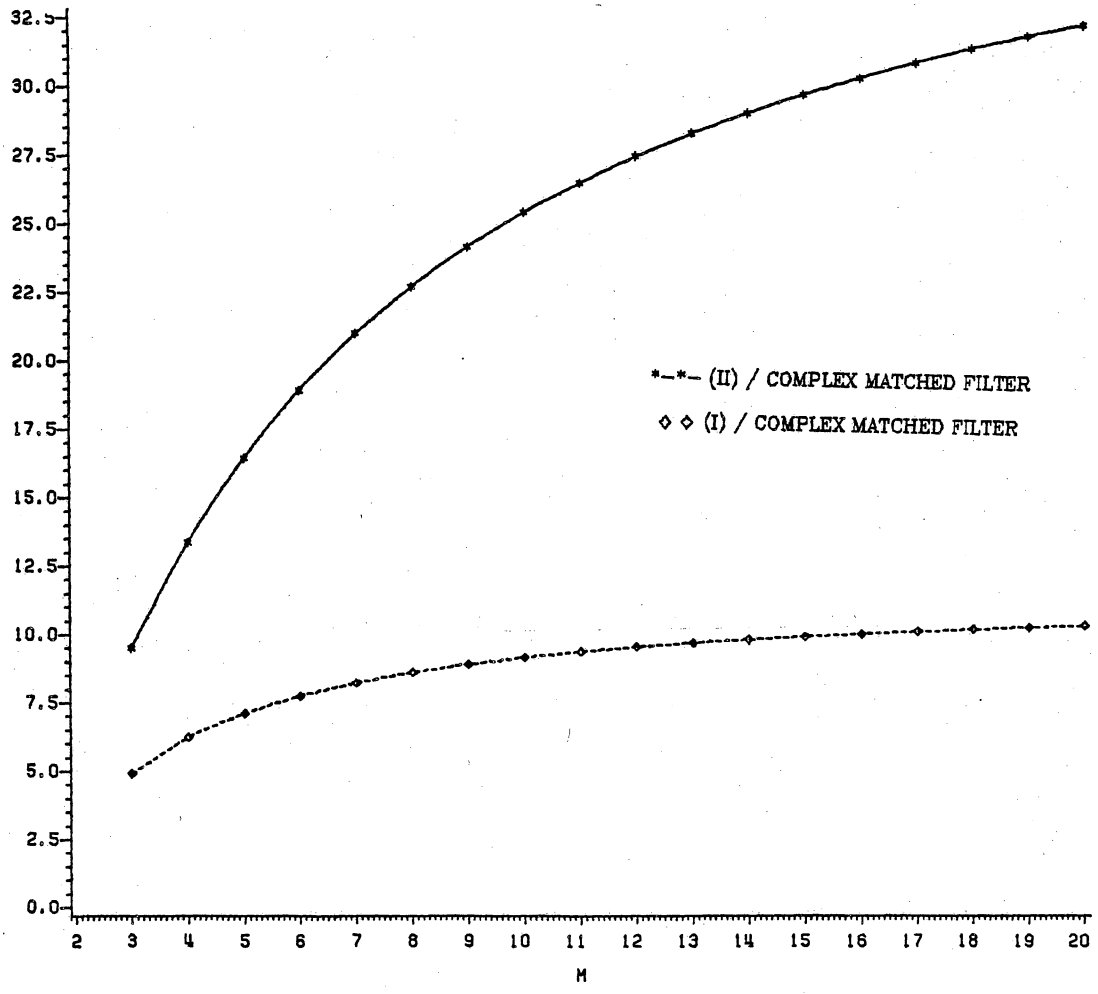

Figure 32. ARE versus (M) for Complex Matched Filter as Reference Detector and Correlation of $\rho = 0.7$, and $\alpha = 1.7$.

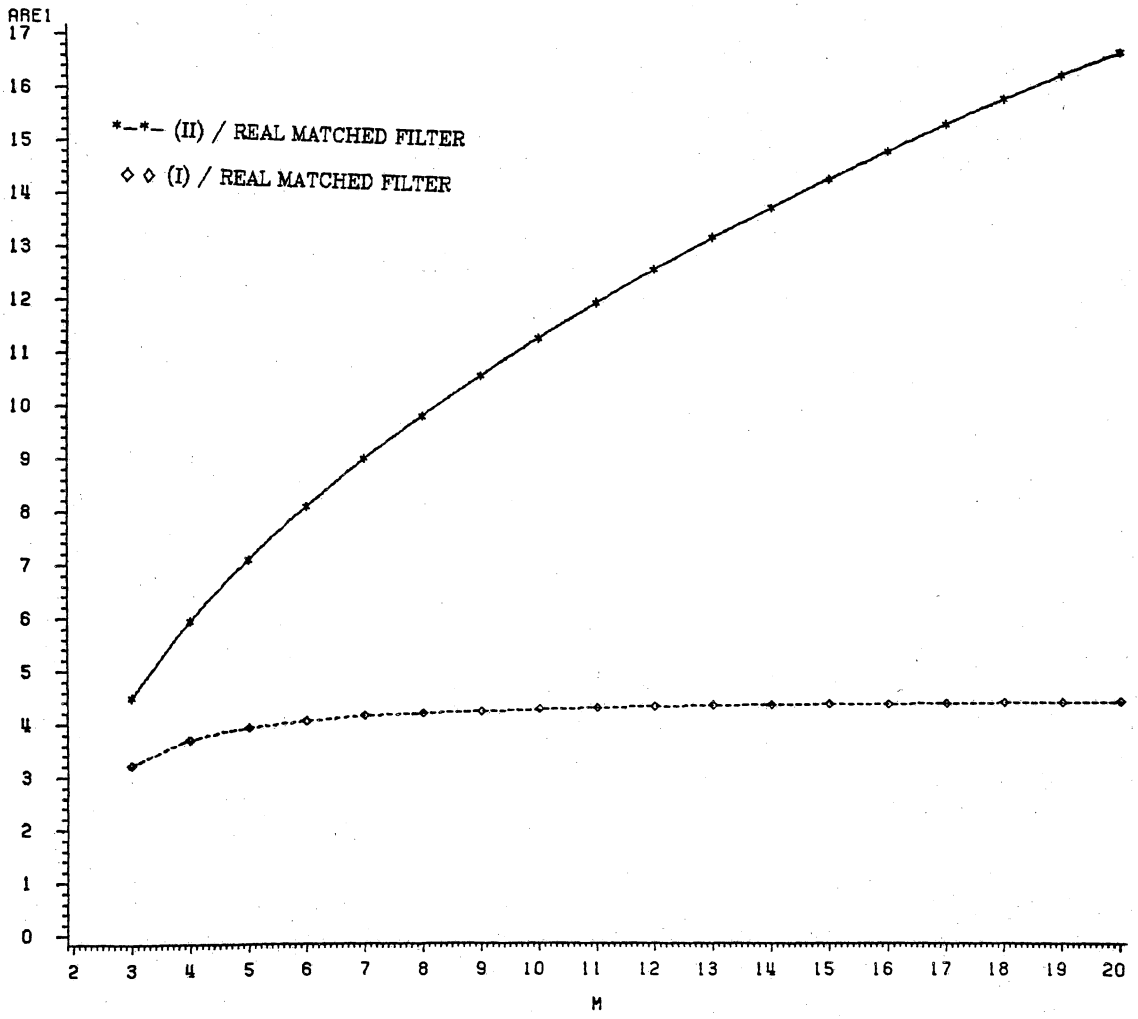

Figure 33. ARE versus (M) for Real Matched Filter as Reference Detector and Correlation of ρ = 0.7, and α = 1.5.

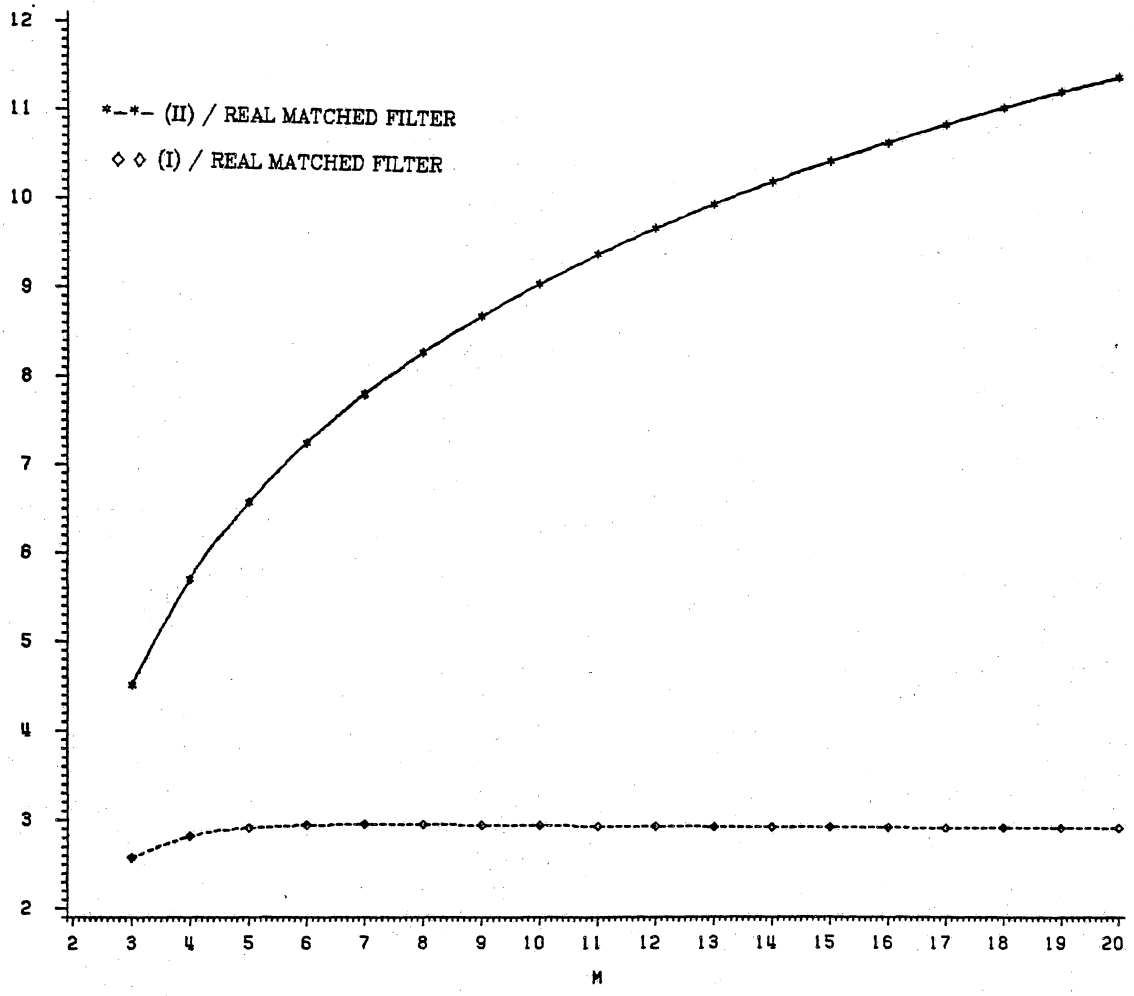

Figure 34. ARE versus (M) for Real Matched Filter as Reference Detector and Correlation of ρ = 0.7, and α = 1.6.

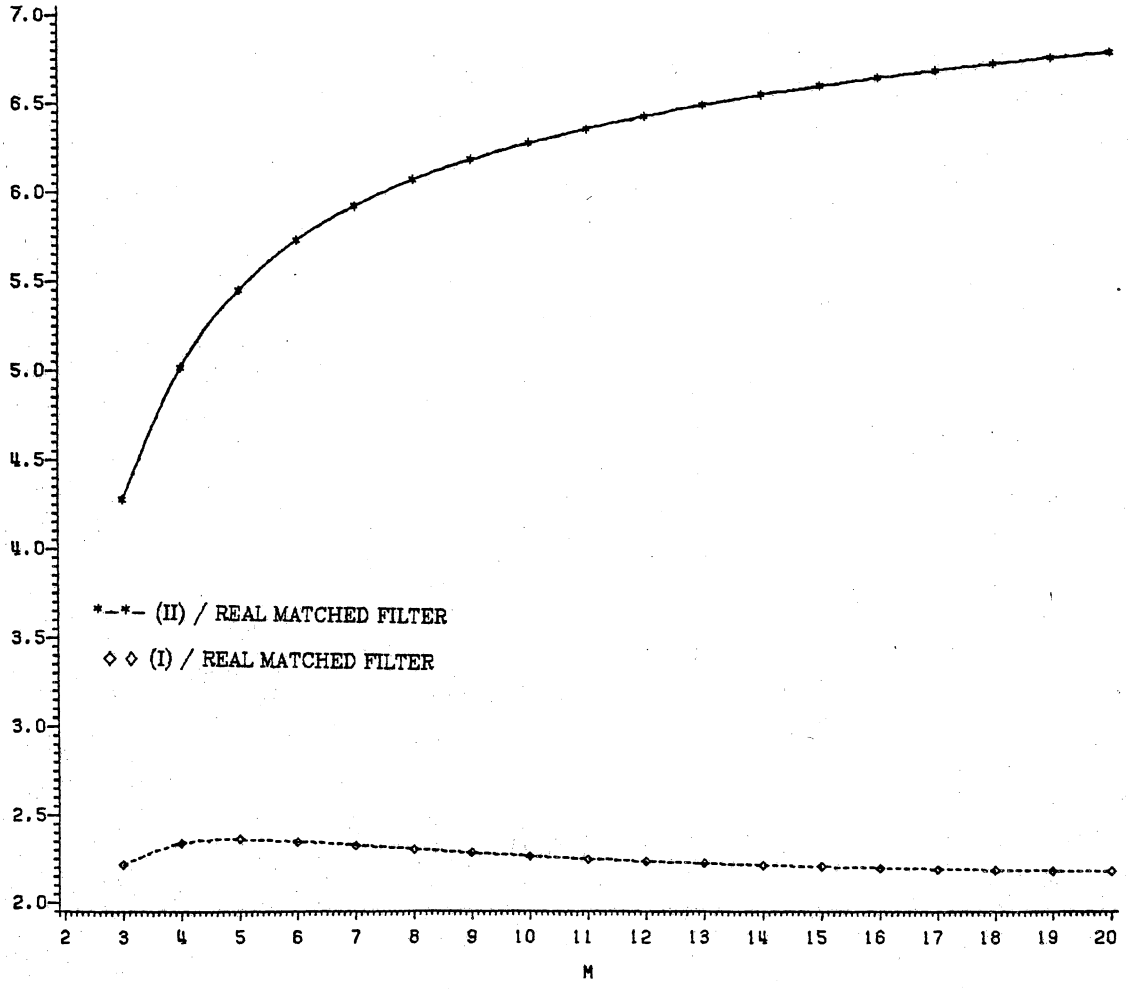

Figure 35. ARE versus (M) for Real Matched Filter as Reference Detector and Correlation of $\rho = 0.7$, and $\alpha = 1.7$.

V. Sub-optimum Detection and Signal Processing Considerations

5.1. Statement of the Problem

This Chapter is concerned with the sub-optimum detection of weak signals in multivariate non-Gaussian noise. In Chapter III, two non-linear detectors were developed, based on amplitude and complex density models as:

$$(LOD)_I = \sum_{i=1}^{M}\sum_{j=1}^{M} \alpha_{ij} \frac{Real(\tilde{y}_i\,\tilde{s}_i^*)}{|\tilde{y}_i|} g'(|\tilde{y}_i|)\; g(|\tilde{y}_j|)$$

$$- \sum_{i=1}^{M} \frac{Real(\tilde{y}_i\,\tilde{s}_i^*)}{|\tilde{y}_i|} \frac{g''(|\tilde{y}_i|)}{g'(|\tilde{y}_i|)} \qquad (5.1-1)$$

$$(LOD)_{II} = \sum_{i=1}^{M}\sum_{j=1}^{M} \alpha_{ij} \frac{Real(\tilde{y}_i\,\tilde{s}_i^*)}{|\tilde{y}_i|} g'(|\tilde{y}_i|)\; g(|\tilde{y}_j|)$$

$$- \sum_{i=1}^{M} \frac{Real(\tilde{y}_i \tilde{s}_i^*)}{|\tilde{y}_i|} \left[\frac{g''(|\tilde{y}_i|)}{g'(|\tilde{y}_i|)} - \frac{1}{|\tilde{y}_i|} \right] \qquad (5.1-2)$$

The various non-linear components, $g(.)$, $g'(.)$, and $g''(.)$ in the LOD structure are implemented on the basis of exact a priori knowledge of the parameters of the underlying noise statistics. However, due to prevailing non-stationarity of the noise environment (i.e., dependence of the sea-clutter on various sea-states), the correlation structure and the parameters of the density function change. Consequently, the shape of the non-linearities in the detector structure changes. Thus, it is both of practical and theoretical interest to investigate the sensitivity of these non-linearities with respect to the parametric variations in the range of interest.

Also, the computationally efficient estimate of the covariance sequence of the multivariate Gaussian density, arising in the modeling of the multivariate non-Gaussian density is of great practical significance.

In section (5.2), variations of different ARE measures with respect to changes in the parameter of Weibull density function are illustrated, and the sensitivity of the non-linearities are investigated. Section (5.3) consideres the computational aspects of the covariance sequence. Finally, section (5.4) deals with the Asymptotic Optimal Detection (AOD).

5.2. Sub-Optimum Approximation to LOD Non-Linearity under Weibull Distribution

In this section, the sensitivity of various non-linearities involved in the structure of $(LOD)_I$ and $(LOD)_{II}$ with respect to parameter variation of the underlying density functions are investigated. As in Chapter II, the density function is chosen to be Weibull, since it represents a well-established density function for amplitude distribution of sea-clutter. The range of interest for the shape parameter (α) of the Weibull distribution, given by:

$$f_{NG}(x) = \alpha\, x^{\alpha-1} e^{-x^{\alpha}} \quad x > 0 \;\; \alpha > 0 \qquad (5.2-1)$$

is : $1 < \alpha < 2$.

The required non-linearities, derived in Chapter IV, are as follows:

$$g(x) = \Phi^{-1}\,[\, F_{NG}(x)\,] \qquad (5.2-2)$$

$$g'(x) = \sqrt{2\pi}\; p_{NG}(x)\; \exp\,\{\,\frac{g^2(x)}{2}\,\} \qquad (5.2-3)$$

$$g''(x) = \sqrt{2\pi}\,[\,p'_{NG}(x) + g'(x)\,g(x)\,p_{NG}(x)\,]\,\exp\,\{\,\frac{g^2(x)}{2}\,\} \qquad (5.2-4)$$

$$g^{(3)}(x) = \sqrt{2\pi}\,[\,p''_{NG}(x) + g''(x)\,g(x)\,p_{NG}(x) + g'^2(x)\,p_{NG}(x) +$$

$$2\,g(x)\,g'(x)\,p'_{NG}(x) + g'^2(x)\,g^2(x)\,p_{NG}(x)\,]\,\exp\,\{\,\frac{g^2(x)}{2}\,\} \qquad (5.2-5)$$

where Φ^{-1} is the inverse Error function and $F_{NG}(x)$ is the Weibull Cumulative Distribution Function (CDF):

$$F_{NG}(x) = 1 - e^{-x^{\alpha}} \qquad (5.2 - 6)$$

In order to obtain some insight into the scale of variation of various ARE measures with respect to changes in the parameter of the density function, four different ARE measures are plotted for three values of (α) . The selected ARE measures are for LOD_{II} with respect to $LOD_{II,i.i.d}$, LOD_{I} with respect to $LOD_{I,i.i.d}$, $LOD_{II,i.i.d}$ with respect to $LOD_{I,i.i.d}$, and LOD_{II} with respect to LOD_{I} . These measures are illustrated in Figures (36) through (39) respectively, for three values of α : 1.3, 1.5, and 1.7. As noticed from these Figures, the values of ARE are all in the same order of magnitude for the selected parameter values, and are all non-decreasing. Also, for a given (M), the difference between ARE measures is less than (8). Consequently, from observation of these results, the next stage is to investigate the degree of robustness that can be incorporated into the structure of these detectors.

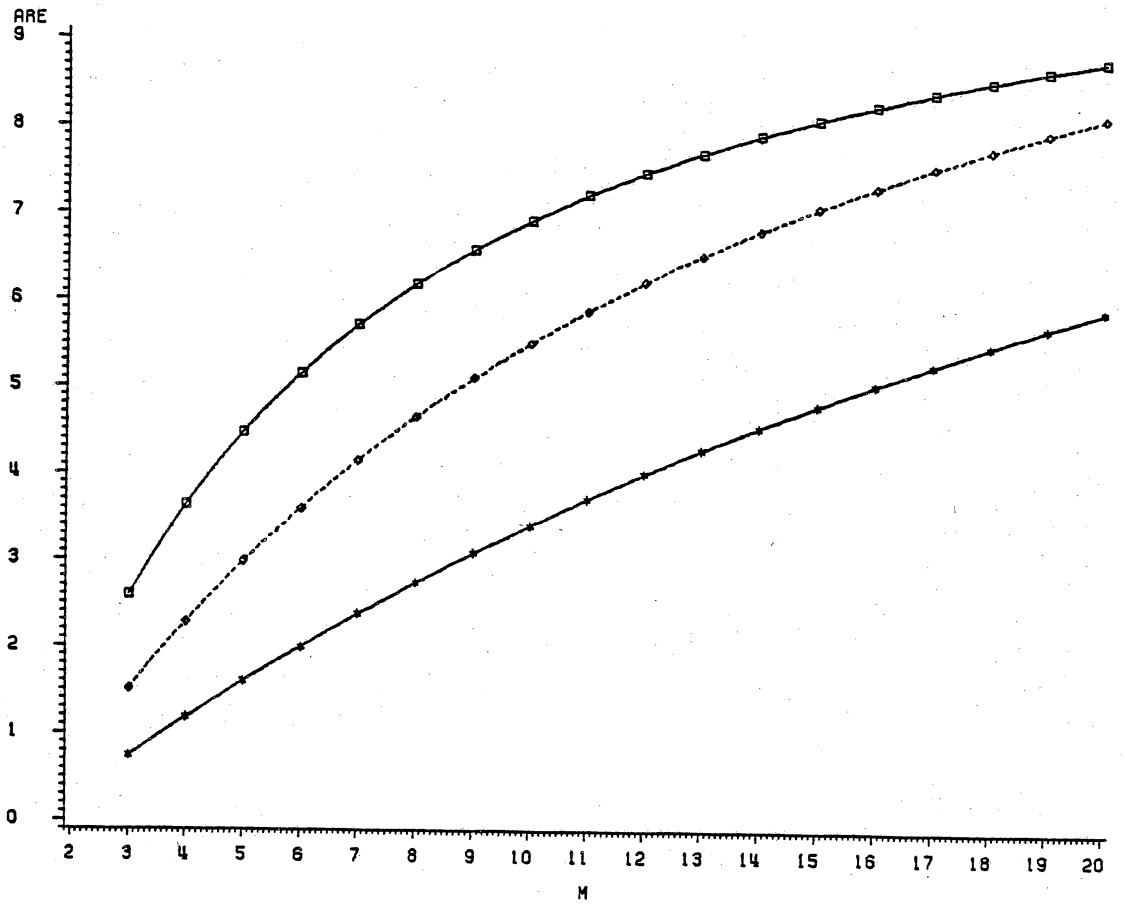

Figure 36. ARE [(II) / (II,i.i.d)] vs (M) for Three Values of α = 1.3, 1.5, 1.7.

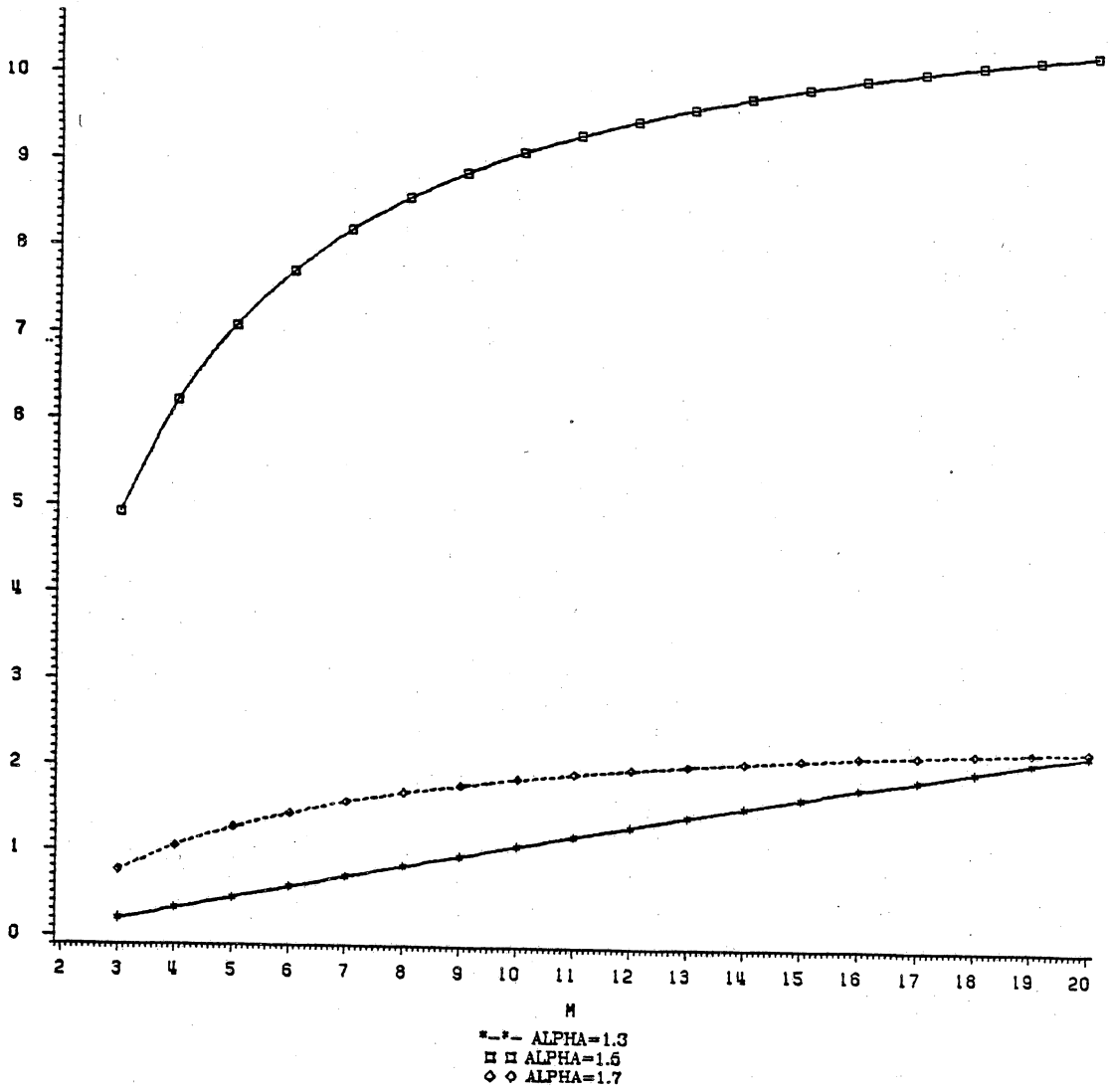

Figure 37. ARE [(I) / (I,i.i.d)] vs (M) for Three Values of α= 1.3, 1.5, 1.7.

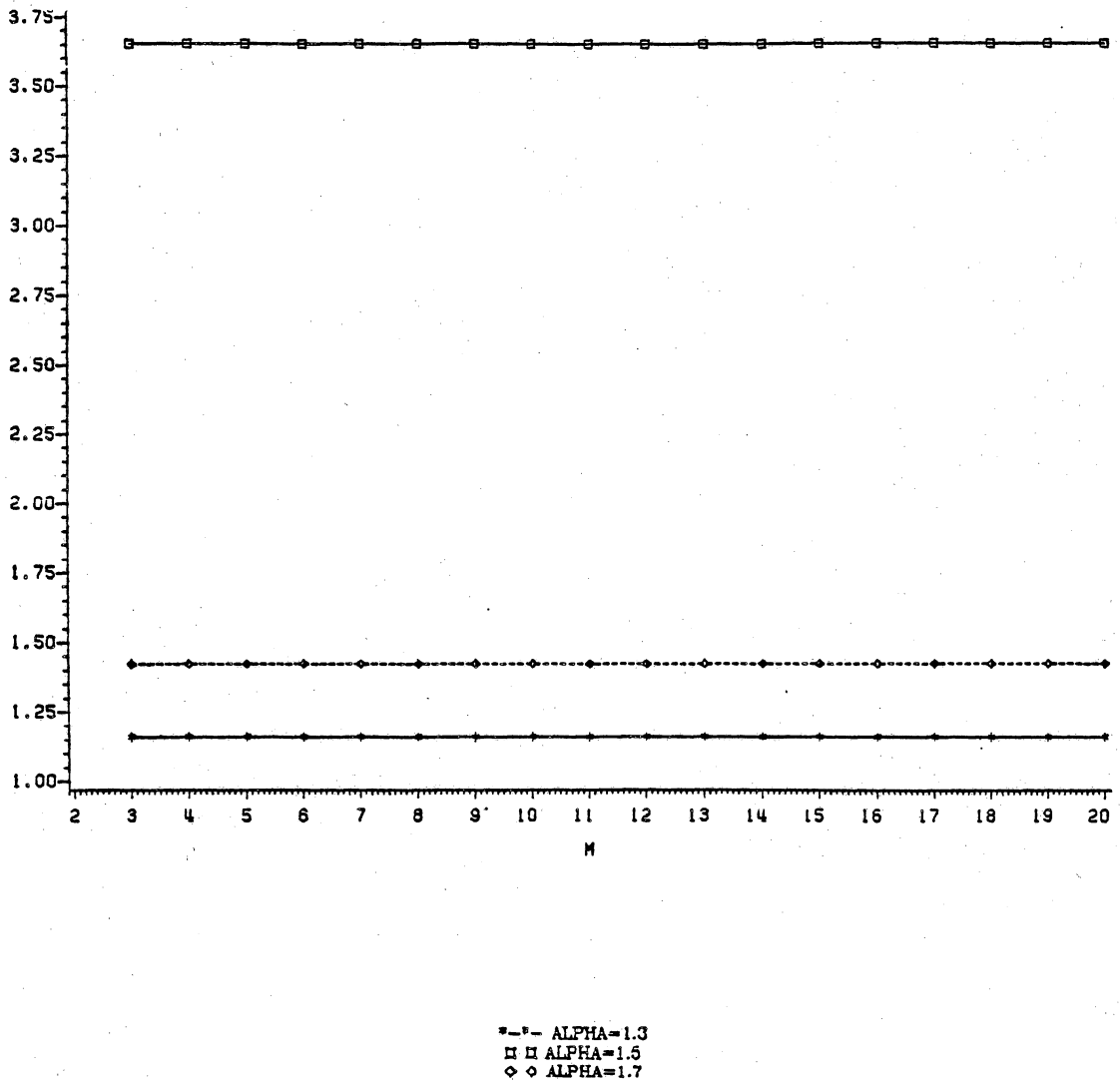

Figure 38. ARE [(II,i.i.d) / (I,i.i.d)] vs (M) for Three Values of α= 1.3, 1.5, 1.7.

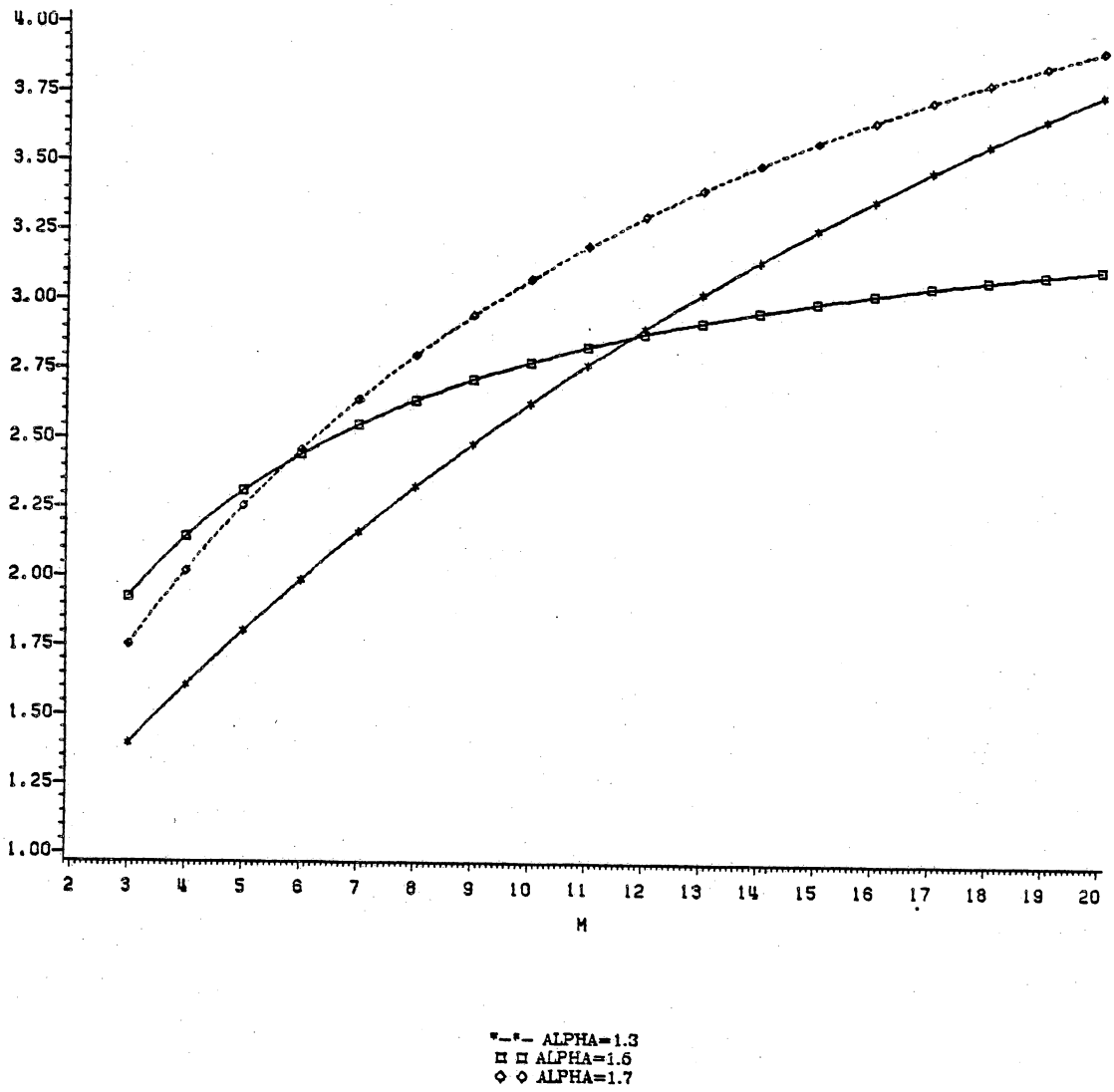

Figure 39. ARE [(II) / (I)] vs (M) for Three Values of α= 1.3, 1.5, 1.7.

As observed from the detector structure, there are several building blocks of non-linearities that can be recognized as:

$$G_1(x) = \frac{g'(x)}{x} \qquad (5.2-7)$$

$$G_2(x) = \frac{g''(x)}{x\, g'(x)} \qquad (5.2-8)$$

$$G_3(x) = \frac{g''(x)}{g'(x)} \qquad (5.2-9)$$

$$G_4(x) = \frac{g''(x)}{g'(x)} - \frac{1}{x} \qquad (5.2-10)$$

$$G_5(x) = \frac{1}{x}\left[\frac{g''(x)}{g'(x)} - \frac{1}{x}\right] \qquad (5.2-11)$$

These non-linearities are plotted for nine values of the Weibull parameter (α) in Figures (40) through (44). As noticed from these Figures, the variation of the non-linearity $G_1(x)$ for the nine values of the parameter α is distinguishable. However, for $G_2(x)$, $G_3(x)$, $G_4(x)$, and $G_5(x)$ the shape of the non-linearity is approximately the same for various values of α .

For practical implementation, it is proposed to set the non-linearities at a fixed value of (α) . For example, $\alpha = 1.5$ is a fairly reasonable value for the non-linearities. Therefore, the overall complexity of the LOD_I and LOD_{II} structures can be reduced to "Robust" structures as:

$$(LOD)_{I,Rob} \cong \sum_{i=1}^{M} \sum_{j=1}^{M} \alpha_{ij}\ Real(\tilde{y}_i\ \tilde{s}_i^*)\ G_1(|\tilde{y}_i|)\ g(|\tilde{y}_j|)$$

$$- \sum_{i=1}^{M} Real(\tilde{y}_i\ \tilde{s}_i^*)\ G_2(|\tilde{y}_i|) \qquad (5.2-12)$$

$$(LOD)_{II,Rob} \cong \sum_{i=1}^{M} \sum_{j=1}^{M} \alpha_{ij}\ Real(\tilde{y}_i\ \tilde{s}_i^*)\ G_1(|\tilde{y}_i|)\ g(|\tilde{y}_j|)$$

$$- \sum_{i=1}^{M} Real(\tilde{y}_i\ \tilde{s}_i^*)\ G_5(|\tilde{y}_i|) \qquad (5.2-13)$$

Thus, for the implementation of each detector, only three non-linear structures are required: $G_1(.)$, g(.), $G_2(.)$ for $(LOD)_{I,Rob}$, and $G_1(.)$, g(.), $G_5(.)$ for $(LOD)_{II,Rob}$.

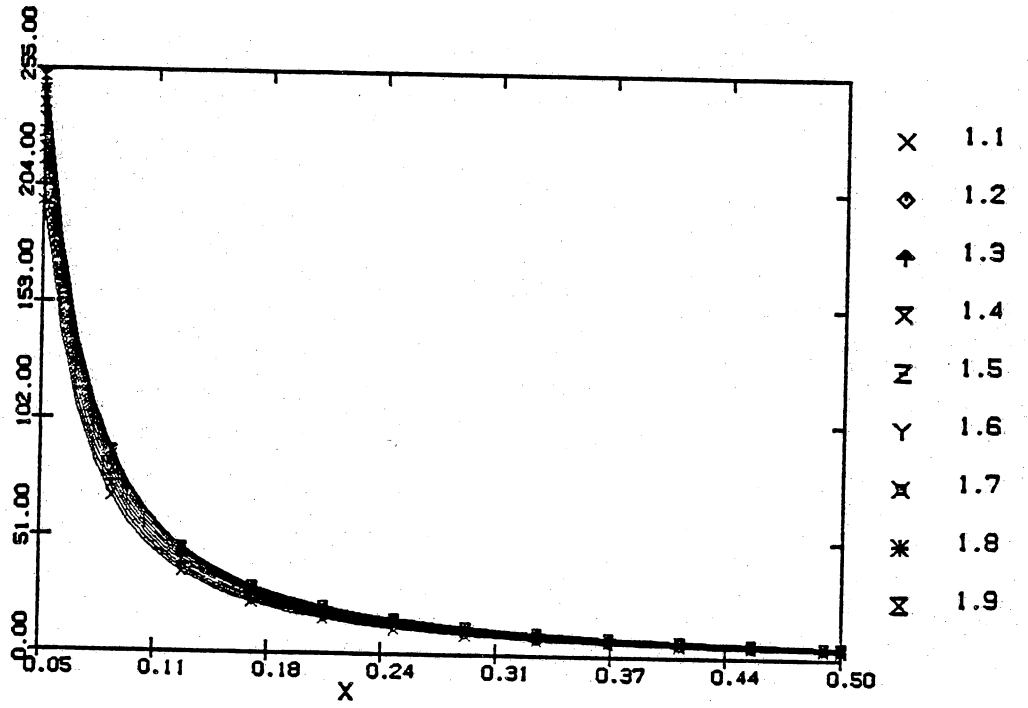

Figure 40. Non-linearity [g'(x)/x] for Various Values of the Univariate Weibull Distribution.

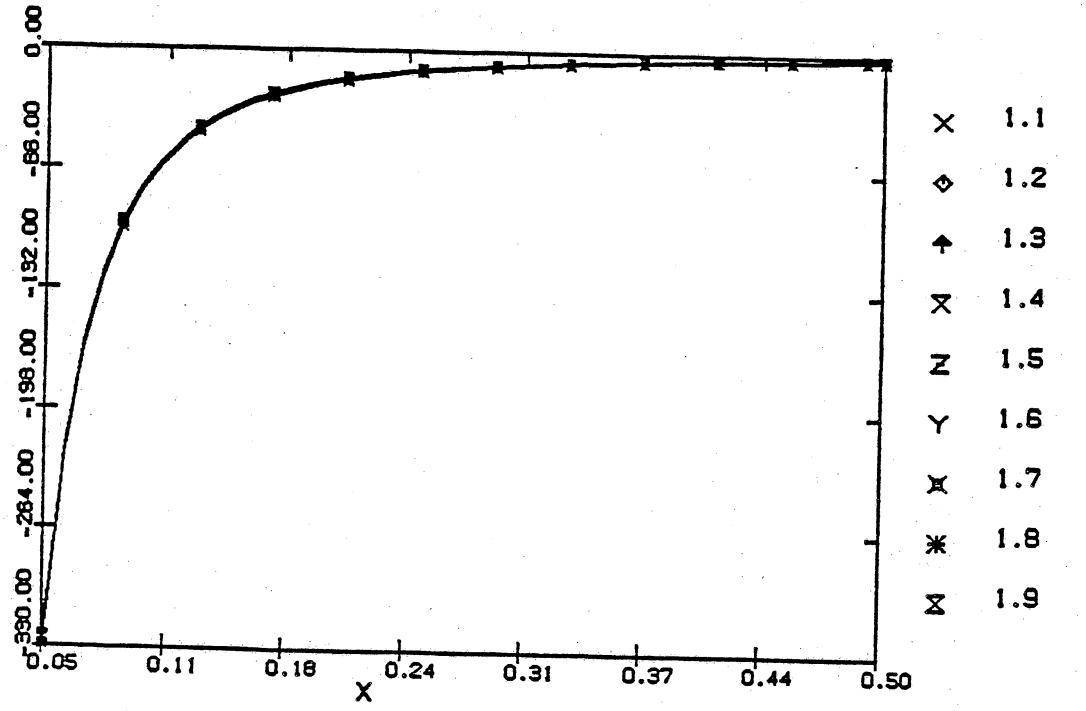

Figure 41. Non-linearity [g″(x)/xg′(x)] for Various Values of the Univariate Weibull Distribution.

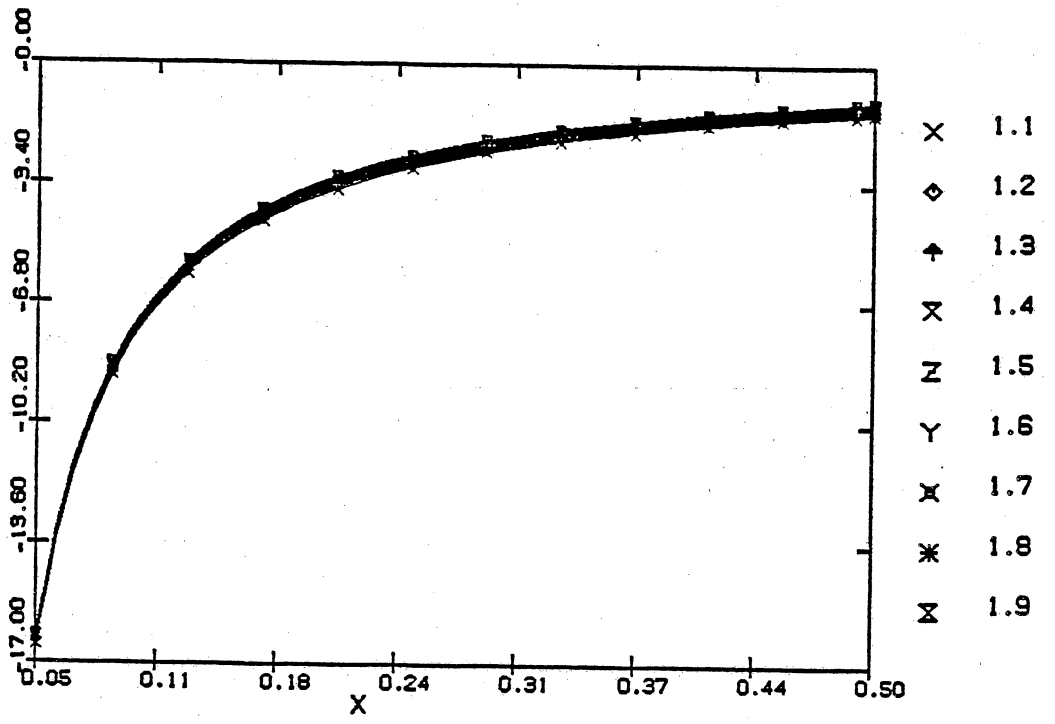

Figure 42. Non-linearity [g″(x)/g′(x)] for Various Values of the Univariate Weibull Distribution.

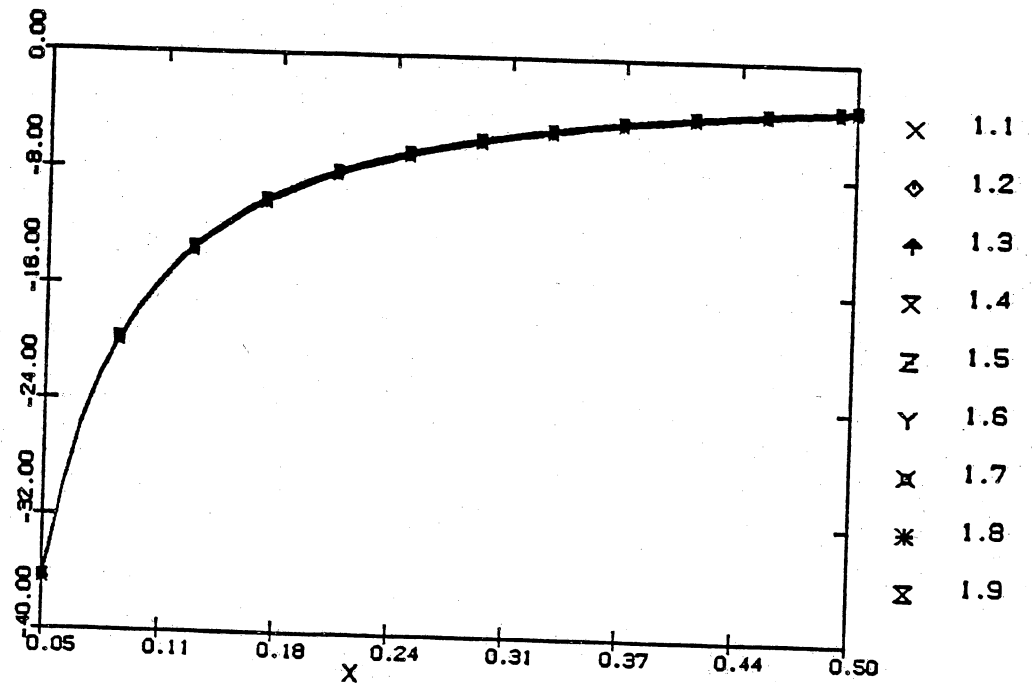

Figure 43. Non-linearity [g″(x)/g′(x) - 1/x] for Various Values of the Univariate Weibull Distribution.

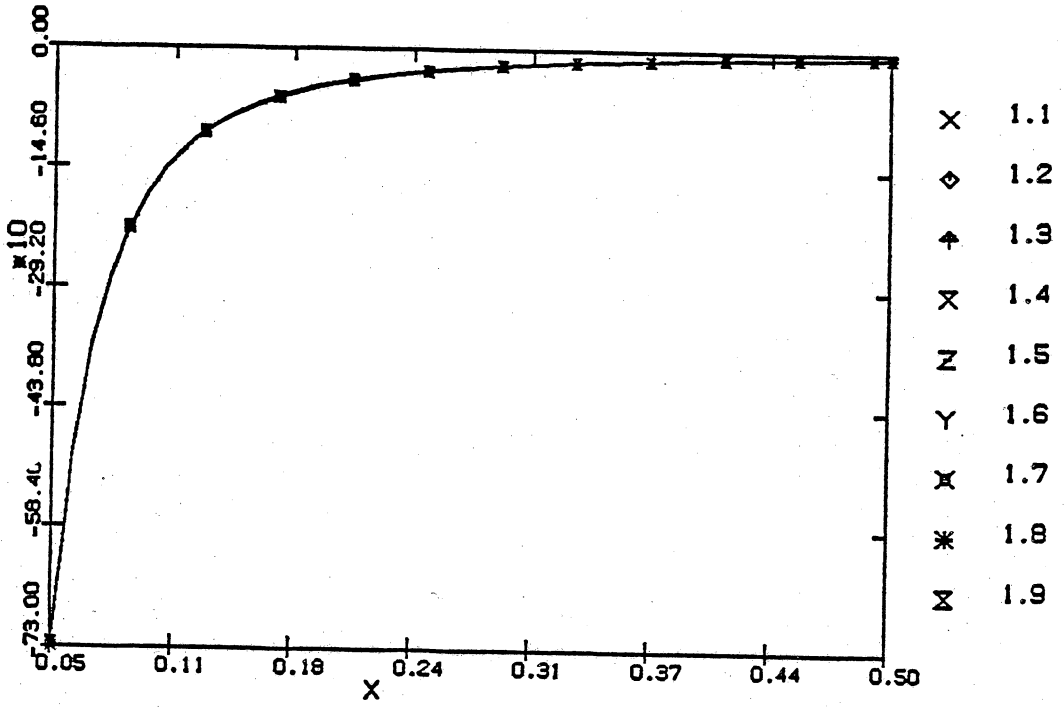

Figure 44. Non-linearity { (1/x) [g''(x)/g'(x) - 1/x] } for Various Values of the Univariate Weibull Distribution.

The next step is to carry out the performance evaluation of these proposed robust detectors with respect to $(LOD)_I$, and $(LOD)_{II}$. Since, the structure of the non-linearities of the $(LOD)_{I,Rob}$, and $(LOD)_{II,Rob}$ are different, the Efficacy of each of the detectors should be derived, based on the new structure.

First, the Efficacy of the $(LOD)_{I,Rob}$ with the test statistic $T_{I,Rob}$ is evaluated. Following the procedures of section (4.4), one can obtain the square root of the numerator of the Efficacy as:

$$E\left\{\frac{\partial T_{I,Rob}}{\partial\theta}\Big|_{\theta=0}\right\} =$$

$$\left\{\sum_{i=1}^{M}\sum_{\substack{j=1\\ j\neq i}}^{M}\alpha_{ij}\,E_i\int_0^\infty dx\int_0^\infty dy\,\left[\,G_1(x)+\frac{x}{2}G'_1(x)\,\right]g(y)\,p_{ij}(x,y)\right\}$$

$$+\left\{\sum_{i=1}^{M}\alpha_{ii}\,E_i\int_0^\infty dx\,\left[\,G_1(x)+\frac{x}{2}G'_1(x)\,\right]g(x)\,p(x)\right\}$$

$$-\left\{\sum_{i=1}^{M}E_i\int_0^\infty dx\,\left[\,G_2(x)+\frac{x}{2}G'_2(x)\,\right]p(x)\right\}$$

$$+\frac{1}{2}\sum_{i=1}^{M}\alpha_{ii}\,E_i\int_0^\infty dx\,[\,x\,G_1(x)\,]g'(x)\,p(x)\,dx \qquad (5.2-14)$$

Similarly, the denominator of the expression for Efficacy is obtained as:

$$Var\left\{\,T^2_{I,Rob}/H_0\,\right\} = \quad + \frac{1}{2}$$

$$\sum_{i=1}^{M}\sum_{\substack{j=1\\ j\neq i}}^{M}\sum_{\substack{k=1\\ k\neq j\\ k\neq i}}^{M} E_i\,(\alpha_{ij}\alpha_{ik})\int_0^\infty dx\int_0^\infty dy\int_0^\infty dz\, x^2 G_1^2(x)\; g(y)\; g(z)\; p_{ijk}(x,y,z)$$

$$+\;\frac{1}{2}\sum_{i=1}^{M}\sum_{\substack{j=1\\ j\neq i}}^{M} E_i\,(\alpha_{ij})^2\int_0^\infty dx\int_0^\infty dy\; x^2 G_1^2(x)\; g^2(y)\; p_{ij}(x,y)$$

$$+\sum_{i=1}^{M}\sum_{\substack{j=1\\ j\neq i}}^{M} E_i\,\alpha_{ii}\,\alpha_{ij}\int_0^\infty dx\int_0^\infty dy\; x^2 G_1^2(x)\; g(x)\; g(y)\; p_{ij}(x,y)$$

$$-\sum_{i=1}^{M}\sum_{\substack{j=1\\ j\neq i}}^{M} E_i\alpha_{ij}\int_0^\infty dx\int_0^\infty dy\; x^2 G_1(x)\,G_2(x)\;\; g(y)\; p_{ij}(x,y)$$

$$+\;\frac{1}{2}\sum_{i=1}^{M} E_i\,(\alpha_{ii})^2\int_0^\infty dx\; x^2 G_1^2(x)\; g^2(x)\; p(x)$$

$$-\sum_{i=1}^{M} E_i\;\alpha_{ii}\int_0^\infty dx\;\; x^2 G_1(x)\,G_2(x)\;\; g(x)\;\; p(x)$$

$$+\;\frac{1}{2}\sum_{i=1}^{M} E_i\int_0^\infty dx\;\; x^2\;\; G_2^2(x)\;\;\; p(x) \qquad (5.2-15)$$

Next, the required expression for the Efficacy of $(LOD)_{II,Rob}$ are derived. As before, it can be shown that the square root of the numerator has the following form:

$$E\left\{\frac{\partial T_{II,Rob}}{\partial\theta}\Big|_{\theta=0}\right\} =$$

$$\left\{\sum_{i=1}^{M}\sum_{\substack{j=1\\ j\neq i}}^{M}\alpha_{ij}\,E_i\int_0^\infty dx\int_0^\infty dy\,\left[\,G_1(x)+\frac{x}{2}G'_1(x)\,\right]g(y)\,p_{ij}(x,y)\right\}$$

$$+\left\{\sum_{i=1}^{M}\alpha_{ii}\,E_i\int_0^\infty dx\,\left[\,G_1(x)+\frac{x}{2}G'_1(x)\,\right]g(x)\,p(x)\right\}$$

$$-\left\{\sum_{i=1}^{M}E_i\int_0^\infty dx\,\left[\,G_5(x)+\frac{x}{2}G'_2(x)\,\right]p(x)\right\}$$

$$+\frac{1}{2}\sum_{i=1}^{M}\alpha_{ii}\,E_i\int_0^\infty dx\,[\,x\,G_1(x)\,]g'(x)\,p(x)\,dx \qquad (5.2-16)$$

Similarly, the denominator can be shown to have the following form:

$$Var\left\{\,T^2_{II,Rob}/H_0\,\right\} = +\frac{1}{2}$$

$$\sum_{i=1}^{M}\sum_{\substack{j=1\\ j\neq i}}^{M}\sum_{\substack{k=1\\ k\neq j\\ k\neq i}}^{M}E_i\,(\alpha_{ij}\alpha_{ik})\int_0^\infty dx\int_0^\infty dy\int_0^\infty dz\,x^2\,G_1^2(x)\;g(y)\;g(z)\;p_{ijk}(x,y,z)$$

$$+\frac{1}{2}\sum_{i=1}^{M}\sum_{\substack{j=1\\ j\neq i}}^{M}E_i\,(\alpha_{ij})^2\int_0^\infty dx\int_0^\infty dy\;x^2\,G_1^2(x)\;g^2(y)\;p_{ij}(x,y)$$

$$+ \sum_{i=1}^{M} \sum_{\substack{j=1 \\ j \neq i}}^{M} E_i \, \alpha_{ii} \, \alpha_{ij} \int_0^\infty dx \int_0^\infty dy \; x^2 \, G_1^2(x) \; g(x) \; g(y) \; p_{ij}(x,y)$$

$$- \sum_{i=1}^{M} \sum_{\substack{j=1 \\ j \neq i}}^{M} E_i \, \alpha_{ij} \int_0^\infty dx \int_0^\infty dy \; x^2 \, G_1(x) \, G_5(x) \; g(y) \; p_{ij}(x,y)$$

$$+ \frac{1}{2} \sum_{i=1}^{M} E_i \, (\alpha_{ii})^2 \int_0^\infty dx \; x^2 \, G_1^2(x) \; g^2(x) \; p(x)$$

$$- \sum_{i=1}^{M} E_i \, \alpha_{ii} \int_0^\infty dx \; x^2 \, G_1(x) \, G_5(x) \; g(x) \; p(x)$$

$$+ \frac{1}{2} \sum_{i=1}^{M} E_i \int_0^\infty dx \; x^2 \; G_5^2(x) \; p(x) \qquad (5.2-17)$$

Next, using the equations (5.2-14) through (5.2-17), the "robustness measure" defined as the ratio of the Efficacy of the $(LOD)_{I,Rob}$ (or $(LOD)_{II,Rob}$) with respect to $(LOD)_I$ (or $(LOD)_{II}$) are calculated for various parameters of the Weibull density function. This measure is essentially the same as (ARE), where the reference detector is $(LOD)_{Rob}$.

Figures (45) through (52) illustrate the ARE versus (M), the number of measurement samples, for correlation coefficient of $\rho = 0.7$, and the density parameter α =1.1,1.2,1.3,1.4,1.6,1.7,1.8, and 1.9.

Careful examination of this robustness measure for various parameters and the number of samples (M) indicate that as the non-Gaussianiy diminishes (i.e., α increases), the robust detectors for both $(LOD)_I$ and $(LOD)_{II}$ show degrada-

tion. This phenomenon is also true, in general, as (M) increases. Furthermore, under different values of the parameter α, the robustness of the $(LOD)_{I,Rob}$ shows steady and consistent superior performance with respect to $(LOD)_I$. This is due to the fact that the structure of the $(LOD)_{II}$ is more complex than $(LOD)_I$.

In summary, it is possible to reduce the structural complexity of $(LOD)_I$ and $(LOD)_{II}$ by introducing the "robust" detectors. However, the type of the detector(I,II), or the number of samples (M) should be examined.

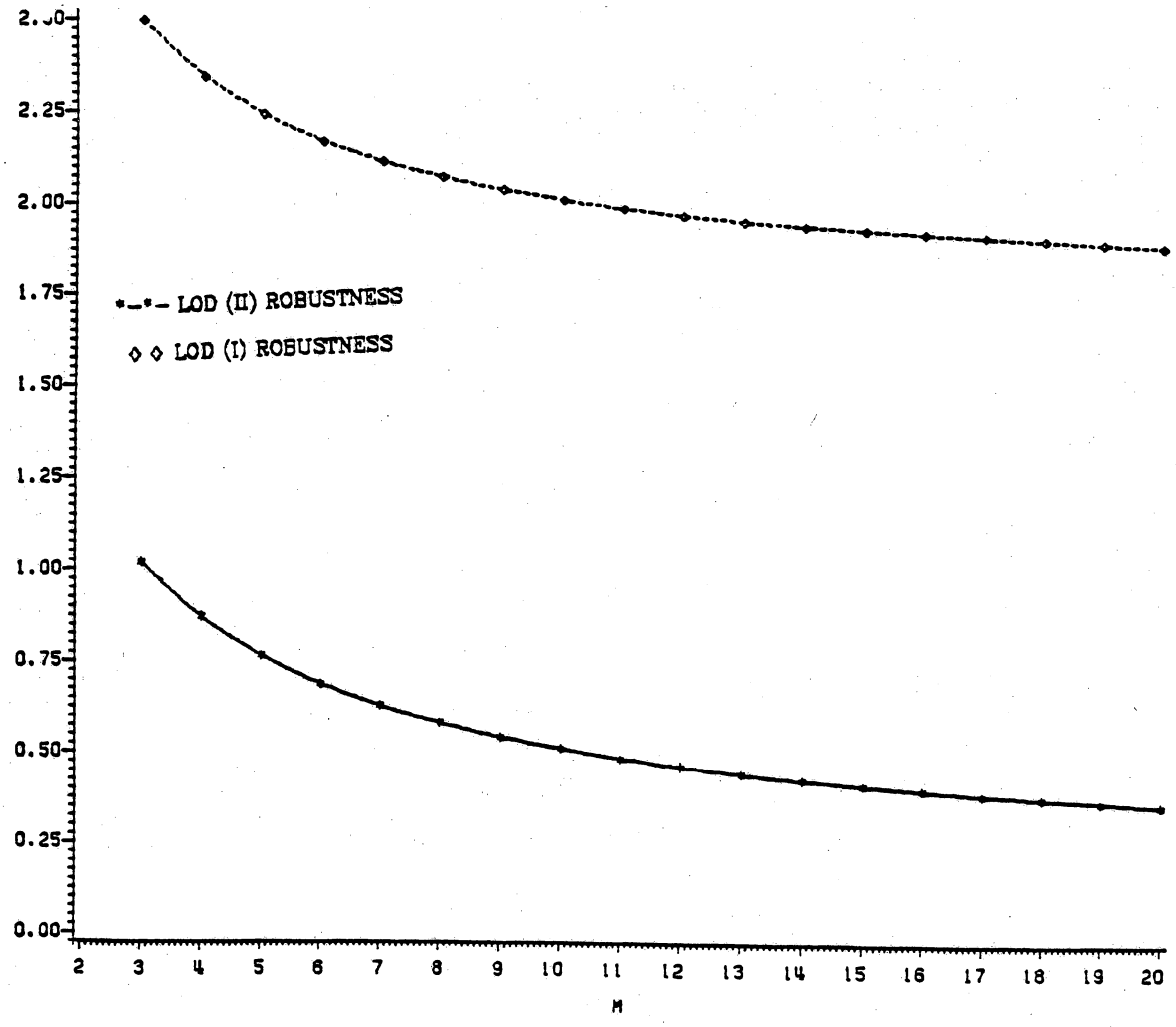

Figure 45. ARE versus (M) for Parametric Detector with respect to Robust Detector for Weibull Parameter of (α = 1.1).

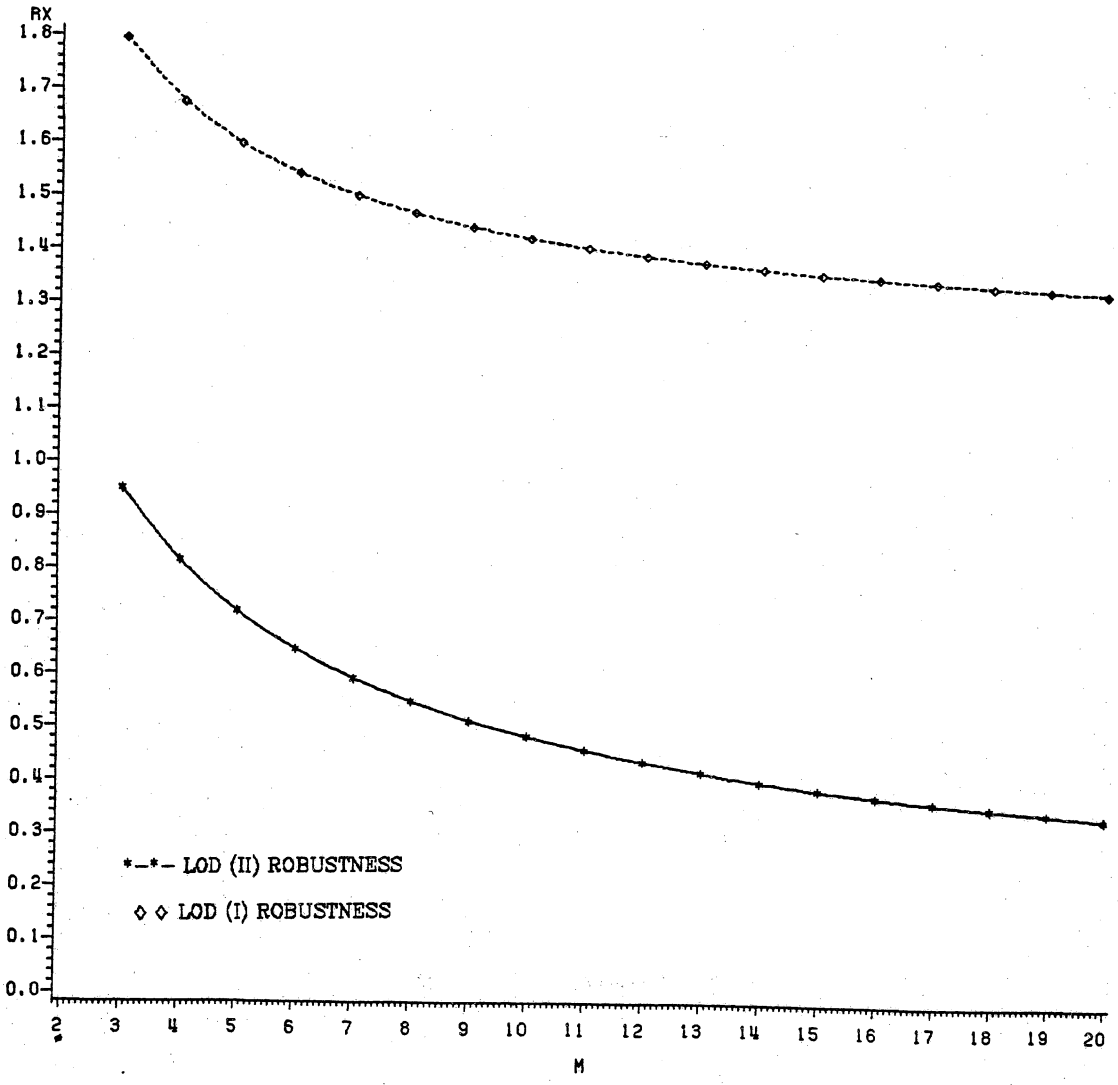

Figure 46. ARE versus (M) for Parametric Detector with respect to Robust Detector for Weibull Parameter of ($\alpha = 1.2$).

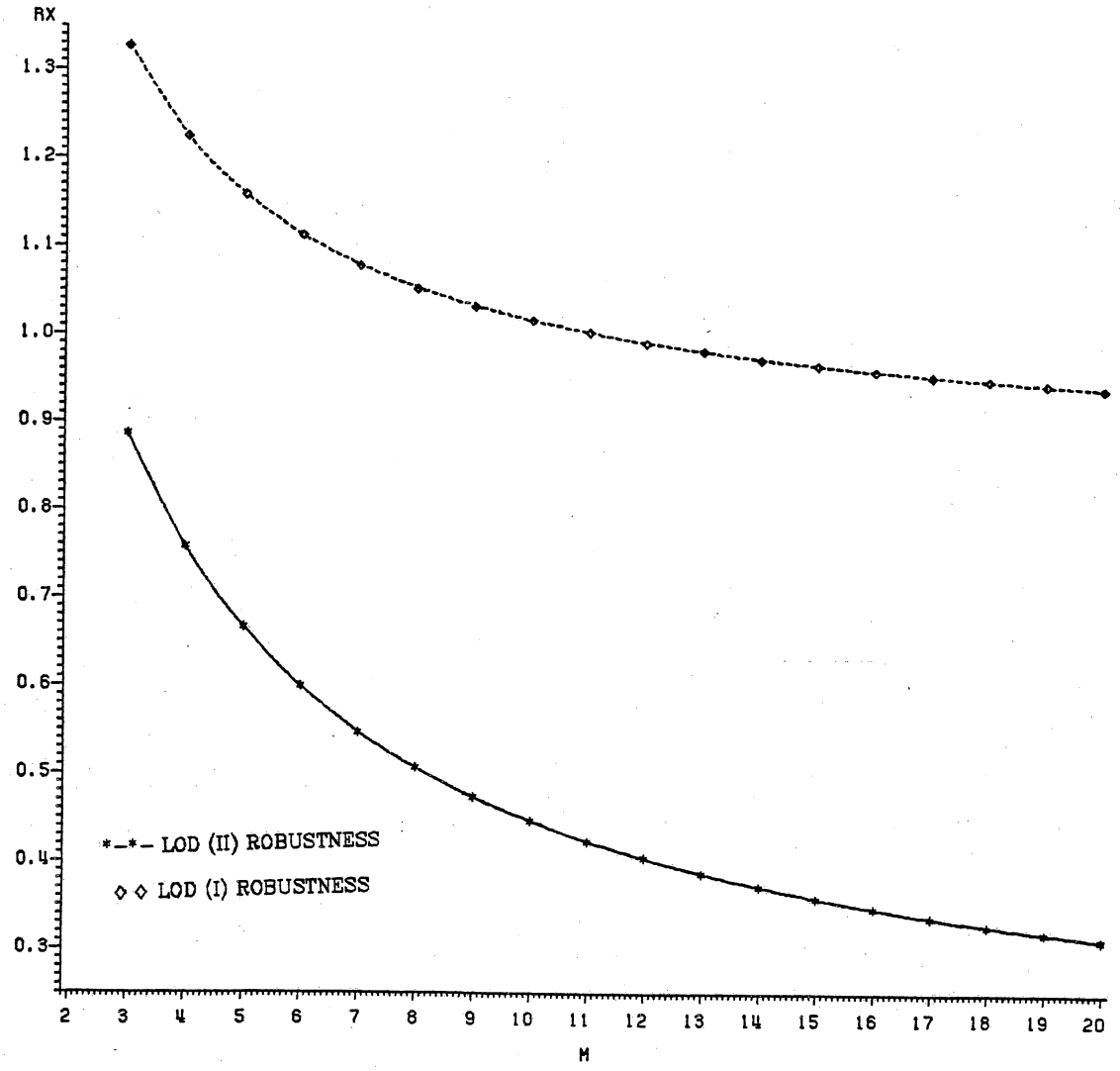

Figure 47. ARE versus (M) for Parametric Detector with respect to Robust Detector for Weibull Parameter of ($\alpha = 1.3$).

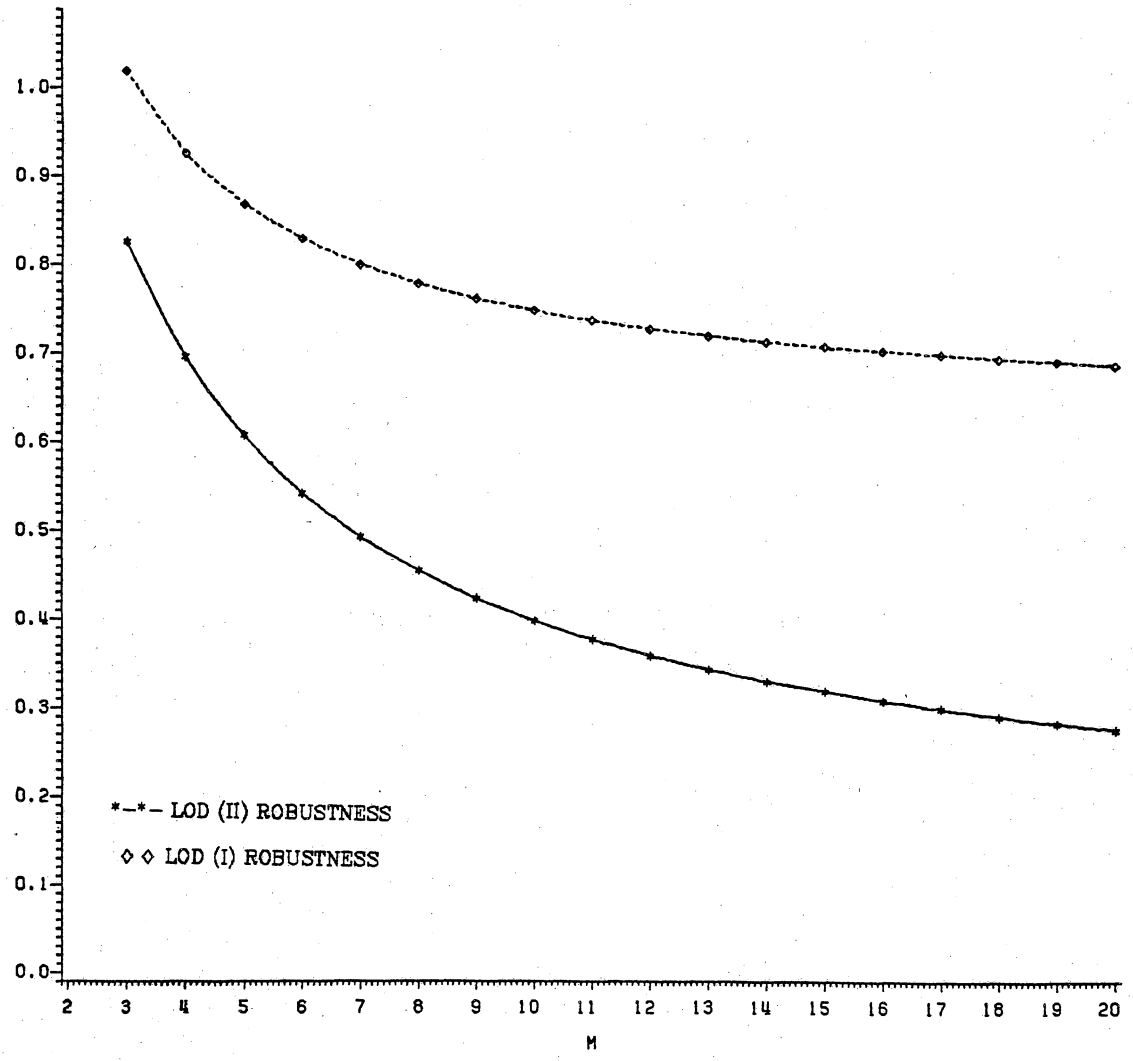

Figure 48. ARE versus (M) for Parametric Detector with respect to Robust Detector for Weibull Parameter of ($\alpha = 1.4$).

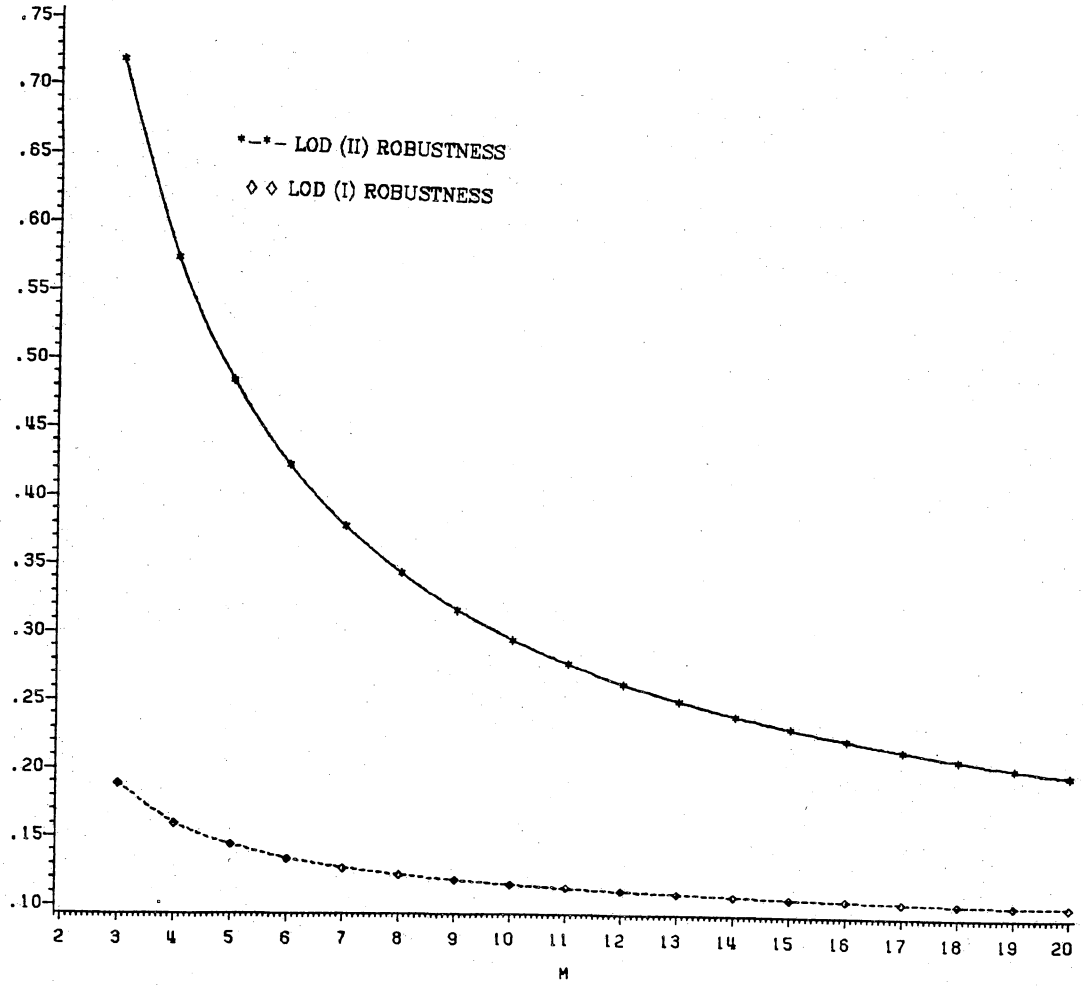

Figure 49. ARE versus (M) for Parametric Detector with respect to Robust Detector for Weibull Parameter of ($\alpha = 1.6$).

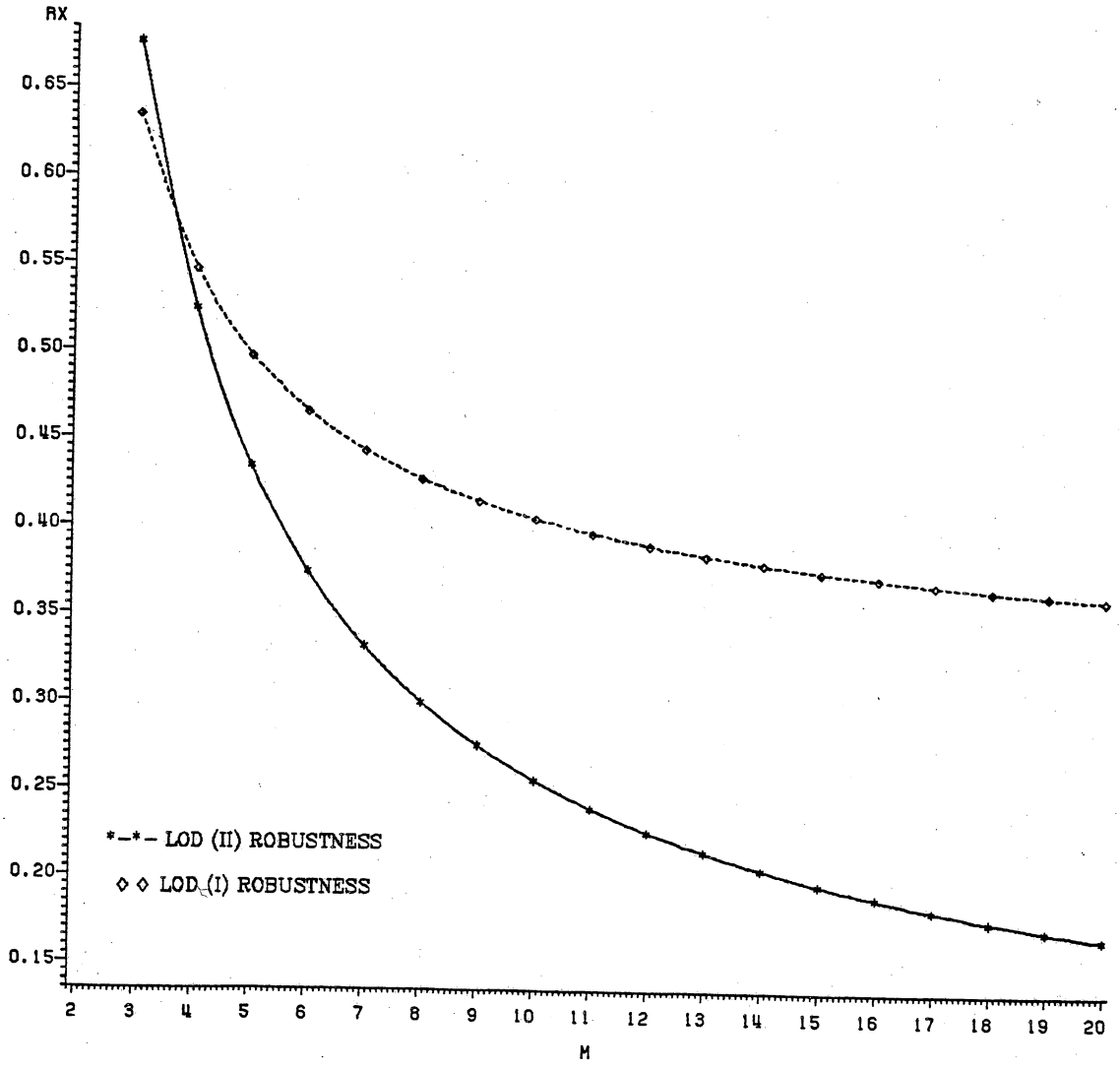

Figure 50. ARE versus (M) for Parametric Detector with respect to Robust Detector for Weibull Parameter of (α = 1.7).

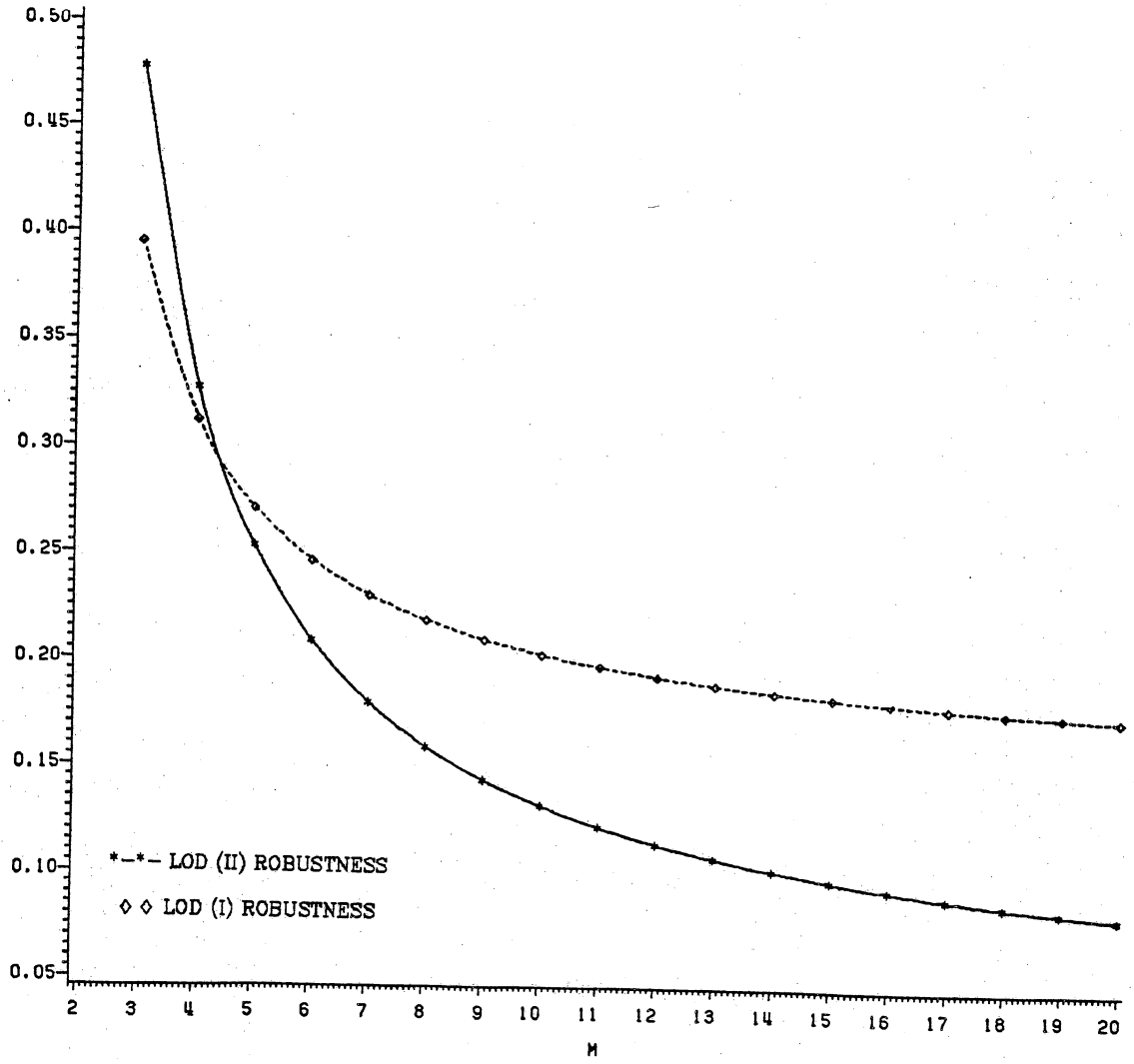

Figure 51. ARE versus (M) for Parametric Detector with respect to Robust Detector for Weibull Parameter of (α = 1.8).

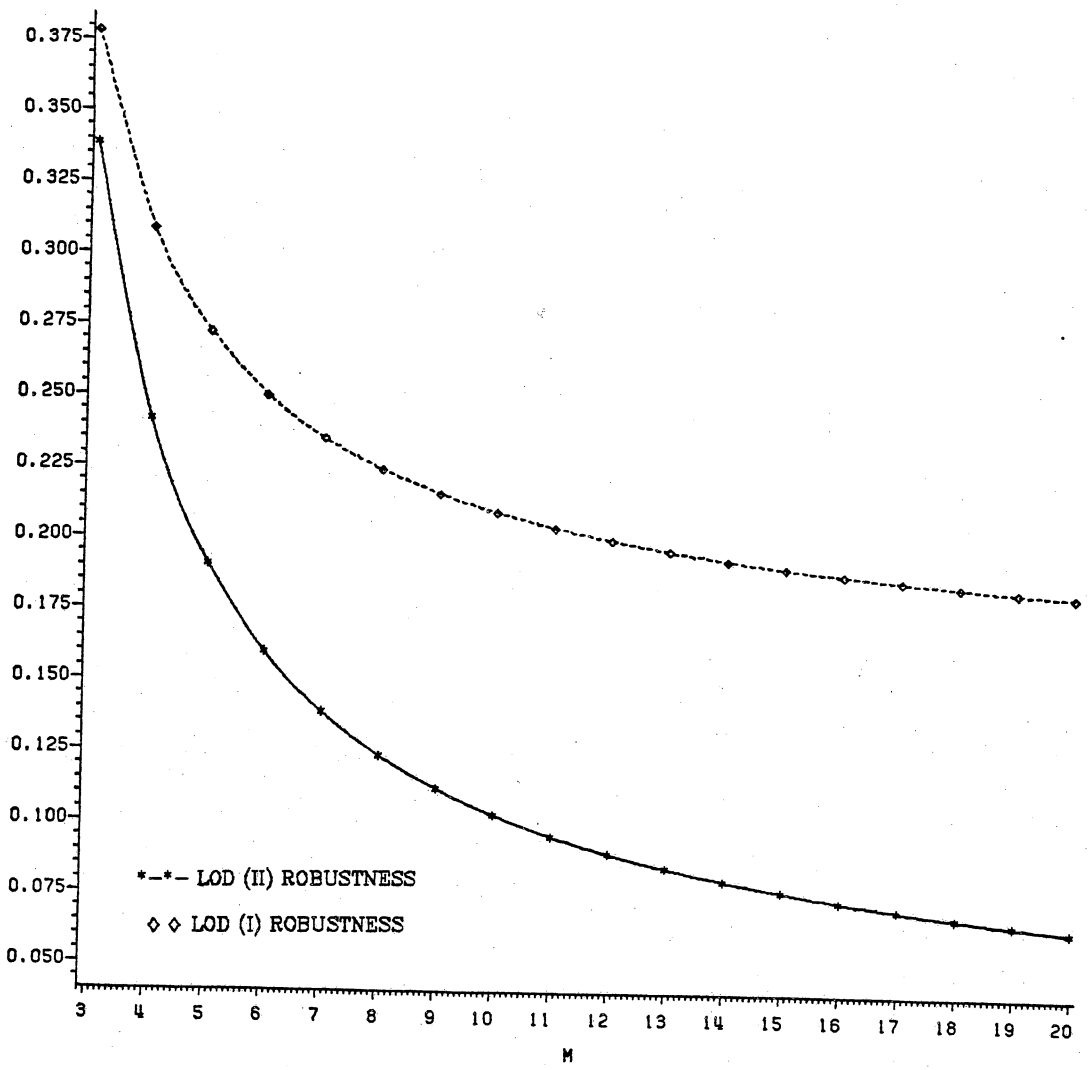

Figure 52. ARE versus (M) for Parametric Detector with respect to Robust Detector for Weibull Parameter of (α = 1.9).

5.3. Computational Aspects of The Correlation Sequence

This section is concerned with performance evaluation of the (LOD)'s using an approximation for the input correlation sequence. In the implementation of the $(LOD)_{II}$ and $(LOD)_{I}$, the weighting coefficients α_{ij} are required. These coefficients are obtained from inversion of the correlation matrix of the multivariate Gaussian density, arising in the modeling of the non-Gaussian amplitude density function.

The relationship between Gaussian input and non-Gaussian output correlation sequence is given by (2.2-20) as:

$$R_n(m) = \sum_{k=0}^{\infty} d_k^2 \left[\rho_x(m)\right]^k \qquad (5.3-1)$$

where

$$d_k^2 = \frac{1}{k!}\left[\int_{-\infty}^{+\infty} g^{-1}(x)\, H_k(\frac{x}{\sigma_x}) \frac{e^{-\frac{x^2}{2\sigma_x^2}}}{\sqrt{2\pi}\,\sigma_x} dx\right]^2 \qquad (5.3-2)$$

where the ZMNL is related to d_k by:

$$g^{-1}(x) = \sum_{k=0}^{\infty} (\frac{d_k}{\sqrt{k!}})\; H_k(\frac{x}{\sigma_x}) \qquad (5.3-3)$$

Ideally, it is desired to obtain $\rho_x(m)$ from (5.3-1) by solution of non-linear system of equations. The detailed discussion of the method and the regularity conditions for valid solutions are given by Liu [23]. However, it has been shown

that for ZMNL non-linearities, the $R_x(m)$ and $R_n(m)$ are very close to each other. This was demonstrated for the triangular and Markovian example under univariate Weibull density function in Chapter II. This phenomenon can be shown as a first order approximation by computation of d_k^2 from (5.3-2).

For a ZMNL obtained under Weibull distribution, and Markovian input covariance sequence ($\rho = 0.7$), and three different values of density parameter α, numerical solution of (5.3-2) yields:

	$\alpha = 1.7$	$\alpha = 1.5$	$\alpha = 1.3$
d_0^2	0.952	0.935	0.897
d_1^2	0.047	0.069	0.101
d_2^2	0.402E-4	0.415E-4	0.283E-3
d_3^2	0.880E-4	0.178E-4	0.266E-3
d_4^2	0.234E-4	0.144E-4	0.277E-5
d_5^2	0.132E-5	0.463E-7	0.566E-6

As noticed, only the first two d_k^2 are significant. That is,with Var(x) = 1, the output correlation sequence can be written as:

$$R_n(m) \cong d_0^2 R_x(m) + d_1^2 R_x^2(m) \qquad (5.3-4)$$

This suggests an approximation scheme for $R_x(m)$. That is, one can assume as a zero-order approximation that: $R_x(m) \cong R_n(m)$.

The performance evaluation of the LOD_{II} has been carried out using the true and approximate values of the input correlation sequence $R_x(m)$. Figures (53) through (55) are ARE's versus (M) for different density parameters. Figure (53) is for $\alpha = 1.3$, Figure (54) is for $\alpha = 1.5$, and Figure (55) is for $\alpha = 1.7$. The evaluated ARE's are for $(LOD)_{II,Approximate}/(LOD)_{II,True}$. As observed, upto $M = 10$, the ARE's are close to each other. However, for long correlated sequences, the approximation will lead to significant degradation. For other non-Gaussian distributions, if the ZMNL is piecewise linear, this approximation can be applied.

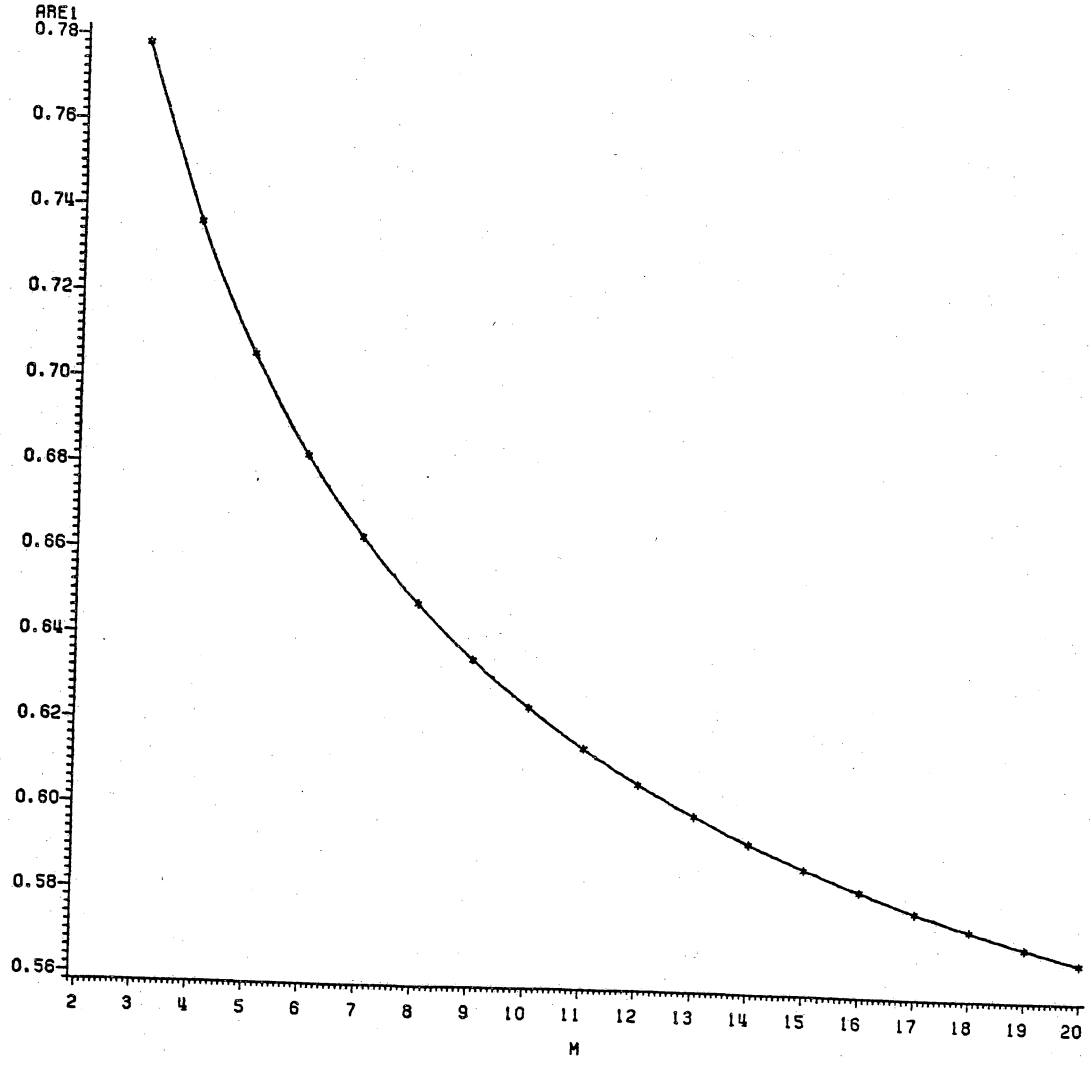

Figure 53. ARE [(II,Approximate) / (II,True)] vs (M) for (α = 1.3).

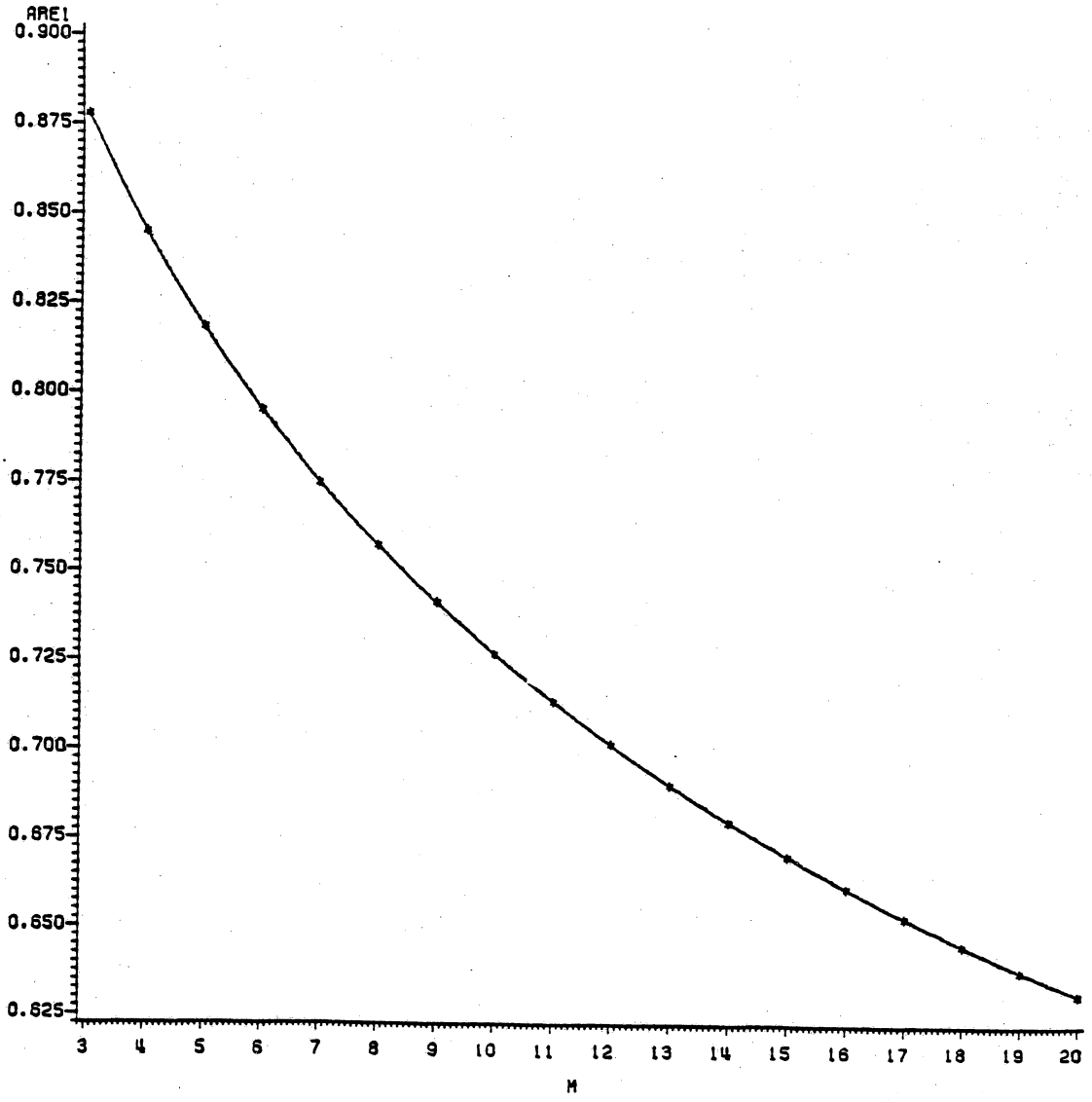

Figure 54. ARE [(II,Approximate) / (II,True)] vs (M) for (α= 1.5).

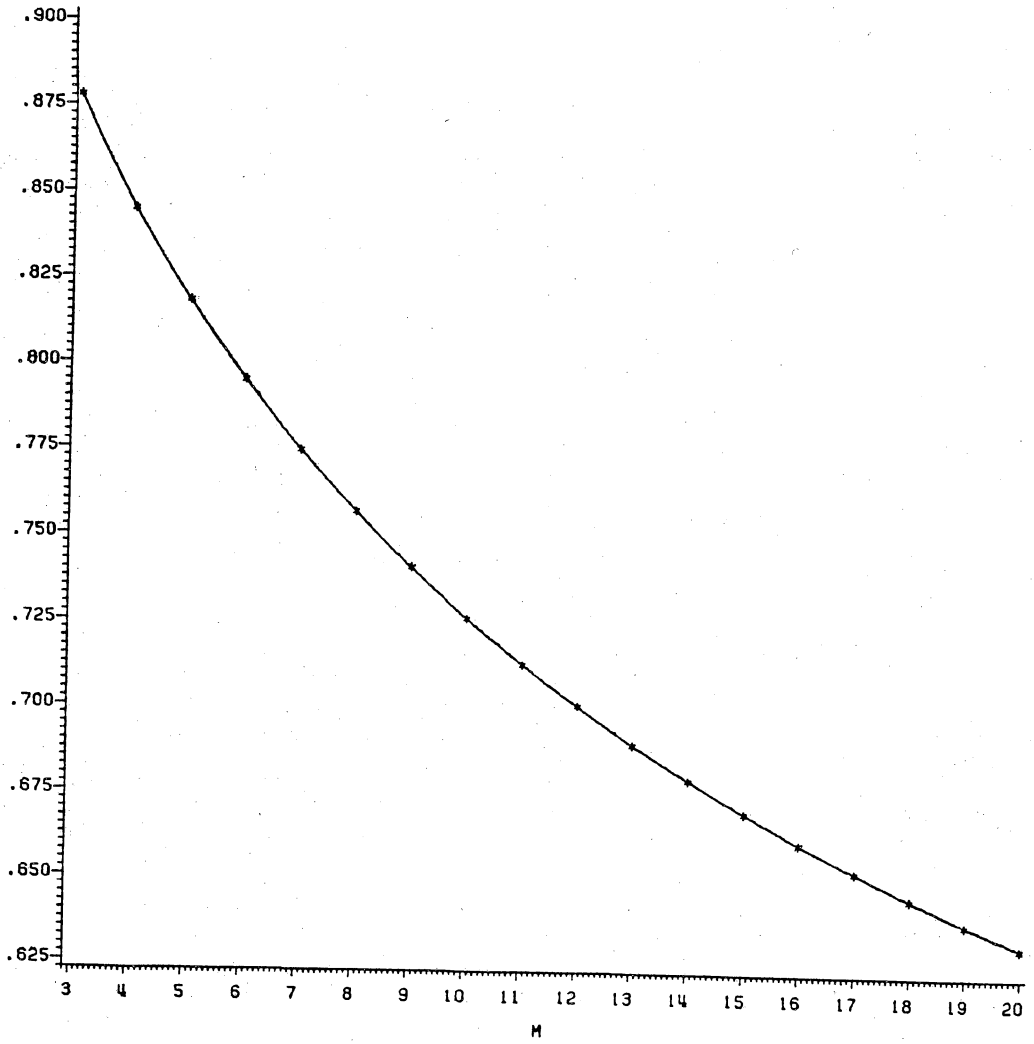

Figure 55. ARE [(II,Approximate) / (II,True)] vs (M) for (α = 1.7).

5.4. Asymptotic Optimum Detection (AOD) of Weak Signals in Non-Gaussian Noise

Thus far, throughout the presentation of this research, one of the fundamental assumption has been based on the weak signal condition. That is, it has been assumed that the signal is vanishingly small ($\theta \rightarrow 0$). This results in the development of non-linear detector structures called: Locally Optimum Detector (LOD), where optimality criterion of maximizing the slope of the power function while keeping a fixed false alarm rate, is achieved as signal approaches to zero. However, there has been no specific criterion on the limiting procedure or the rate of the convergence of the signal to zero.

Recently, there has been new developments on the performance of (LOD) under practical conditions [56-58]. As reported, a satisfactory system performance, under weak signal condition, requires a large number of samples (i.e., M $>$ 10) [56]. However, as the number of samples increases, the LOD becomes sub-optimum [58].

In order to gain some insight, consider the LR expansion for the real signal case as:

$$\Lambda(\underline{y}) = 1 - \theta \underline{s}^T \left(\frac{\nabla_{\underline{y}} p_{\underline{n}}(\underline{y})}{p_{\underline{n}}(\underline{y})}\right) + \frac{1}{2}\theta^2 \underline{s}^T \left(\frac{\nabla^2_{\underline{y}} p_{\underline{n}}(\underline{y})}{p_{\underline{n}}(\underline{y})}\right) \underline{s} + O(\theta^3) \qquad (5.4-1)$$

When the volume of observation is small, it is sufficient to have ($\theta << 1$) in order to approximate (5.4-1) as:

$$\Lambda(\underline{y}) \cong 1 - \theta \underline{s}^T \left(\frac{\nabla_{\underline{y}} p_{\underline{n}}(\underline{y})}{p_{\underline{n}}(\underline{y})}\right) \qquad (5.4-2)$$

However for large value of (M), the contribution of the coefficient of (θ^2) can not be neglected. Thus, in order to have valid approximation as in (5.4-2), the magnitude of (θ) should be restricted by considering:

$$E \mid \Lambda(\underline{y}) - 1 + \theta \underline{s}^T \left(\frac{\nabla_{\underline{y}} p_{\underline{n}}(\underline{y})}{p_{\underline{n}}(\underline{y})}\right) \mid \leq \theta^2 M C \qquad (5.4-3)$$

where (C) is a constant. Thus the condition on θ should be:

$$\theta << \frac{1}{\sqrt{M}} \qquad (5.4-4)$$

so as to justify the approximation of (5.4-2). This is the reason for sub-optimality of the LOD if this condition is not satisfied.

This phenomenon has lead to synthesis of a new class of detectors: Asymptotic Optimum Detectors (AOD). This class of detectors is directed towards a different class of signals where the convergence rate has an explicit dependence on the number of samples. Specifically, the signal level (θ) is proportional to:

$$\theta = k \frac{1}{\sqrt{M}} \qquad (5.4-5)$$

where k is the proportionality constant and (M) is the number of measurement samples. As observed, as ($M \rightarrow \infty$), the signal level approaches to zero, thus satisfying the weak signal condition in a controlled manner. This assumed law of decrease of the signal level assures that the Signal to Noise Ratio (SNR) is finite for a fixed value of (M) [57,58].

Formally, the difference between (LOD) and (AOD) can be stated by the following formulation. In general, the Neyman-Pearson Detector(NPD) has the optimal property that for any arbitrary value of θ_0, the power of (NPD) is greater than the power of (LOD). That is, for a given probability of false alarm:

$$P_{\text{det}}(\theta_0 / LOD) < P_{\text{det}}(\theta_0 / NPD) \qquad (5.4-6)$$

This relation holds for any arbitrary small value of θ_0. By employment of the (LOD), only maximization of the derivative of the power function at $\theta = 0$ is insured: $P'_{\text{det}}(\theta = 0 / LOD)$.

Also, for a given fixed value of (M), as the signal amplitude approaches zero ($\theta \rightarrow 0$), probability of detection approaches to probability of false alarm ($P_{\text{det}} \rightarrow P_{fa}$) which is not, in general, useful. Similarly, with fixed level of (θ), and (M) approaching infinity ($(M) \rightarrow \infty$), probability of detection approaches one ($P_{\text{det}} \rightarrow 1$). However, what is desired is that $\theta \rightarrow 0$ and $M \rightarrow \infty$ so that P_{det} converges to $P_{\text{det}}(\theta / NPD)$. These conditions can be satisfied [45] if one considers the sequence of detectors, where the parametric dependency is allowed to be incorporated into the constant θ as: $\theta_M = \frac{k}{\sqrt{M}}$ for fixed (k). That is, $(M\theta^2)$ remains fixed as $M \rightarrow \infty$.

Thus, one can define the Asymptotic Optimal Detector (AOD) as the sequence of (LOD) with dependence on (M) incorporated into $\theta_M = \frac{k}{\sqrt{M}}$ with the following conditions [45]:

$$\underset{M\to\infty}{Limit}\ [\ P_{\det}(\theta_M / NPD) - P_{\det}(\theta_M / AOD)\ ] = 0 \qquad (5.4-7)$$

and

$$\underset{M\to\infty}{Limit}\ P_{\det}(\theta_M = 0 / AOD) \le P_{fa} \qquad (5.4-8)$$

and

$$P_{fa} < \underset{\substack{M\to\infty \\ \theta\neq 0}}{Limit}\ P_{\det}(\theta_M / AOD) < 1 \qquad (5.4-9)$$

Consequently, the detection problem can be formulated in the context of Hypothesis testing as:

$$H_0 : \underset{\sim}{y} = \underset{\sim}{n} \qquad (5.4-10)$$

$$H_1 : \underset{\sim}{y} = \underset{\sim}{n} + \frac{k}{\sqrt{M}}\underset{\sim}{s} \qquad (5.4-11)$$

where $\underset{\sim}{n} \equiv [\tilde{n}_1, ..., \tilde{n}_M]^T$, $\underset{\sim}{s} \equiv [\tilde{s}_1, ..., \tilde{s}_M]^T$, and $\underset{\sim}{y} \equiv [\tilde{y}_1, ...\tilde{y}_M]^T$ are the M-vector complex noise, signal, and measured samples respectively. The constant $(\frac{k}{\sqrt{M}})$ is a real positive constant, proportional to the amplitude of the signal.

The structure of AOD, based on the asymptotic expansion of the Likelihood Ratio (LR), can be expressed as:

$$\Lambda(\tilde{\underset{\sim}{y}}) = 1 - \frac{k}{\sqrt{M}} \{ \underset{\sim}{s}_I^T \frac{\nabla_{\underset{\sim}{y}_I} p_{\underset{\sim}{n}}(\tilde{\underset{\sim}{y}})}{p_{\underset{\sim}{n}}(\tilde{\underset{\sim}{y}})} + \underset{\sim}{s}_Q^T \frac{\nabla_{\underset{\sim}{y}_Q} p_{\underset{\sim}{n}}(\tilde{\underset{\sim}{y}})}{p_{\underset{\sim}{n}}(\tilde{\underset{\sim}{y}})} \} + O(\frac{k^2}{M}) \qquad (5.4-12)$$

The expression in the brace is proportional to the structure of the $(LOD)_{III}$ which is independent of (M). Now, as $(M \to \infty)$, the second order and higher terms vanish due to the dependence of the expressions on $\frac{1}{M}$. Thus, (5.4-12) can be approximated by:

$$\Lambda(\tilde{\underset{\sim}{y}}) \cong 1 - \frac{k}{\sqrt{M}} \{ \underset{\sim}{s}_I^T \frac{\nabla_{\underset{\sim}{y}_I} p_{\underset{\sim}{n}}(\tilde{\underset{\sim}{y}})}{p_{\underset{\sim}{n}}(\tilde{\underset{\sim}{y}})} + \underset{\sim}{s}_Q^T \frac{\nabla_{\underset{\sim}{y}_Q} p_{\underset{\sim}{n}}(\tilde{\underset{\sim}{y}})}{p_{\underset{\sim}{n}}(\tilde{\underset{\sim}{y}})} \} \qquad (5.4-13)$$

From (5.4-13), the sufficient statistic can be recognized as the structure of the Asymptotic Optimum Detector (AOD) :

$$AOD = \frac{1}{\sqrt{M}} \{ \underset{\sim}{s}_I^T \frac{\nabla_{\underset{\sim}{y}_I} p_{\underset{\sim}{n}}(\tilde{\underset{\sim}{y}})}{p_{\underset{\sim}{n}}(\tilde{\underset{\sim}{y}})} + \underset{\sim}{s}_Q^T \frac{\nabla_{\underset{\sim}{y}_Q} p_{\underset{\sim}{n}}(\tilde{\underset{\sim}{y}})}{p_{\underset{\sim}{n}}(\tilde{\underset{\sim}{y}})} \} \qquad (5.4-14)$$

As noticed, the basic difference between the structure of (LOD) and (AOD) is the normalization of the test statistic which is dependent on the number of measurement samples.

The performance evaluation of (AOD) can also be carried out using the concept of Asymptotic Relative Efficiency (ARE). Since, the test statistics of (LOD) and (AOD) differ by a non-random variable, the ARE type performance evaluation yields the same results. Thus, all the analytical formulation of Chapter IV is also applicable to the case of (AOD).

In general, the employment of (LOD) and (AOD) depend strongly on the application under consideration and the required number of measurement samples. In the next Chapter, the topics of interest that deserve furthur attention will be discussed.

VI. Summary and Concluding Remarks

6.1. Summary, Advantages, and Drawbacks of the Proposed Techniques

In this dissertation, a class of non-linear receivers for detection of weak narrow-band signals in complex multivariate non-Gaussian clutter is investigated. First, the complex multivariate non-Gaussian clutter is characterized by two distinct models. Model (I) is based on a priori knowledge of the marginal density function, the covariance structure, and the circular-symmetry assumption of the in-phase and quadrature phase components. This modeling is implemented by Zero-Memory Non-Linear (ZMNL) transformation of a multivariate Gaussian noise with covariance based on the desired non-Gaussian covariance structure. The information requirements for Model (II) are the first-order in-phase and quadrature phase densities and the complex correlation structure. The implementation of this model is based on ZMNL transformation of the in-phase and

quadrature phase components of a complex multivariate Gaussian clutter whose complex correlation is related to the desired structure.

Second, a class of optimum non-linear receiver structures based on weak signal level, canonically known as Locally Optimum Detectors (LOD), are derived. The optimality criterion is the maximization of the derivative of the power function at zero signal level, subject to fixed false alarm probability. It is shown that the structural complexity depends on whether the underlying hypothesis testing model is real or complex. It is also observed that this is a generalization of the LOD for the independent and identically distributed (i.i.d) clutter.

Third, the performance of each of the proposed detector structures, based on the concept of Efficacy, is formulated analytically. Then, relative performance of the non-linear detectors with respect to a reference detector is evaluated. The comparative performance criterion is Asymptotic Relative Efficiency (ARE). Specifically, computer simulation using Weibull distribution is carried out. Also, performance enhancement of multivariate noise model with respect to independent and identically distributed noise is illustrated.

It should be emphasized that the results of the simulations are based on the model of the underlying multivariate noise density. However, modeling of the noise density is based on the utilization of partial information, i.e., first-order density and correlation structure. Thus, the results presented here might be biased to some extent. That is, using actual data, the performance might be suboptimum.

Unfortunately, the proposed detectors are based on the exact a priori knowledge of the underlying marginal density and covariance parameters of the noise. However, due to non-stationarity of the noise in realistic environments, these parameters vary. To circumvent this problem, and reduce the structural complexity as well, a robust detector is proposed for the Weibull density function with specific range of the density parameter. It is shown that the performance of the robust detector is sensitive to the number of samples and density parameter.

The condition of weak signal is encountered frequently in practice. Although, a detector which is designed to operate optimally for a weak signal is suboptimum for a strong signal, it has reasonable performance on an absolute scale. However, it has been reported recently that in practical situations of interest, a large number of samples are required for reliable detection. Since, as the number of samples increases, the optimality of LOD is degraded, attention has to be directed towards employment of Asymptotic Optimal Detectors (AOD). Thus, a brief discussion on AOD is presented, and its relation with LOD is pointed out.

6.2. Specific Contributions of this Dissertation

The following is a list of specific contributions that have resulted during the course of this research:

1) Modeling of the complex multivariate non-Gaussian density function by imposing "circular symmetry" assumption on the joint in-phase and quadrature phase density function, and invoking the "Transformation Noise" model for the multivariate amplitude density function.

2) Modeling of the complex multivariate non-Gaussian density function by Zero Memory Non-Linear (ZMNL) transformation of the in-phase and quadrature phase components of a complex multivariate Gaussian density.

3) Development of non-linear receiver structures for detection of constant narrow-band complex weak signal in complex multivariate non-Gaussian noise, using the amplitude density model.

4) Development of non-linear receiver structures for detection of constant narrow-band complex weak signal in complex multivariate non-Gaussian noise, using the complex density model.

5) Analytical evaluation of the Asymptotic Relative Efficiency (ARE) for non-linear detector structures by deriving explicit expressions for Efficacy of the test statistic.

6.3. Suggestions for Further Research

As in any other theoretical investigation, during the course of this research, many issues have come to be of significant value that deserve further attention. These issues are either mentioned in the dissertation and are unresolved (i.e., due to the limitation of scope), or they are topics that can be dealt with, having acquired the background material that this dissertation presents. The following is a list of possible topics:

1) If the information on the density of the test statistics for $(LOD)_I$ and $(LOD)_{II}$ are available, one task would be to calculate the probability of detection, and the probability of false alarm versus threshold. This will lead to system performance characterization in terms of the well-known Receiver Operating Characteristic (ROC).

2) In practical situations, due to the non-stationarity of the clutter environment, the noise power level varies. Consequently, the detector threshold should be adjusted to retain constant probability of false alarm. It would be of great practical interest to change the threshold adaptively. This requires an adaptive noise power estimator that can be incorporated into the structure of the $(LOD)_I$ and $(LOD)_{II}$.

3) The weak constant signal detection in multivariate non-Gaussian noise, can be extended to the case of weak stochastic signal. In this case, the structure of detectors will take different forms depending on the mean of the signal. That is, to realize the Local Optimality criterion under the Generalized Neyman-Pearson scheme, either the first or second derivative of the Likelihood Ratio (LR) will be utilized.

4) As was mentioned and illustrated in Chapter II, the K-distributed clutter is both analytically and computationally a difficult problem. It would be desirable to carry out the computational procedures as it was performed for Weibull distribution. This will require computation of Modified Bessel Functions of the Second Kind with non-integer order, and numerical integrations of such functions.

5) In the case of Asymptotic Optimal Detector (AOD), further investigation is required to determine the required sample size for the performance of (AOD) to approach the Neyman-Pearson Detector(NPD).

6) The analytical and experimental results presented in this dissertation, can be extended to the "multi-sensor" detection problem. This is the so-called "diversity" scheme, where the final outcome of the decision process depends on each of the sensors (detectors).

Bibliography

1. D.Middleton,"Canonically Optimum Threshold Detection," IEEE Trans. on Information Theory, Vol.IT-12, No.2, pp.230-243, April 1966.

2. T.S.Ferguson, Mathematical Statistics: A Decision Theoretic Approach Academic Press, 1967.

3. S.Rapport,L.Kurz,"An Optimal Non-linear Detector For Digital Data Transmission Through Non-Gaussian Channels," IEEE Trans. on Communications Technology, Vol.COM-14, pp.266-274, June 1966.

4. J.H.Miller,J.B.Thomas,"Detectors For Discrete-Time Signals In Non-Gaussian Noise," IEEE Trans. on Information Theory, Vol.IT-18, No.2, March 1972.

5. J.H.Miller,J.B.Thomas,"The Detection Of Signals In Impulsive Noise Modeled As A Mixture Process," IEEE Trans. on Communications, Vol.COM-24, pp.559-562, May 1976.

6. J.H.Miller,J.B.Thomas,"Robust Detectors For Signals In Non-Gaussian Noise," IEEE Trans. on Communications, pp.686-690, July 1977.

7. J.J.Sheehy,"Optimum Detection Of Signals In Non-Gaussian Noise," Journal. Acoust. Soc. Am. 63(1), pp.81-90, January 1978.

8. H.V.Poor,J.B.Thomas,"Locally Optimum Detection Of Discrete-Time Stochastic Signals In Non-Gaussian Noise," Journal. Acoust. Soc. Am. 63(1), pp.75-80, January 1978.

9. S.A.Kassam,"Locally Robust Array Detectors For Random Signals," IEEE Trans. on Information Theory, Vol.IT-24, pp.309-316, May 1978.

10. L.M.Nirenberg,"Low SNR Digital Communication Over Certain Additive Non-Gaussian Channels," IEEE Trans. on Communications, Vol. COM-23, No.3, pp.332-341, March 1975.

11. J.W.Modestino,A.Y.Ningo,"Detection Of Weak Signals In Narrow-Band Non-Gaussian Noise," IEEE Trans. on Information Theory, Vol.IT-25, No.5, pp.592-600, September 1979.

12. N.H.Lu,B.A.Eisenstein,"Detection Of Weak Signals In Non-Gaussian Noise," IEEE Trans. on Information Theory, Vol.IT-27, No.6, pp.755-771, November 1981.

13. H.V.Poor,J.B.Thomas,"Memoryless Discrete-Time Detection Of A Constant Signal In m-Dependent Noise," IEEE Trans. on Information Theory, Vol.IT- 25, No.1, pp.54-61, January 1979.

14. D.R.Halverson,G.L.Wise,"A Detection Scheme For Dependent Noise Processes," Journal of The Franklin Institute, Vol.309, No.5, pp.287-300, May 1980.

15. D.R.Halverson,G.L.Wise,"Asymptotic Memoryless Detection Of Random Signals In Dependent Noise," Journal of The Franklin Institute, Vol.312, No.1, pp.13-29, July 1981.

16. H.V.Poor,"Signal Detection In The Presence Of Weakly Dependent Noise-Part I : Optimum Detection," IEEE Trans. on Information Theory, Vol.IT-28, No.5, pp.735-744, Sept 1982.

17. A.B.Martinez, P.F.Swaszek,J.B.Thomas,"Locally Optimum Detection In Multivariate Non-Gaussian Noise," IEEE Trans. on Information Theory, Vol.IT-30, No.6, pp.815-822, November 1984.

18. A.D.Whalen, Detection Of Signals In Noise , Academic Press, 1971.

19. D.K.McGraw,J.F.Wagner,"Elliptically Symmetric Distributions," IEEE Trans. on Information Theory, Vol.IT-14, No.1, pp.110-120, January 1968.

20. S.C.Schwartz,"A Series Technique For The Optimum Detection Of Stochastic Signals In Noise," IEEE Trans. on Information Theory, Vol.IT- 15, No.3, pp.362-369, May 1969.

21. J.K.Ord, Families of Frequecny Distributions , Hafner, 1977.

22. G.L.Wise,A.P.Traganitis,J.B.Thomas,"The Effects Of A Memoryless Non-linearity On The Spectrum Of A Random Process," IEEE Trans. on Information Theory, Vol.IT-23, No.1, pp.84-89, January 1977.

23. B.Liu,D.C.Munson,Jr,"Generation Of A Random Sequence Having A Jointly Specified Marginal Distribution And Autocovariance," IEEE Trans. on ASSP, Vol.ASSP-30, No.6, pp.973-983, December 1982.

24. M.I.Skolnik, Introduction to Radar Systems , McGraw-Hill, 1980.

25. M.Katzin,"On The Mechanism Of Radar Sea Clutter," Proceedings of IRE, pp.44-53, January 1957.

26. N.W.Guinard,J.C.Daley,"An Experimental Study Of A Sea Clutter Model," Proceedings of The IEEE, Vol.58, No.4, pp.543-550, April 1970.

27. G.V.Trunk,S.F.George,"Detection Of Targets In Non-Gaussian Sea-Clutter," IEEE Trans. on Aerospace and Electronic Systems, Vol.AES-6, No.5, pp.620-628, September 1970.

28. E.Jakeman,P.N.Pusey,"Statistics Of Non-Rayleigh Microwave Sea Echo," IEEE International Conference on Radar, pp.105-109, 1977.

29. F.A.Fay,J.Clarke,R.S.Peters,"Weibull Distribution Applied To Sea-Clutter,"IEEE International Radar Conference, pp.101-104, 1977.

30. K.D.Ward,"Compound Representation Of High Resolution Sea Clutter," Electronic Letters, Vol.17, No.16, August 1981.

31. H.C.Glaser,T.F.Havig,"Radar Backscattering From Ocean Waves At Low Grazing Angles," NAECON Records, pp.406-411, 1981.

32. J.Maaloe,"Sea Clutter Statistics," IEEE International Radar Conference, pp.193-197, 1982.

33. P.Z.Peebles,JR.,"The Generation of Correlated Log-Normal Clutter for Radar Simulations," IEEE Trans. on Aerospace and Electronic Systems, pp.1215-1217, November 1971.

34. W.J.Szajnowski,"Generation of Correlated Log-Normal Clutter Samples," Electronic Letters, Vol.12, No.19, pp.497-498, September 1976.

35. W.J.Szajnowski,"The Generation of Correlated Weibull Clutter for Signal Detection Problems," IEEE Trans. on Aerospace and Electronic Systems, pp.536-540, Vol.AES-13, No.5, September 1977.

36. D.C.Schleher,F.Kozin,"Radar Signal Processing Using Digital Non-Linear Filters," IEEE International Conference on Acoustics, Speech, and Signal Processing, pp.854-858, May 1977.

37. A.Farina,A.Russo,F.A.Studer,"Advanced Models of Targets and Disturbances and Related Radar Signal Processors," IEEE International Radar Conference, pp.151-158, 1985.

38. A.Farina,A.Russo,F.A.Studer,"Coherent Radar Detection in Log-Normal Clutter," IEE Proceedings, Vol.133, Pt.F, No.1, pp.39-54, February 1986.

39. P.K.Enge,"Discrete Time Detection in m-Dependent Narrowband Noise," Proceedings of the 19-th Annual Conference on Information Sciences and Sysems, Johns Hopkins University, Baltimore, Maryland, (1985).

40. H.L.Van Trees, Detection, Estimation, and Modulation Theory, Part I , John Wiley & Sons, 1968.

41. D.Middleton, Statistical Communication Theory , McGraw Hill, 1960.

42. C.W.Helstrom, Statistical Theory Of Signal Detection , Pergamon Press, 1960.

43. D.Middleton, Topics In Communication Theory , McGraw Hill, 1965.

44. J.Capon, "On The Asymptotic Efficiency Of Locally Optimum Detectors," IRE Trans. on Information Theory, pp.67-71, April 1961.

45. I.F.Blake, H.V.Poor, Communications and Networks: A Survey of Recent Advances , Springer-Verlag 1986.

46. E.L.Lehmann, Testing Statistical Hypothesis , John Wiley & Sons, 1959.

47. P.Billingsley, Probability and Measure , John Wiley & Sons, 1979.

48. W.A.Gardner,"A Unifying View Of Second-Order Measure Of Quality For Signal Classification," IEEE Trans. on Communications, Vol.Com-28, No.6, pp.807-816, June 1980.

49. S.A.Kassam,T.L.Lim,"Coefficient and Data Quantization in Matched Filters for Detection," IEEE Trans. on Communications, Vol.Com.26, pp.124-127, January 1978.

50. B.Picinbono,"Detection with Uncertainty: Non-parametric, Robust or Adaptive Approaches," in Adaptive Methods in Underwater Acoustics , NATO ASI Series, edited by H.G.Urban, 1985.

51. G.E.Noether,"On A Theorem Of Pitman," Annals of Math.Stat, Vol.26, pp.64-68, 1955.

52. E.J.G.Pitman, Some Basic Theory for Statistical Inference , Chapman and Hall, London 1979.

53. M.Kanefsky,J.B.Thomas,"On Polarity Detection Schemes with Non-Gaussian Inputs," Journal of the Franklin Institute, Vol.280, No.2, pp.120-138, August 1965.

54. A.Papoulis, Probability, Random Variables, and Stochastic Process , McGraw Hill 1984.

55. H.Urkowitz, Signal Theory and Random Processes , ARTECH House. Inc, 1983.

56. A.Farina,G.Galati,"Surveillance Radars: State of the Art, Research and Perspective," ALTA Frequenza, Vol.LIV, No.4, pp.243-260, July-August 1985.

57. E.Conte,L.Izzo,M.Longo,L.Paura,"Asymptotically Optimum Radar Detection In Sea Clutter," MELECON 85, Vol II, pp.339-343,Digital Signal Processing ,Elsevier Science Publishers, IEEE 1985.

58. L.Izzo,L.Paura,"Asymptotically Optimum Space-Diversity Detection in Non-Gaussian Noise," IEEE Trans. on Communications, Vol.COM-34, No.2, pp. 97-103, February 1986.

The vita has been removed from the scanned document